

Bent Naphthodithiophenes: Synthesis and Characterisation of Isomeric Fluorophores

Emmanuel B.A. Adusei,^[a] Vincent T. Casetti,^[a] Calvin D. Goldsmith,^[a] Madison Caswell,^[a] Drecila Alinj,^[a] Jimin Park,^[a] Matthias Zeller,^[b] Alexander A. Rusakov,^[a] and Zacharias J. Kinney^{[a]*}

Electronic Supporting Information

*email: kinney@oakland.edu

| | |
|---|----|
| 1) Experimental Procedures | 2 |
| 2) NMR Spectra | 8 |
| 3) Photophysical Properties of $\alpha(\text{OHex})\text{R}_2$ and $\beta(\text{O}i\text{-Pent})\text{R}_2$ | 53 |
| 4) Solution-State Analysis | 56 |
| 5) Computational Analysis | 63 |
| 6) Crystallographic Analysis | 69 |
| 7) References | 76 |

1) Experimental Procedures

Unless otherwise noted, all starting materials, reagents, and solvents were purchased from commercial sources and used without further purification. Anhydrous solvents (dichloromethane, hexanes, tetrahydrofuran, toluene) were purified using an Inert PureSolv solvent purification system equipped with an alumina column. NMR spectra were measured on a Bruker Avance III 400 MHz spectrometer, with all samples referenced to the residual solvent signal. High resolution mass spectra were obtained by dissolving samples in dichloromethane/methanol and analysed on a LTQ Orbitrap (ionisation method: APCI+). Absorbance spectra were recorded on a Cary 100Bio spectrophotometer and corrected for solvent background absorbance. Emission spectra were recorded on a Horiba Jobin-Yvon Fluorolog-3 fluorometer. All spectra were recorded at room temperature using 1 cm path length quartz cuvettes with spectrometric grade solvents. Fluorescence quantum yield (ϕ) measurements were performed on solutions prepared under inert atmosphere in a Vacuum Atmosphere Company NexGen glovebox with dry, degassed solvents. Quantum yields were determined by reference to 9,10-diphenylanthracene in cyclohexane ($\phi = 0.91$) which was cross-checked with quinine bisulfate in 0.5 M H₂SO₄ (aq) ($\phi = 0.54$). Five solutions of varying concentration were prepared for each sample and good fits ($R^2 \geq 0.99$) were obtained in all cases. The absorbance of all sample solutions was kept below 0.10 to avoid the inner-filter effect. Measurements were performed at room temperature with both sample and standard excited at the same wavelength (365 nm).¹ Procedures for **1(OHex)**, **1(OMe)**, **2(OHex)**, **2(OMe)**, **3**, **α (OMe)**, and **α (OMe)Br₂** are given for clarity with appropriate literature references containing spectral identification. All procedures detailed below were carried out multiple times and the yields reported represent the median outcome of an experiment. Common reagent and solvent abbreviations: ethyl acetate (EtOAc), dichloromethane (DCM), tetrahydrofuran (THF), chloroform-d (CDCl₃), *N*-bromosuccinimide (NBS), 2,3-dichloro-5,6-dicyano-*p*-benzoquinone (DDQ).

Synthesis of α (OHex)**R**₂ Series

1,2-dibromo-4,5-dihexyloxybenzene, **1(OHex)**

4,5-dibromocatechol (19.0 mmol) was massed into a 250 mL round bottom flask and dissolved in 2-butanone (150 mL). A stir bar was added, followed by K₂CO₃ (57.0 mmol) and a reflux condenser. The reaction flask was flushed with argon for 5 minutes, then iodoethane (34.2 mmol) was added in one portion. The reaction temperature was then raised to 80 °C and allowed to stir for 24 hours. After 24 hours the reaction flask was cooled to RT and poured into H₂O (50 mL), extracted with EtOAc (2x50 mL), washed with brine (2x50 mL), dried over anhydrous Na₂SO₄, decanted, and concentrated to yield crude product. Purification via silica gel flash column with Hexanes:EtOAc (99:1) mobile phase afforded 1,2-dibromo-4,5-dihexyloxybenzene (**1(OHex)**) as a colorless oil (R_f 0.56), 5.46 g (82%). Spectral details match literature values.²

1,2-di(3-thienyl)-4,5-dihexyloxybenzene, **2(OHex)**

A 100 mL Schlenk tube was charged with **1(OHex)** (7.23 mmol), 3-thiophene boronic acid (21.8 mmol), Pd(PPh₃)₂Cl₂ (1.13 mmol), and a stir bar added. The reaction flask was then backfilled with argon (x3), after which 40 mL dry THF and 15 mL degassed 2 M K₂CO₃ (aq) were added under positive pressure of argon. The tube was sealed under argon, and the reaction was allowed to stir in an oil bath at 80 °C overnight. After overnight stirring the reaction tube was cooled to RT, poured into H₂O (25 mL), extracted with EtOAc (2x50 mL), washed with brine (2x50 mL), dried over anhydrous Na₂SO₄, decanted, and concentrated to yield crude product. Purification via silica gel flash column with Hexanes:DCM (4:1) eluent to afford 1,2-di(3-thienyl)-4,5-dihexyloxybenzene (**2(OHex)**) as a tacky colorless oil (R_f 0.33), 2.20 g (69%). Spectral details match literature values.³

5,6-bis(hexyloxy)naphtho[2,1-*b*:3,4-*b'*]dithiophene, **α (OHex)**

A 500 mL Schlenk flask was charged with **2(OHex)** (1.64 mmol) and a stir bar, then was sparged with argon for 10 minutes. After 10 minutes dry DCM (75 mL) was added and the reaction flask was equipped with a pressure equalising funnel. The reaction flask was then cooled to 0 °C and equilibrated for 15 minutes under argon. FeCl₃ (3.86 mmol) was massed into a beaker and dissolved in MeNO₂ (14 mL), then added to the pressure equalising funnel. The FeCl₃/MeNO₂ solution was added dropwise over five minutes to the reaction flask, after which the ice bath was removed and the reaction was allowed to come to RT over an hour. The reaction was quenched with MeOH (10x MeNO₂) and concentrated. The crude reaction was resuspended in DCM (50 mL) and H₂O (50 mL), extracted with DCM (2x50 mL), washed with brine (2x50 mL), dried over anhydrous Na₂SO₄, decanted, and concentrated to yield crude product. Purification via silica gel flash column with Hexanes:DCM (4:1) affords pure **α (OHex)** as an off-white solid (R_f 0.28), 422 mg (58%): ¹H NMR (400 MHz, CDCl₃) δ 7.87 (d, $J = 5.4$ Hz, 2H), 7.47 (d, $J = 5.3$ Hz, 2H), 4.21 (t, $J = 6.6$ Hz, 4H), 1.95 (p, $J = 6.9$ Hz, 4H), 1.62 – 1.51 (m, 4H), 1.41 (m, 8H), 0.97 – 0.90 (m, 6H); ¹³C NMR (101 MHz, CDCl₃) δ 148.9, 133.9, 130.4, 123.4, 122.7, 122.5, 106.8, 69.3, 31.6, 29.2, 25.8, 22.6, 14.0.; HRMS (APCI+) calcd for C₂₆H₃₃O₂S₂ (M+H)⁺ 441.192199, found 441.19289 (1.56 ppm).

2,9-dibromo-5,6-bis(hexyloxy)naphtho[2,1-*b*:3,4-*b'*]dithiophene, **$\alpha(\text{OHex})\text{Br}_2$**

$\alpha(\text{OHex})$ (3.32 mmol) was massed into a 250 mL round bottom flask and dissolved in CHCl_3 (56 mL). A stir bar was added and the reaction was allowed to stir under argon for 5 minutes, after which NBS (9.10 mmol) was added in portions. The reaction was left to stir for 3 days and quenched in DI water (100 mL), extracted with DCM (2x50 mL), washed with brine (2x50 mL), dried with anhydrous Na_2SO_4 , decanted, and concentrated to yield crude product as a pale-yellow solid. Purification via silica gel flash column with Hexanes:DCM (19:1) as mobile phase afforded pure **$\alpha(\text{OHex})\text{Br}_2$** as an off-white solid (R_f 0.15), 1.23 g (62%): ^1H NMR (400 MHz, CDCl_3) δ 7.80 (s, 2H), 7.49 (s, 2H), 4.17 (t, J = 6.6 Hz, 4H), 1.93 (m, 4H), 1.61 – 1.50 (m, 4H), 1.45 – 1.33 (m, 8H), 0.99 – 0.91 (m, 6H); ^{13}C NMR (101 MHz, CDCl_3) δ 149.3, 133.7, 130.2, 125.4, 121.7, 112.1, 106.1, 69.2, 31.6, 29.2, 25.8, 22.6, 14.0; HRMS (APCI+) calcd for $\text{C}_{26}\text{H}_{31}\text{Br}_2\text{O}_2\text{S}_2$ (M+H)⁺ 597.013220, found 597.01476 (2.57 ppm).

5,6-bis(hexyloxy)-2,9-diphenylnaphtho[2,1-*b*:3,4-*b'*]dithiophene, **$\alpha(\text{OHex})\text{Ph}_2$**

A 25 mL Schlenk tube was charged with **$\alpha(\text{OHex})\text{Br}_2$** (0.539 mmol), phenylboronic acid (1.780 mmol), $\text{Pd}(\text{PPh}_3)_2\text{Cl}_2$ (0.129 mmol), and a stir bar. The reaction tube was backfilled with argon (3x), after which 5 mL dry THF and 1 mL degassed 2M K_2CO_3 solution were added under positive pressure of argon. The reaction tube was sealed under argon and stirred in an oil bath at 80 °C overnight. The reaction was cooled to RT, poured into H_2O (15 mL), extracted with EtOAc (2x50 mL), washed with brine (2x50 mL), dried over anhydrous Na_2SO_4 , decanted, and concentrated to yield crude product. Purification was achieved via silica gel flash column Hexanes:EtOAc (49:1) followed by recrystallisation from hexanes to afford **$\alpha(\text{OHex})\text{Ph}_2$** as a pale yellow solid (R_f 0.22), 204 mg (64%): ^1H NMR (400 MHz, CDCl_3) δ 7.95 (s, 2H), 7.78 (d, J = 7.6 Hz, 4H), 7.59 (s, 2H), 7.45 (t, J = 7.6 Hz, 4H), 7.35 (t, J = 7.4 Hz, 2H), 4.20 (t, J = 6.7 Hz, 4H), 1.96 (p, J = 6.9 Hz, 4H), 1.58 (m, 4H), 1.42 (m, 8H), 1.00 – 0.91 (m, 6H); ^{13}C NMR (101 MHz, CDCl_3) δ 149.0, 141.9, 134.8, 134.5, 129.8, 129.1, 128.0, 126.3, 122.8, 118.2, 106.7, 69.4, 31.8, 29.5, 26.0, 22.8, 14.2; HRMS (APCI+) calcd for $\text{C}_{38}\text{H}_{41}\text{O}_2\text{S}_2$ (M+H)⁺ 593.254799, found 593.25632 (2.56 ppm).

5,6-bis(hexyloxy)-2,9-di-*p*-tolyl naphtho[2,1-*b*:3,4-*b'*]dithiophene, **$\alpha(\text{OHex})\text{Tot}_2$**

A 50 mL Schlenk tube was charged with **$\alpha(\text{OHex})\text{Br}_2$** (0.424 mmol), *p*-methylphenylboronic acid (1.101 mmol), $\text{Pd}(\text{PPh}_3)_2\text{Cl}_2$ (0.115 mmol), and a stir bar. The reaction tube was backfilled with argon (3x), after which 4 mL dry THF and 0.85 mL degassed 2M K_2CO_3 solution were added under positive pressure of argon. The reaction tube was sealed under argon and stirred in an oil bath at 80 °C overnight. The reaction was cooled to RT, poured into H_2O (15 mL), extracted with EtOAc (2x50 mL), washed with brine (2x50 mL), dried over anhydrous Na_2SO_4 , decanted, and concentrated to yield crude product. Purification was achieved via silica gel flash column Hexanes:Toluene (7:3) followed by recrystallisation from hexanes to afford **$\alpha(\text{OHex})\text{Tot}_2$** as a pale yellow solid (R_f 0.35), 100 mg (38%): ^1H NMR (400 MHz, CDCl_3) δ 7.92 (s, 2H), 7.67 (d, J = 7.7 Hz, 4H), 7.60 (s, 2H), 7.25 (d, J = 7.6 Hz, 5H), 4.20 (t, J = 6.6 Hz, 4H), 2.42 (s, 6H), 1.96 (p, J = 6.9 Hz, 4H), 1.58 (m, 4H), 1.42 (m, 8H), 1.01 – 0.92 (m, 6H); ^{13}C NMR (101 MHz, CDCl_3) δ 149.0, 142.1, 138.0, 134.8, 131.8, 129.8, 129.5, 126.2, 122.8, 117.6, 106.8, 69.4, 31.8, 29.5, 26.0, 22.8, 21.4, 14.2; HRMS (APCI+) calcd for $\text{C}_{40}\text{H}_{45}\text{O}_2\text{S}_2$ (M+H)⁺ 621.286099, found 621.28751 (2.27 ppm).

5,6-bis(hexyloxy)-2,9-di(4-methoxyphenyl)naphtho[2,1-*b*:3,4-*b'*]dithiophene, **$\alpha(\text{OHex})(\text{PhOMe})_2$**

A 50 mL Schlenk tube was charged with **$\alpha(\text{OHex})\text{Br}_2$** (0.512 mmol), *p*-methoxyphenylboronic acid (1.429 mmol), $\text{Pd}(\text{PPh}_3)_2\text{Cl}_2$ (0.102 mmol), and a stir bar. The reaction tube was backfilled with argon (3x), after which 5 mL dry THF and 1 mL degassed 2M K_2CO_3 solution were added under positive pressure of argon. The reaction tube was sealed under argon and stirred in an oil bath at 80 °C overnight. The reaction was cooled to RT, poured into H_2O (15 mL), extracted with EtOAc (2x50 mL), washed with brine (2x50 mL), dried over anhydrous Na_2SO_4 , decanted, and concentrated to yield crude product. Purification was achieved via silica gel flash column Hexanes:EtOAc (9:1) followed by recrystallisation from hexanes to afford **$\alpha(\text{OHex})(\text{PhOMe})_2$** as a pale yellow solid (R_f 0.49), 98 mg (29%): ^1H NMR (400 MHz, CDCl_3) δ 7.84 (s, 2H), 7.69 (d, J = 8.1 Hz, 4H), 7.60 (s, 2H), 6.97 (d, J = 8.1 Hz, 4H), 4.20 (t, J = 6.6 Hz, 4H), 3.87 (s, 6H), 2.00 – 1.90 (m, 4H), 1.59 (m, 4H), 1.42 (m, 8H), 0.96 (m, 6H); ^{13}C NMR (101 MHz, CDCl_3) δ 159.7, 148.9, 141.7, 134.7, 127.5, 127.4, 122.8, 117.0, 114.5, 106.8, 69.4, 55.5, 31.8, 29.5, 26.0, 22.8, 14.2; HRMS (APCI+) calcd for $\text{C}_{40}\text{H}_{45}\text{O}_4\text{S}_2$ (M+H)⁺ 653.275929, found 653.27712 (1.82 ppm).

5,6-bis(hexyloxy)-2,9-di(4-trifluoromethylphenyl)naphtho[2,1-*b*:3,4-*b'*]dithiophene, **$\alpha(\text{OHex})(\text{PhCF}_3)_2$**

A 100 mL Schlenk tube was charged with **$\alpha(\text{OHex})\text{Br}_2$** (0.231 mmol), *p*-(trifluoromethyl)phenylboronic acid (0.636 mmol), $\text{Pd}(\text{PPh}_3)_2\text{Cl}_2$ (0.049 mmol), and a stir bar. The reaction tube was backfilled with argon (3x), after which 4 mL dry THF and 0.50 mL degassed 2M K_2CO_3 solution were added under positive pressure of argon. The reaction tube was sealed under argon and stirred in an oil bath at 80 °C overnight. The reaction was cooled to RT, poured into H_2O (15 mL), extracted with EtOAc (2x50 mL), washed with brine (2x50 mL), dried over anhydrous Na_2SO_4 , decanted, and concentrated to yield crude product. Purification was achieved via silica gel flash column Hexanes:Toluene (9:1) followed by recrystallisation from toluene to afford **$\alpha(\text{OHex})(\text{PhCF}_3)_2$** as a bright yellow solid (R_f 0.19), 70 mg (42%):

^1H NMR (400 MHz, CDCl_3) δ 8.15 (s, 2H), 7.92 (d, $J = 8.1$ Hz, 4H), 7.72 (d, $J = 7.8$ Hz, 6H), 4.25 (t, $J = 6.6$ Hz, 4H), 1.97 (p, $J = 6.8$ Hz, 4H), 1.64 – 1.57 (m, 4H), 1.47 – 1.35 (m, 8H), 0.98 – 0.91 (m, 6H); Due to poor solubility, only ^{13}C signals obtained from ^1H - ^{13}C HSQC were obtained. ^{13}C NMR (101 MHz, CDCl_3) δ 126.3, 119.8, 106.6, 69.5, 31.8, 29.2, 25.7, 22.8, 14.1; HRMS (APCI+) calcd for $\text{C}_{40}\text{H}_{39}\text{F}_6\text{O}_2\text{S}_2$ ($\text{M}+\text{H}$) $^+$ 729.229567, found 729.23127 (2.33 ppm).

Synthesis of $\alpha(\text{OMe})\text{R}_2$ Series

1,2-dibromo-4,5-dimethoxybenzene, **1(OMe)**

Veratrole (39 mmol), $\text{AcOH}/\text{CHCl}_3$ (36 mL:36 mL), and stir bar were combined in a 250 mL round bottom flask. The reaction flask was placed under argon for 5 minutes after which NBS (87.60 mmol) was added in portions. After complete addition of NBS reaction was left under static argon to stir overnight. The reaction was quenched with aqueous Na_2SO_3 , extracted with DCM (3x30 mL), washed with brine (2x30 mL), dried over anhydrous Na_2SO_4 , decanted, and concentrated to yield crude product. Recrystallisation from ethanol affords **1(OMe)** as colorless crystals, 6.34 g (37%). Spectral details match literature values.⁴

1,2-di(3-thienyl)-4,5-dimethoxybenzene, **2(OMe)**

A 100 mL Schlenk tube was charged with **1(OMe)** (6.79 mmol), 3-thiophene boronic acid (17.65 mmol), $\text{Pd}(\text{PPh}_3)_2\text{Cl}_2$ (1.09 mmol), and a stir bar, then was backfilled with argon (3x). Under positive pressure of argon dry THF (27 mL) and degassed 2M K_2CO_3 (14 mL) were added and the tube was sealed. The reaction was placed into an oil bath and stirred at 80 °C overnight. The next day, the reaction was cool to RT and poured into H_2O (25 mL), extracted with EtOAc (2x50 mL), washed with brine (2x50 mL), dried over anhydrous Na_2SO_4 , decanted, and concentrated to yield crude product. Purification was achieved through silica gel flash column with Hexanes:EtOAc (9:1) as mobile phase to afford **2(OMe)** as a colorless oil (R_f 0.40), 1.36 g (66%). Spectral details match literature values.⁴

5,6-bis(methoxy)naphtho[2,1-*b*:3,4-*b'*]dithiophene, $\alpha(\text{OMe})$

A 500 mL round bottom flask was charged with **2(OMe)** (3.40 mmol) and a stir bar, then was sparged with argon for 10 minutes. After 10 minutes dry DCM (136 mL) was added and the reaction flask was equipped with a pressure equalising funnel. The reaction flask was then cooled to 0 °C and equilibrated for 15 minutes under argon. FeCl_3 (7.92 mmol) was massed into a beaker and dissolved in MeNO_2 (32 mL), then added to the pressure equalising funnel. The $\text{FeCl}_3/\text{MeNO}_2$ solution was added dropwise over five minutes to the reaction flask, after which the ice bath was removed and the reaction was allowed to come to RT over an hour. The reaction was quenched with MeOH (10x MeNO_2) and concentrated. The crude reaction was resuspended in DCM (50 mL) and H_2O (50 mL), extracted with DCM (2x50 mL), washed with brine (2x50 mL), dried over anhydrous Na_2SO_4 , decanted, and concentrated to yield crude product. Purification was achieved through silica gel flash column Hexanes:DCM (4:1) to afford pure $\alpha(\text{OMe})$ as a pale yellow solid (R_f 0.28), 564 mg (55%). Spectral details match literature values.⁴

2,9-dibromo-5,6-bis(methoxy)naphtho[2,1-*b*:3,4-*b'*]dithiophene, $\alpha(\text{OMe})\text{Br}_2$

$\alpha(\text{OMe})$ (2.96 mmol) was massed into a 250 mL round bottom flask. A stir bar and CHCl_3 (34 mL) were added, followed by vigorous stirring under argon (5 minutes). After equilibration NBS (7.69 mmol) was added in portions over 5 minutes. Upon complete addition of NBS the reaction was left to stir for 48 hours. After 48 hours the reaction was poured into H_2O (100 mL), extracted with DCM (2x50 mL), washed with brine (2x50 mL), dried over anhydrous Na_2SO_4 , decanted, and concentrated to yield crude product as a yellow solid. Crude product was dissolved in 15 mL CHCl_3 then poured into MeOH (4x volume of CHCl_3), yielding pure $\alpha(\text{OMe})\text{Br}_2$ as pale-yellow precipitate (1.04 g, 77%). Spectral details match literature values.⁵

5,6-bis(methoxy)-2,9-diphenylnaphtho[2,1-*b*:3,4-*b'*]dithiophene, $\alpha(\text{OMe})\text{Ph}_2$

A 25 mL Schlenk tube was charged with $\alpha(\text{OMe})\text{Br}_2$ (0.549 mmol), phenylboronic acid (1.41 mmol), $\text{Pd}(\text{PPh}_3)_2\text{Cl}_2$ (0.083 mmol), and a stir bar. The reaction tube was backfilled with argon (3x), after which 4 mL dry THF and 1 mL degassed 2M K_2CO_3 solution were added under positive pressure of argon. The reaction tube was sealed under argon and stirred in an oil bath at 80 °C overnight. The reaction was cooled to RT, poured into H_2O (15 mL), extracted with EtOAc (2x50 mL), washed with brine (2x50 mL), dried over anhydrous Na_2SO_4 , decanted, and concentrated to yield crude product. Purification was achieved via silica gel flash column Toluene:EtOAc (49:1) to afford $\alpha(\text{OMe})\text{Ph}_2$ as a pale yellow solid (R_f 0.29), 109 mg (55%). Single crystals suitable for x-ray diffraction were obtained from vapor diffusion of hexanes into a solution of $\alpha(\text{OMe})\text{Ph}_2$ in THF, yielding yellow crystals. ^1H NMR (400 MHz, CDCl_3) δ 7.95 (s, 1H), 7.79 (d, $J = 7.4$ Hz, 4H), 7.56 (s, 2H), 7.46 (t, $J = 7.6$ Hz, 4H), 7.36 (t, $J = 7.4$ Hz, 2H), 4.09 (s, 6H); ^{13}C NMR (101 MHz, CDCl_3) δ 148.9, 142.1, 134.8, 134.5, 129.9, 129.2, 128.1, 126.3, 122.7, 118.1, 104.7, 77.5, 77.2, 76.8, 56.2; HRMS (APCI+) calcd for $\text{C}_{28}\text{H}_{21}\text{O}_4\text{S}_2$ ($\text{M}+\text{H}$) $^+$ 453.098299, found 453.09829 (-0.01 ppm).

5,6-bis(methoxy)-2,9-di-*p*-tolyl naphtho[2,1-*b*:3,4-*b'*]dithiophene, ***a*(OMe)Tol₂**

A 25 mL Schlenk tube was charged with ***a*(OMe)Br₂** (0.557 mmol), *p*-methylphenylboronic acid (1.489 mmol), Pd(PPh₃)₂Cl₂ (0.084 mmol), and a stir bar. The reaction tube was backfilled with argon (3x), after which 4 mL dry THF and 0.85 mL degassed 2M K₂CO₃ solution were added under positive pressure of argon. The reaction tube was sealed under argon and stirred in an oil bath at 80 °C overnight. The reaction was cooled to RT, poured into H₂O (15 mL), extracted with EtOAc (2x50 mL), washed with brine (2x50 mL), dried over anhydrous Na₂SO₄, decanted, and concentrated to yield crude product. Purification was achieved via silica gel flash column Toluene:EtOAc (49:1) to afford ***a*(OMe)Tol₂** as a pale yellow solid (R_f 0.32), 170 mg (63%). Single crystals suitable for x-ray diffraction were obtained from vapor diffusion of hexanes into a solution of ***a*(OMe)Tol₂** in THF, resulting in pale yellow crystals. ¹H NMR (400 MHz, CDCl₃) δ 7.96 (s, 2H), 7.69 (d, *J* = 7.8 Hz, 4H), 7.61 (s, 2H), 7.31 – 7.17 (m, 4H), 4.11 (s, 6H), 2.42 (s, 6H); ¹³C NMR (101 MHz, CDCl₃) δ 148.9, 142.3, 138.1, 134.7, 131.7, 129.8, 129.7, 126.2, 122.7, 117.5, 104.8, 56.2, 21.4; HRMS (APCI+) calcd for C₃₀H₂₅O₄S₂ (M+H)⁺ 481.129599, found 481.13060 (2.08 ppm).

5,6-bis(methoxy)-2,9-di(4-methoxyphenyl)naphtho[2,1-*b*:3,4-*b'*]dithiophene, ***a*(OMe)(PhOMe)₂**

A 25 mL Schlenk tube was charged with ***a*(OMe)Br₂** (0.599 mmol), *p*-methoxyphenylboronic acid (1.589 mmol), Pd(PPh₃)₂Cl₂ (0.118 mmol), and a stir bar. The reaction tube was backfilled with argon (3x), after which 4 mL dry THF and 1.2 mL degassed 2M K₂CO₃ solution were added under positive pressure of argon. The reaction tube was sealed under argon and stirred in an oil bath at 80 °C overnight. The reaction was cooled to RT, poured into H₂O (15 mL), extracted with EtOAc (2x50 mL), washed with brine (2x50 mL), dried over anhydrous Na₂SO₄, decanted, and concentrated to yield crude product. Purification was achieved via silica gel flash column Toluene:EtOAc (49:1) to afford ***a*(OMe)(PhOMe)₂** as a pale yellow solid (R_f 0.16), 123 mg (40%). Vapor diffusion of hexanes into a solution of ***a*(OMe)(PhOMe)₂** in THF resulted in pale yellow crystals suitable for single crystal X-ray diffraction. ¹H NMR (400 MHz, CDCl₃) δ 7.91 (s, 2H), 7.73 (d, *J* = 8.6 Hz, 4H), 7.63 (s, 2H), 6.99 (d, *J* = 8.6 Hz, 4H), 4.11 (s, 6H), 3.88 (s, 6H); ¹³C NMR (101 MHz, CDCl₃) δ 159.8, 148.9, 142.0, 134.7, 129.5, 127.7, 127.3, 122.7, 117.0, 114.6, 104.8, 56.2, 55.6; HRMS (APCI+) calcd for C₃₀H₂₅O₄S₂ (M+H)⁺ 513.119429, found 513.12001 (1.13 ppm).

5,6-bis(methoxy)-2,9-di(4-trifluoromethylphenyl)naphtho[2,1-*b*:3,4-*b'*]dithiophene, ***a*(OMe)(PhCF₃)₂**

A 25 mL Schlenk tube was charged with ***a*(OMe)Br₂** (0.531 mmol), *p*-(trifluoromethyl)phenylboronic acid (1.333 mmol), Pd(PPh₃)₂Cl₂ (0.096 mmol), and a stir bar. The reaction tube was backfilled with argon (3x), after which 4 mL dry THF and 0.50 mL degassed 2M K₂CO₃ solution were added under positive pressure of argon. The reaction tube was sealed under argon and stirred in an oil bath at 80 °C overnight. The reaction was cooled to RT, poured into H₂O (15 mL), extracted with EtOAc (2x50 mL), washed with brine (2x50 mL), dried over anhydrous Na₂SO₄, decanted, and concentrated to yield crude product. Purification was achieved via silica gel flash column Toluene:EtOAc (49:1) to afford ***a*(OMe)(PhCF₃)₂** as a bright yellow solid (R_f 0.34), 240 mg (77%). Vapor diffusion of toluene into a solution of ***a*(OMe)(PhCF₃)₂** in THF resulted in yellowish-green crystals suitable for single crystal X-ray diffraction. ¹H NMR (400 MHz, CDCl₃) δ 8.18 (s, 2H), 7.92 (d, *J* = 8.0 Hz, 4H), 7.72 (d, *J* = 8.6 Hz, 4H), 7.71 (s, 2H), 4.15 (s, 6H); Due to poor solubility, only ¹³C signals obtained from ¹H-¹³C HSQC were obtained. ¹³C NMR (101 MHz, CDCl₃) δ 126.2, 119.4, 104.6, 56.2; HRMS (APCI+) calcd for C₃₀H₁₉F₆O₂S₂ (M+H)⁺ 589.073067, found 589.07387 (1.36 ppm).

Synthesis of ***β*(*Oi*-Pent)*R*₂ Series**

1,2-dibromo-4,5-di-isopentyloxybenzene, **1(*Oi*-Pent)**

4,5-dibromocatechol (18.75 mmol) was massed into a 250 mL round bottom flask and dissolved in 2-butanone (100 mL). A stir bar was added, followed by K₂CO₃ (57.89 mmol) and a reflux condenser. Reaction was flushed with argon for 5 minutes, then isopentyl bromide (41.31 mmol) was added in one portion. Reaction temperature was then raised to 80 °C and allowed to stir for 24 hours. After 24 hours the reaction flask was cooled to RT and poured into H₂O (50 mL), extracted with EtOAc (2x50 mL), washed with brine (2x50 mL), dried over anhydrous Na₂SO₄, decanted, and concentrated to yield crude product. Purification via silica gel flash column with Hexanes:EtOAc (99:1) as mobile phase afforded 1,2-dibromo-4,5-di-isopentyloxybenzene (**1(*Oi*-Pent)**) as a colorless oil (R_f 0.53), 6.40 g (84%). Spectral details match literature values.⁶ ¹H NMR (400 MHz, CDCl₃) δ 7.07 (s, 2H), 3.97 (t, *J* = 6.7 Hz, 4H), 1.83 (dp, *J* = 13.3, 6.9 Hz, 2H), 1.69 (q, *J* = 6.8 Hz, 4H), 0.96 (d, *J* = 6.6 Hz, 12H).

1,2-di(2-thienyl)-4,5-di-isopentyloxybenzene, **3(*Oi*-Pent)**

A 100 mL Schlenk tube was charged with **1(*Oi*-Pent)** (6.19 mmol), 2-thiophene boronic acid (18.64 mmol), and Pd(PPh₃)₂Cl₂ (0.95 mmol), and a stir bar added. Under positive pressure of argon dry THF (30 mL) and degassed 2M

K₂CO₃ (7.5 mL) were added and the tube was sealed. The reaction was placed into an oil bath and stirred at 80 °C overnight. The next day, the reaction was cooled to RT and poured into H₂O (25 mL), extracted with EtOAc (2x50 mL), washed with brine (2x50 mL), dried over anhydrous Na₂SO₄, decanted, and concentrated to yield crude product. Purification was achieved through silica gel flash column with Hexane:EtOAc (99:1) followed by trituration with cold ethanol to afford 1,2-di(2-thienyl)-4,5-di-isopentyloxybenzene (**3(Oi-Pent)**) as a white solid (R_f 0.19), 2.34 g (91%): ¹H NMR (400 MHz, CDCl₃) δ 7.23 (dd, *J* = 5.2, 1.2 Hz, 2H), 7.00 (s, 2H), 6.94 (dd, *J* = 5.1, 3.5 Hz, 2H), 6.85 (dd, *J* = 3.5, 1.2 Hz, 2H), 4.07 (t, *J* = 6.7 Hz, 4H), 1.87 (dp, *J* = 13.3, 6.7 Hz, 2H), 1.74 (q, *J* = 6.7 Hz, 4H), 0.98 (d, *J* = 6.7 Hz, 12H); ¹³C NMR (101 MHz, CDCl₃) δ 148.6, 142.9, 126.8, 126.7, 126.3, 125.4, 116.1, 67.8, 37.9, 25.2, 22.6; HRMS (APCI+) calcd for C₂₄H₃₁O₂S₂ (M+H)⁺ 415.176549, found 415.17750 (2.29 ppm).

1,2-di(2-(5-bromothieryl)-4,5-di-isopentyloxybenzene, **4(Oi-Pent)**

3(Oi-Pent) (3.56 mmol) was massed into a 100 mL round bottom flask. A stir bar and CHCl₃ (60 mL) were added, followed by vigorous stirring under argon (5 minutes). After equilibration NBS (9.70 mmol) was added in portions over 5 minutes. Upon complete addition of NBS the reaction was left to stir for 3 days. After 3 days the reaction was poured into H₂O (100 mL), extracted with DCM (2x50 mL), washed with brine (2x50 mL), dried over anhydrous Na₂SO₄, decanted, and concentrated to yield crude product as a pale-yellow solid. Purification was achieved through silica gel flash column Hexanes:EtOAc (99:1) followed by recrystallization from ethanol to afford pure 1,2-di(2-(5-bromothieryl)-4,5-di-isopentyloxybenzene (**4(Oi-Pent)**) as an off-white solid (R_f 0.31), 1.50 g (74%): ¹H NMR (400 MHz, CDCl₃) δ 6.92 – 6.90 (m, 4H), 6.62 (d, *J* = 3.8 Hz, 2H), 4.05 (t, *J* = 6.6 Hz, 4H), 1.85 (dq, *J* = 13.3, 6.7 Hz, 2H), 1.73 (q, *J* = 6.7 Hz, 4H), 0.98 (d, *J* = 6.6 Hz, 12H); ¹³C NMR (101 MHz, CDCl₃) δ 149.0, 144.0, 129.8, 127.1, 125.3, 115.8, 112.0, 67.8, 37.9, 25.1, 22.6; HRMS (APCI+) calcd for C₂₄H₂₉Br₂O₂S₂ (M+H)⁺ 570.997571, found 570.99892 (2.36 ppm).

2,5-dibromo-8,9-bis(isopentyloxy)naphtho[1,2-*b*:4,3-*b'*]dithiophene, **β(Oi-Pent)Br₂**

A 100 mL Schlenk tube was charged with **5** (1.10 mmol) and a stir bar, then placed under argon atmosphere. Under positive pressure of argon dry DCM (100 mL) was added, then the reaction was cooled to 0 °C and equilibrated for 10 minutes. After 10 minutes MeSO₃H (11 mL) was added and the reaction was stirred 5 additional minutes. DDQ (1.69 mmol) was added to the reaction in one portion and left to stir for 30 minutes at 0 °C. After 30 minutes the reaction was quenched with an aqueous solution of sodium bicarbonate slowly, and then allowed to come to RT. The reaction mixture poured into a separatory funnel and was extracted with DCM (2x50 mL), washed with brine (2x50 mL), dried over anhydrous Na₂SO₄, decanted, and concentrated to yield crude product. Purification was achieved through silica gel flash column with Hexanes:Toluene (4:1) to afford pure **β(Oi-Pent)Br₂** as an off-white solid (R_f 0.58), 269 mg (44%): ¹H NMR (400 MHz, CDCl₃) δ 7.49 (s, 2H), 7.11 (s, 2H), 4.16 (t, *J* = 6.7 Hz, 4H), 1.93 (dt, *J* = 13.5, 6.7 Hz, 2H), 1.82 (q, *J* = 6.8 Hz, 4H), 1.03 (d, *J* = 6.5 Hz, 12H); ¹³C NMR (101 MHz, CDCl₃) δ 149.7, 135.7, 130.5, 125.6, 120.6, 112.4, 105.3, 67.6, 37.8, 25.3, 22.7; HRMS (APCI+) calcd for C₂₄H₂₇Br₂O₂S₂ (M+H)⁺ 568.98121, found 568.98322 (2.28 ppm).

8,9-bis(isopentyloxy)-2,5-diphenylnaphtho[1,2-*b*:4,3-*b'*]dithiophene, **β(Oi-Pent)Ph₂**

A 25 mL Schlenk tube was charged with **β(Oi-Pent)Br₂** (0.308 mmol), phenylboronic acid (1.077 mmol), Pd(PPh₃)₂Cl₂ (0.063 mmol), and a stir bar. The reaction tube was backfilled with argon (3x), after which 5 mL dry THF and 0.6 mL degassed 2M K₂CO₃ solution were added under positive pressure of argon. The reaction tube was sealed under argon and stirred in an oil bath at 80 °C overnight. The reaction was cooled to RT, poured into H₂O (15 mL), extracted with EtOAc (2x50 mL), washed with brine (2x50 mL), dried over anhydrous Na₂SO₄, decanted, and concentrated to yield crude product. Purification was achieved via silica gel flash column Hexanes:DCM (9:1) followed by recrystallisation from hexanes to afford **β(Oi-Pent)Ph₂** as an off-white solid (R_f 0.30), 102 mg (58%): ¹H NMR (400 MHz, CDCl₃) δ 7.95 (s, 2H), 7.82 (d, *J* = 7.7 Hz, 4H), 7.47 (t, *J* = 7.6 Hz, 4H), 7.42 (s, 2H), 7.36 (t, *J* = 7.4 Hz, 2H), 4.24 (t, *J* = 6.6 Hz, 4H), 1.95 (dq, *J* = 13.2, 6.7 Hz, 2H), 1.85 (q, *J* = 6.7 Hz, 4H), 1.05 (d, *J* = 6.5 Hz, 12H); ¹³C NMR (101 MHz, CDCl₃) δ 149.7, 142.6, 134.7, 134.5, 133.0, 129.2, 128.1, 126.4, 121.8, 118.8, 106.2, 67.9, 38.0, 25.5, 22.9; HRMS (APCI+) calcd for C₃₆H₃₇O₂S₂ (M+H)⁺ 565.223499, found 565.22502 (2.69 ppm).

8,9-bis(isopentyloxy)-2,5-di-*p*-tolyl naphtho[1,2-*b*:4,3-*b'*]dithiophene, **β(Oi-Pent)Tol₂**

A 25 mL Schlenk tube was charged with **β(Oi-Pent)Br₂** (0.271 mmol), *p*-methylphenylboronic acid (0.927 mmol), Pd(PPh₃)₂Cl₂ (0.083 mmol) and a stir bar. The reaction tube was backfilled with argon (3x), after which dry THF (5 mL) and degassed 2M K₂CO₃ (0.5 mL) were added under positive pressure of argon. The reaction tube was sealed under argon and stirred in an oil bath at 80 °C overnight. The reaction was cooled to RT, poured into H₂O (15 mL), extracted with EtOAc (2x50 mL), washed with brine (2x50 mL), dried over anhydrous Na₂SO₄, decanted, and concentrated to yield crude product. Purification was achieved via silica gel flash column with Hexanes:DCM (9:1) followed by recrystallisation from hexanes to afford **β(Oi-Pent)Tol₂** as an off-white solid (R_f 0.30), 66 mg (41%): ¹H NMR (400 MHz, CDCl₃) δ 7.87 (s, 2H), 7.70 (d, *J* = 8.1 Hz, 4H), 7.39 (s, 2H), 7.29 – 7.23 (m, 4H), 4.22 (t, *J* = 6.6 Hz, 4H), 2.42 (s, 6H), 1.95 (dp, *J* = 13.2, 6.6 Hz, 2H), 1.85 (q, *J* = 6.7 Hz, 4H), 1.04 (d, *J* = 6.6 Hz, 12H); ¹³C NMR (101 MHz, CDCl₃) δ 149.6,

142.7, 138.0, 134.1, 133.0, 131.9, 129.8, 126.2, 121.7, 118.2, 106.2, 67.8, 38.0, 25.5, 22.9, 21.4; HRMS (APCI+) calcd for C₃₈H₄₁O₂S₂ (M+H)⁺ 593.254799, found 593.25583 (1.73 ppm).

8,9-bis(isopentyloxy)-2,5-di(4-methoxyphenyl)naphtho[1,2-*b*:4,3-*b'*]dithiophene, **β(Oi-Pent)(PhOMe)₂**

A 50 mL Schlenk tube was charged with **β(Oi-Pent)Br₂** (0.360 mmol), *p*-methoxyphenylboronic acid (0.908 mmol), Pd(PPh₃)₂Cl₂ (0.064 mmol), and a stir bar. The reaction tube was backfilled with argon (3x), after which dry THF (2.8 mL) and degassed 2M K₂CO₃ (0.7 mL) were added under positive pressure of argon. The reaction tube was sealed under argon and stirred in an oil bath at 80 °C overnight. The reaction was cooled to RT, poured into H₂O (15 mL), extracted with EtOAc (2x50 mL), washed with brine (2x50 mL), dried over anhydrous Na₂SO₄, decanted, and concentrated to yield crude product. Purification was achieved via silica gel flash column with Hexanes:DCM (2:3) followed by recrystallisation from hexanes to afford **β(Oi-Pent)(PhOMe)₂** as an off-white solid (R_f 0.50), 104 mg (46%): ¹H NMR (400 MHz, CDCl₃) δ 7.81 (s, 2H), 7.74 (d, *J* = 8.7 Hz, 4H), 7.39 (s, 2H), 7.00 (d, *J* = 8.8 Hz, 4H), 4.23 (t, *J* = 6.6 Hz, 4H), 3.88 (s, 6H), 1.95 (dt, *J* = 13.2, 6.6 Hz, 2H), 1.84 (q, *J* = 6.7 Hz, 4H), 1.04 (d, *J* = 6.6 Hz, 12H); ¹³C NMR (101 MHz, CDCl₃) δ 159.7, 149.5, 142.5, 133.8, 133.1, 127.6, 127.5, 121.7, 117.7, 114.6, 106.2, 67.8, 55.6, 38.0, 25.5, 22.9; HRMS (APCI+) calcd for C₃₈H₄₁O₄S₂ (M+H)⁺ 625.244629, found 625.24608 (2.32 ppm).

8,9-bis(isopentyloxy)-2,5-di(4-trifluoromethylphenyl)naphtho[1,2-*b*:4,3-*b'*]dithiophene, **β(Oi-Pent)(PhCF₃)₂**

A 25 mL Schlenk tube was charged with **β(Oi-Pent)Br₂** (0.393 mmol), *p*-(trifluoromethyl)phenylboronic acid (1.146 mmol), Pd(PPh₃)₂Cl₂ (0.070 mmol), and a stir bar. The reaction tube was backfilled with argon (3x), after which dry THF (5 mL) and degassed 2M K₂CO₃ (0.8 mL) were added under positive pressure of argon. The reaction tube was sealed under argon and stirred in an oil bath at 80 °C overnight. The reaction was cooled to RT, poured into H₂O (15 mL), extracted with EtOAc (2x50 mL), washed with brine (2x50 mL), dried over anhydrous Na₂SO₄, decanted, and concentrated to yield crude product. Purification was achieved via silica gel flash column with Hexanes:Toluene (9:1) followed by recrystallisation from toluene to afford **β(Oi-Pent)(PhCF₃)₂** as an off-white solid (R_f 0.38), 145 mg (53%): ¹H NMR (400 MHz, CDCl₃) δ 7.98 (s, 2H), 7.89 (d, *J* = 8.1 Hz, 4H), 7.70 (d, *J* = 8.1 Hz, 4H), 7.38 (s, 2H), 4.22 (t, *J* = 6.6 Hz, 4H), 1.96 (dt, *J* = 13.2, 6.6 Hz, 2H), 1.85 (q, *J* = 6.6 Hz, 4H), 1.05 (d, *J* = 6.5 Hz, 12H); ¹³C NMR (101 MHz, CDCl₃) δ 150.0, 140.6, 137.8, 135.3, 132.6, 129.8, 129.5, 126.2, 126.1, 126.0, 122.8, 121.7, 120.0, 105.9, 67.7, 37.8, 25.3, 22.7; HRMS (APCI+) calcd for C₃₈H₃₅F₆O₂S₂ (M+H)⁺ 701.198267, found 701.20016 (2.69 ppm).

2,9-dibromo-5,6-bis(hexyloxy)naphtho[2,1-b:3,4-b']dithiophene, ***a*(OHex)Br₂**

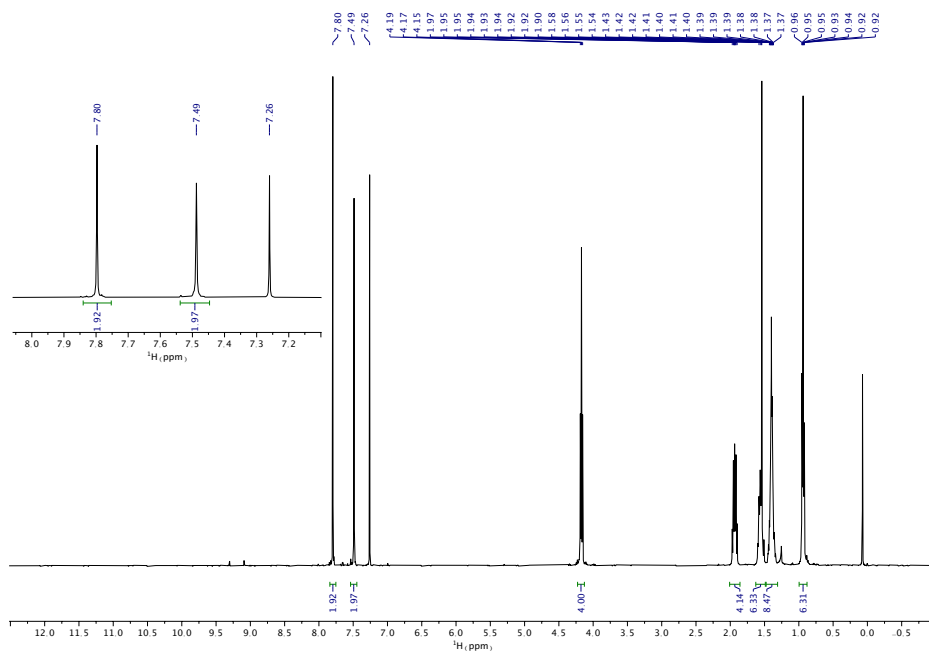


Figure 3. ¹H NMR spectrum of ***a*(OHex)Br₂** (CDCl₃, 400 MHz, 298 K).

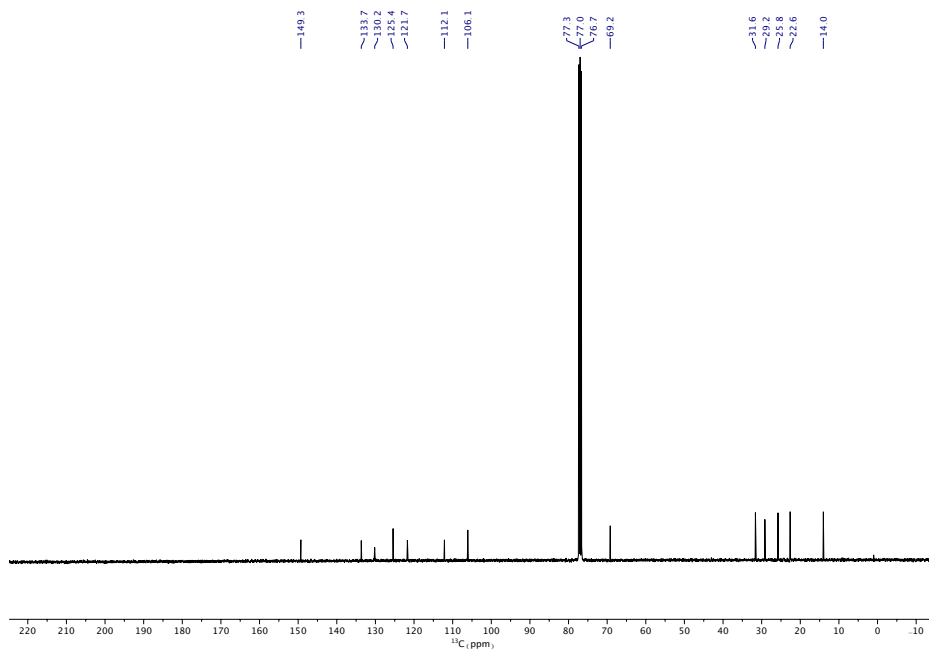


Figure 4. ¹³C{¹H} NMR spectrum of ***a*(OHex)Br₂** (CDCl₃, 101 MHz, 298 K).

5,6-bis(hexyloxy)-2,9-diphenylnaphtho[2,1-b:3,4-b']dithiophene, **a(OHex)Ph₂**

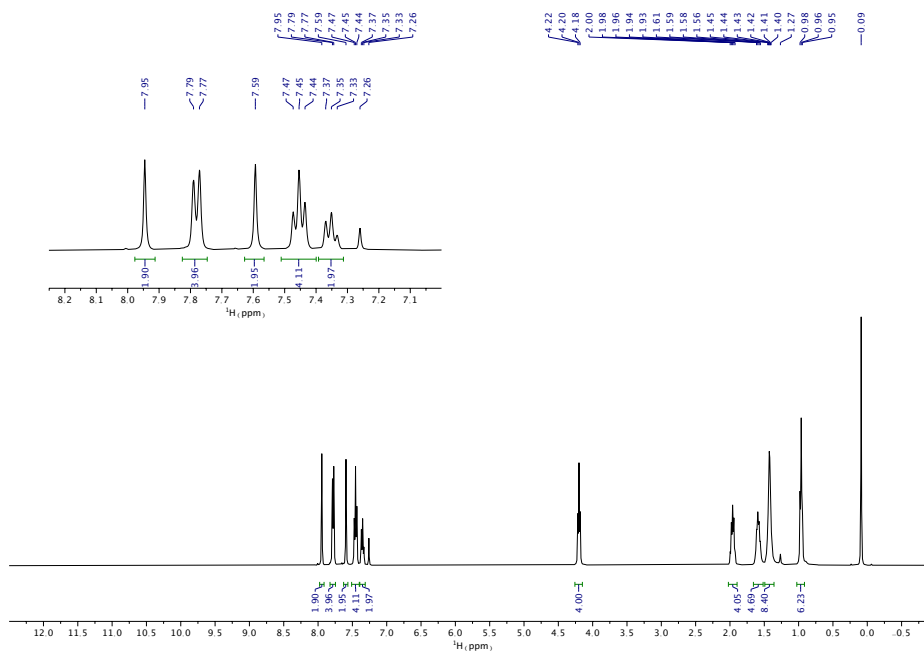


Figure 5. ¹H NMR spectrum of **a(OHex)Ph₂** (CDCl₃, 400 MHz, 298 K).

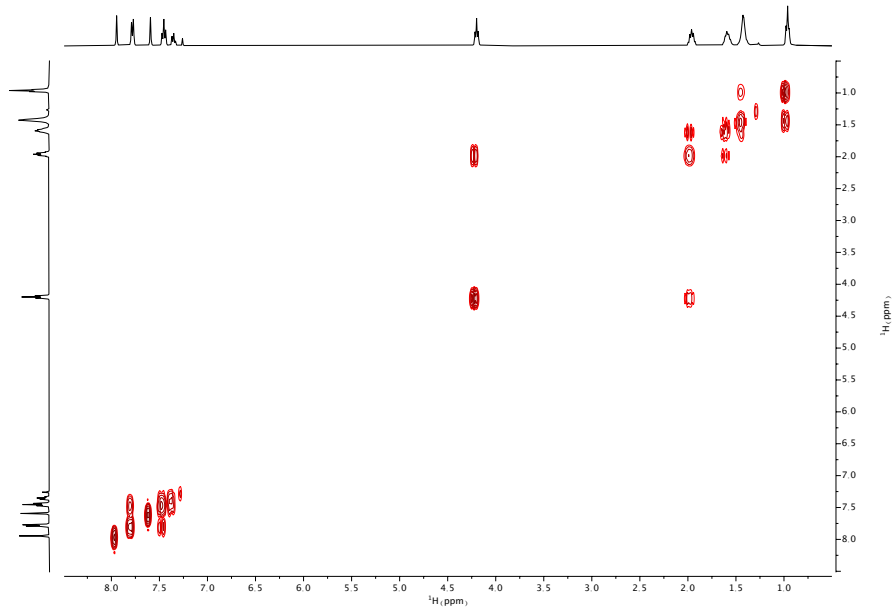


Figure 6. ¹H-¹H COSY spectrum of **a(OHex)Ph₂** (CDCl₃, 400 MHz, 298 K).

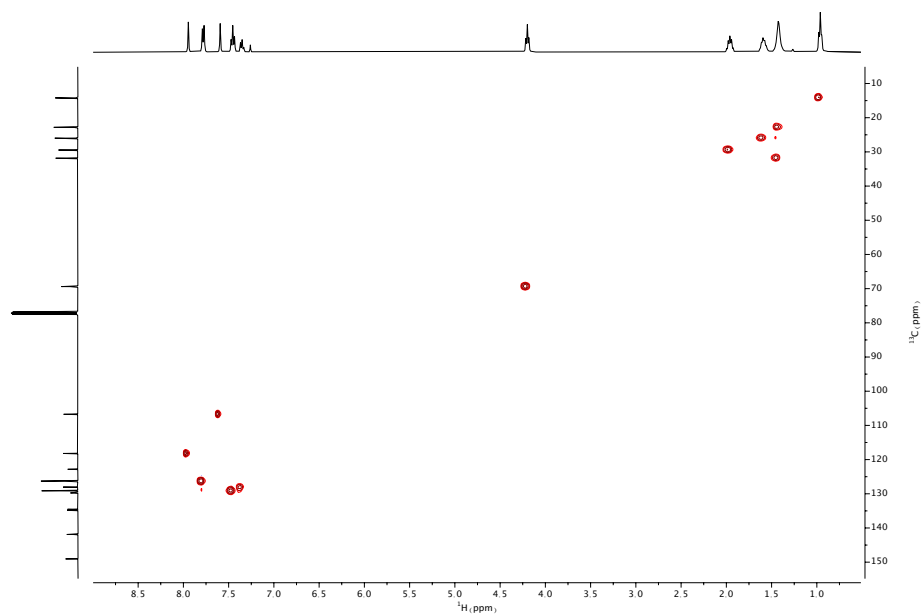


Figure 7. ^1H - ^{13}C HSQC spectrum of $\alpha(\text{OHex})\text{Ph}_2$ (CDCl_3 , 400 MHz, 298 K).

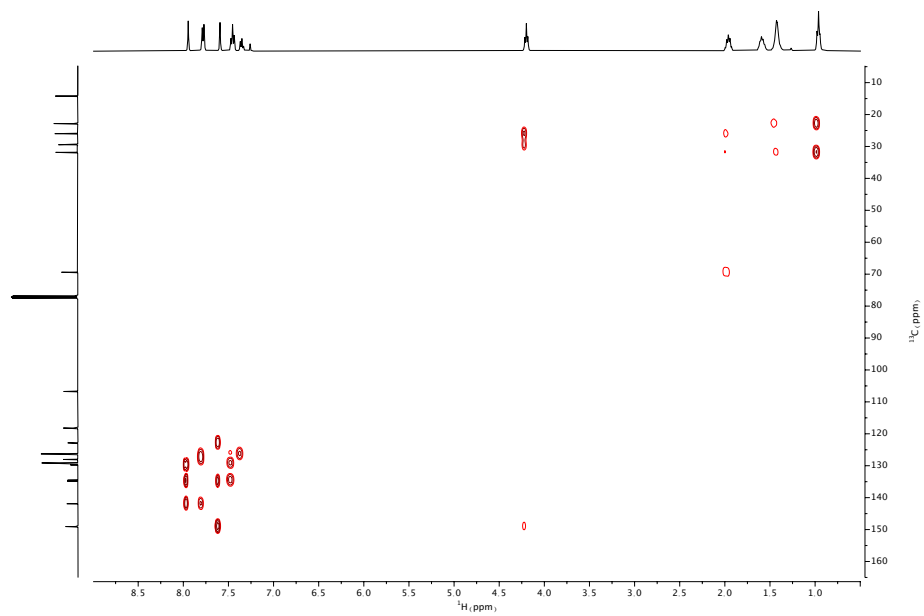


Figure 8. ^1H - ^{13}C HMBC spectrum of $\alpha(\text{OHex})\text{Ph}_2$ (CDCl_3 , 400 MHz, 298 K).

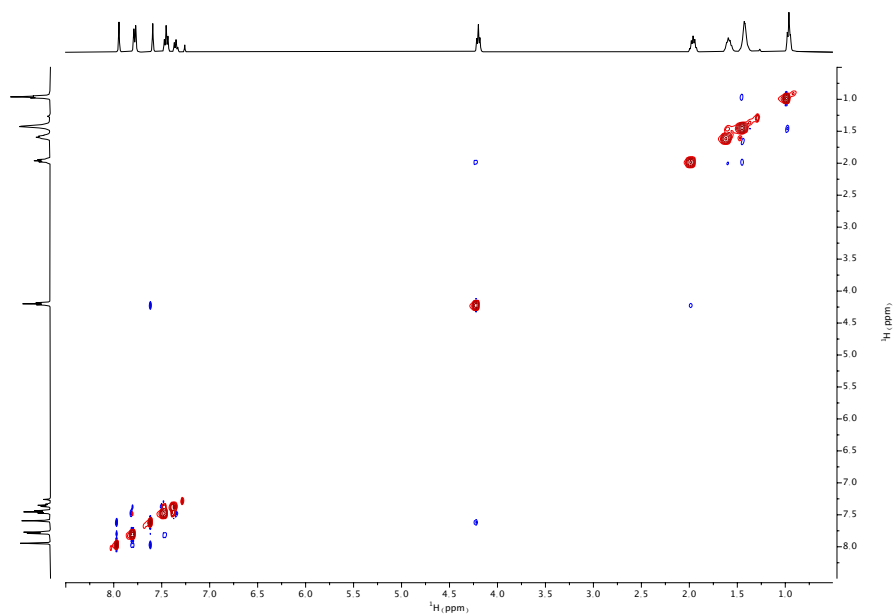


Figure 9. ^1H - ^1H NOESY spectrum of $\alpha(\text{OHex})\text{Ph}_2$ (CDCl_3 , 400 MHz, 298 K).

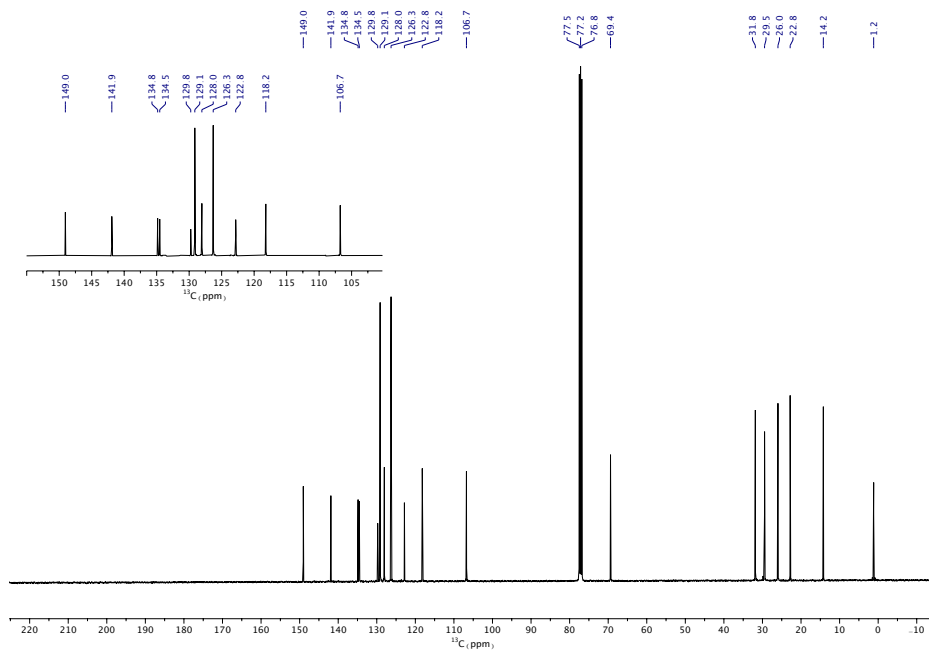


Figure 10. $^{13}\text{C}\{^1\text{H}\}$ NMR spectrum of $\alpha(\text{OHex})\text{Ph}_2$ (CDCl_3 , 101 MHz, 298 K).

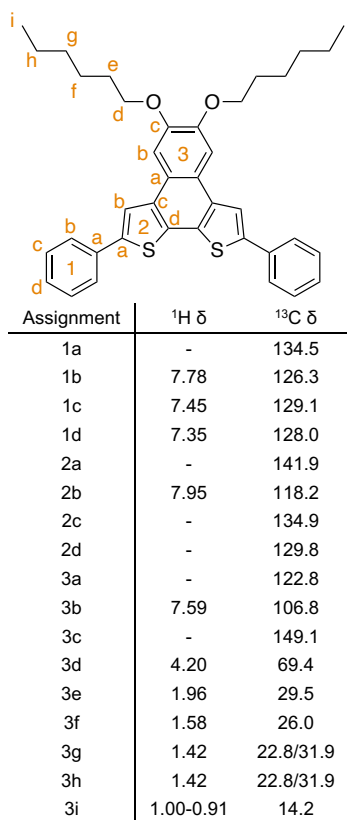


Figure 11. $\alpha(\text{OHex})\text{Ph}_2$ with assignment of ^1H and ^{13}C resonances.

5,6-bis(hexyloxy)-2,9-di-*p*-tolynaphtho[2,1-*b*:3,4-*b'*]dithiophene, $\alpha(\text{OHex})\text{ToI}_2$

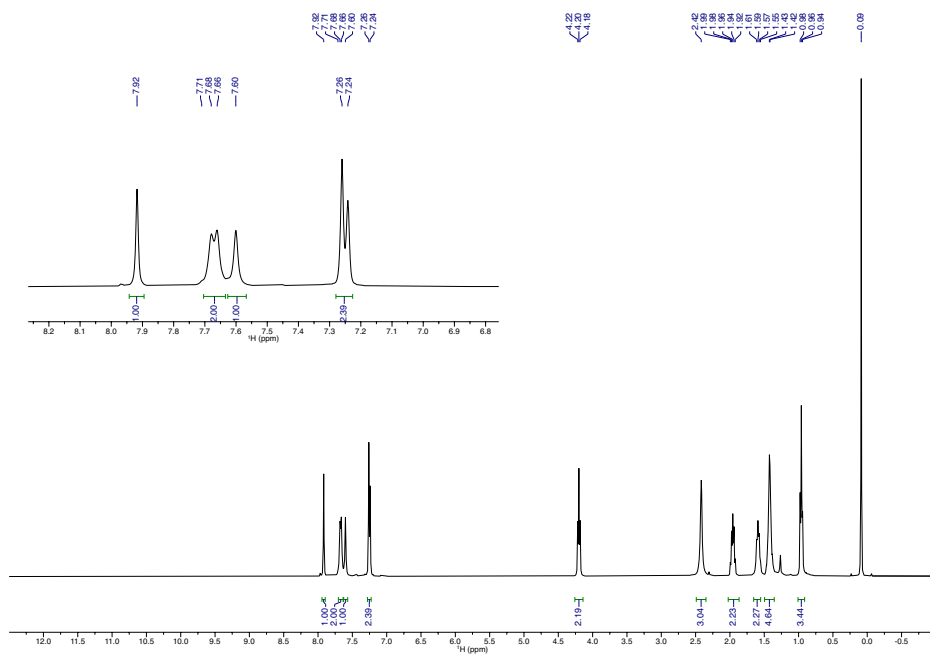


Figure 12. ^1H NMR spectrum of $\alpha(\text{OHex})\text{ToI}_2$ (CDCl_3 , 400 MHz, 298 K).

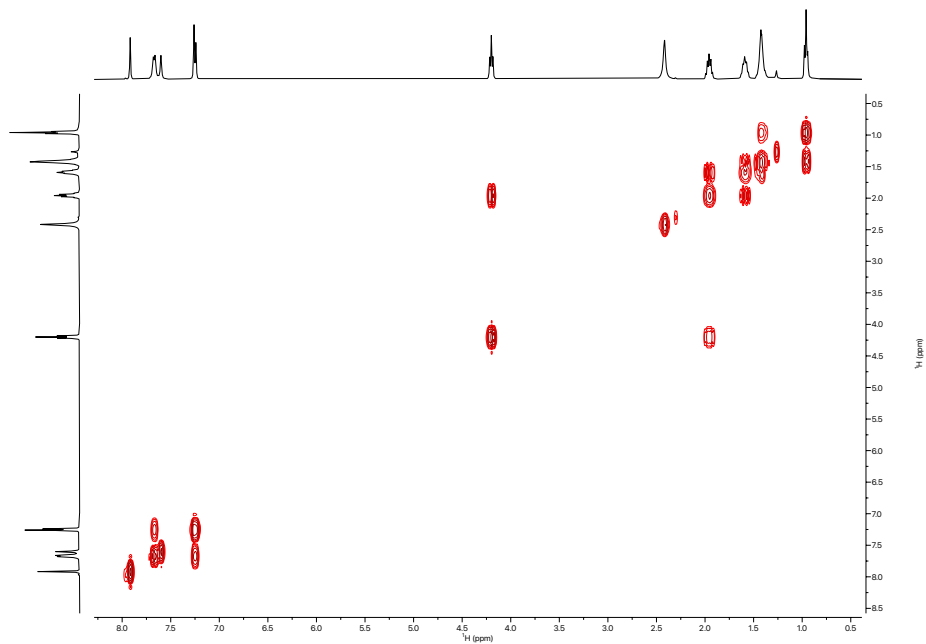


Figure 13. ^1H - ^1H COSY spectrum of $\alpha(\text{OHex})\text{Tol}_2$ (CDCl_3 , 400 MHz, 298 K).

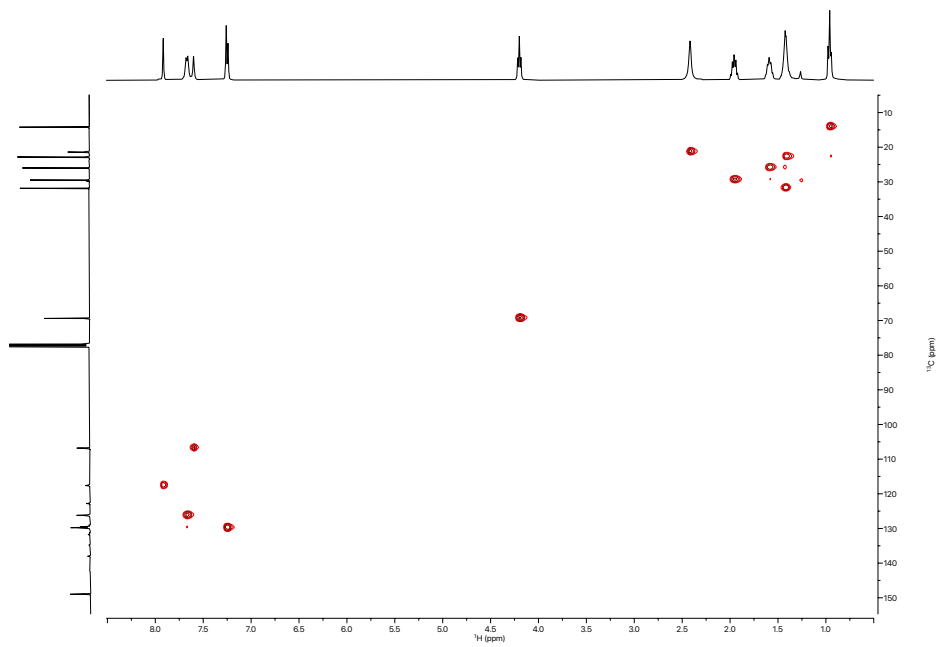


Figure 14. ^1H - ^{13}C HSQC spectrum of $\alpha(\text{OHex})\text{Tol}_2$ (CDCl_3 , 400 MHz, 298 K).

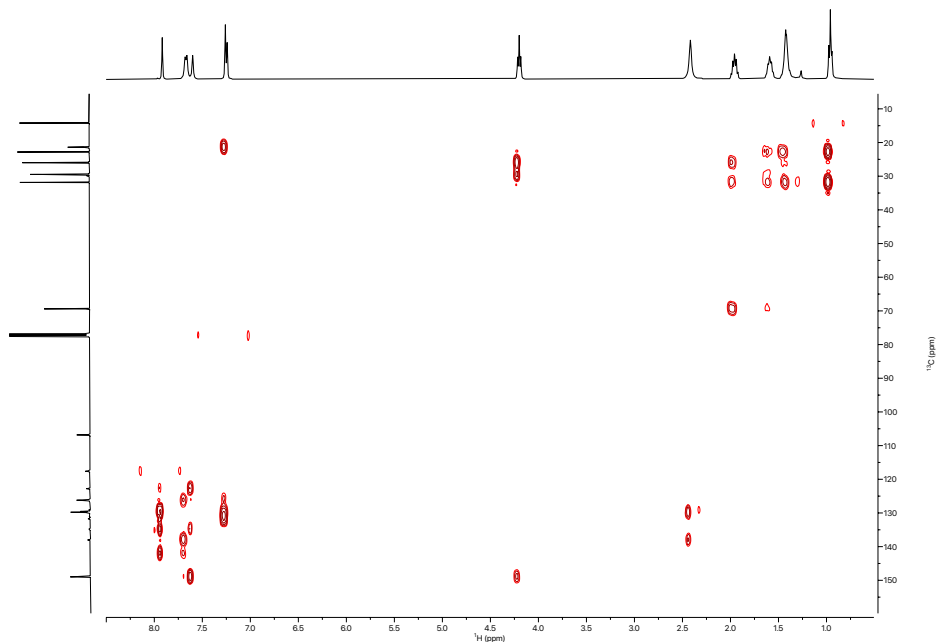


Figure 15. ^1H - ^{13}C HMBC spectrum of $\alpha(\text{OHex})\text{Tol}_2$ (CDCl_3 , 400 MHz, 298 K).

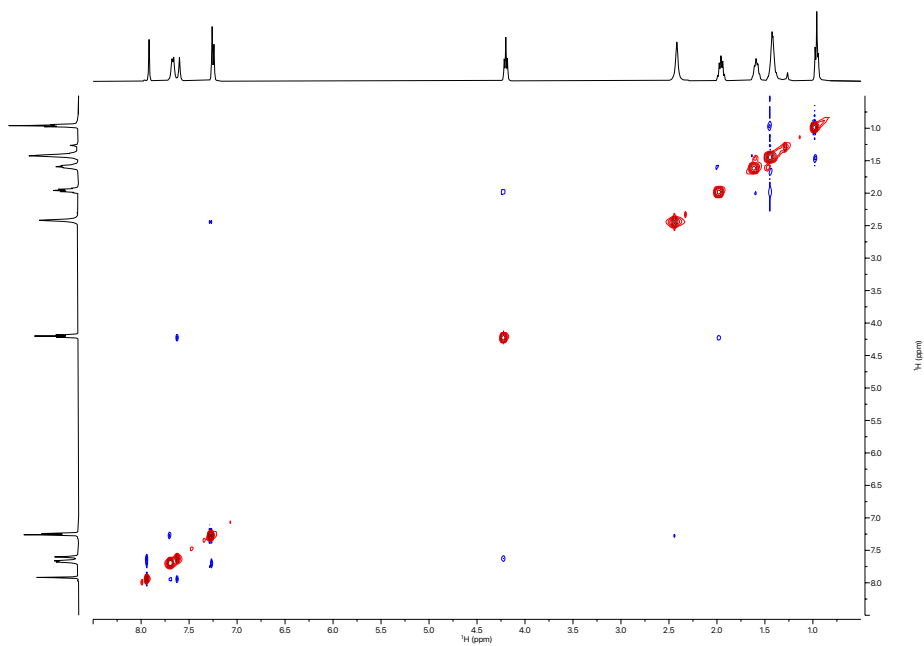


Figure 16. ^1H - ^1H NOESY spectrum of $\alpha(\text{OHex})\text{Tol}_2$ (CDCl_3 , 400 MHz, 298 K).

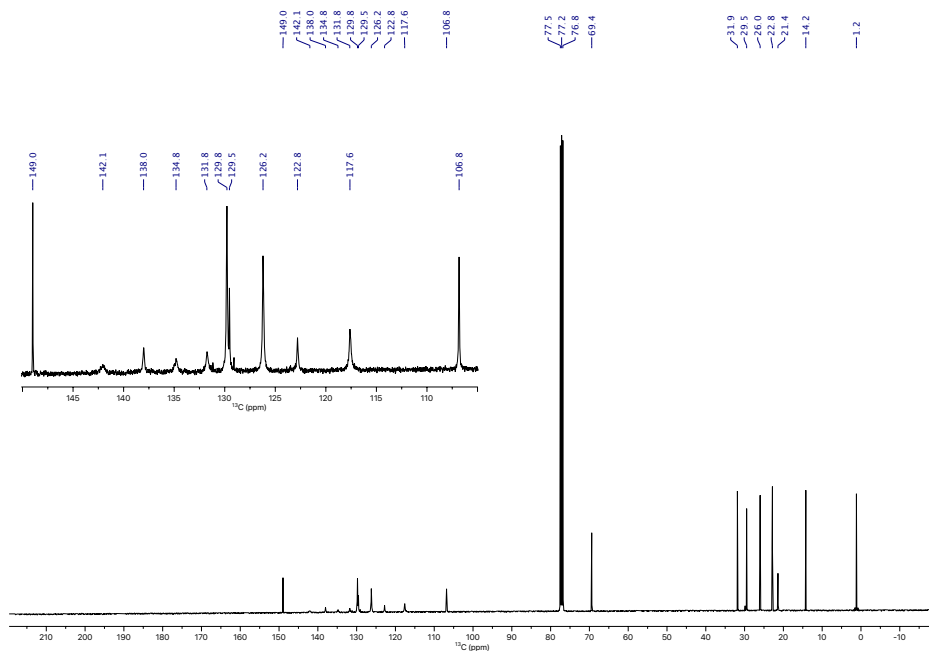


Figure 17. $^{13}\text{C}\{^1\text{H}\}$ NMR spectrum of $\alpha(\text{OHex})\text{ToI}_2$ (CDCl_3 , 101 MHz, 298 K).

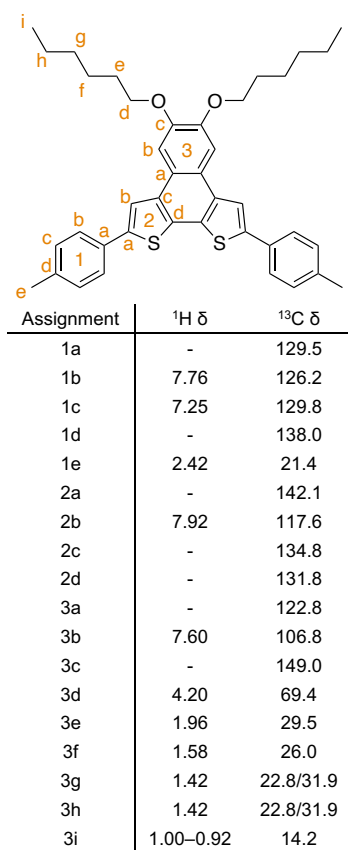


Figure 18. $\alpha(\text{OHex})\text{ToI}_2$ with assignment of ^1H and ^{13}C resonances.

5,6-bis(hexyloxy)-2,9-di(4-methoxyphenyl)naphtho[2,1-*b*:3,4-*b'*]dithiophene, $\alpha(\text{OHex})(\text{PhOMe})_2$

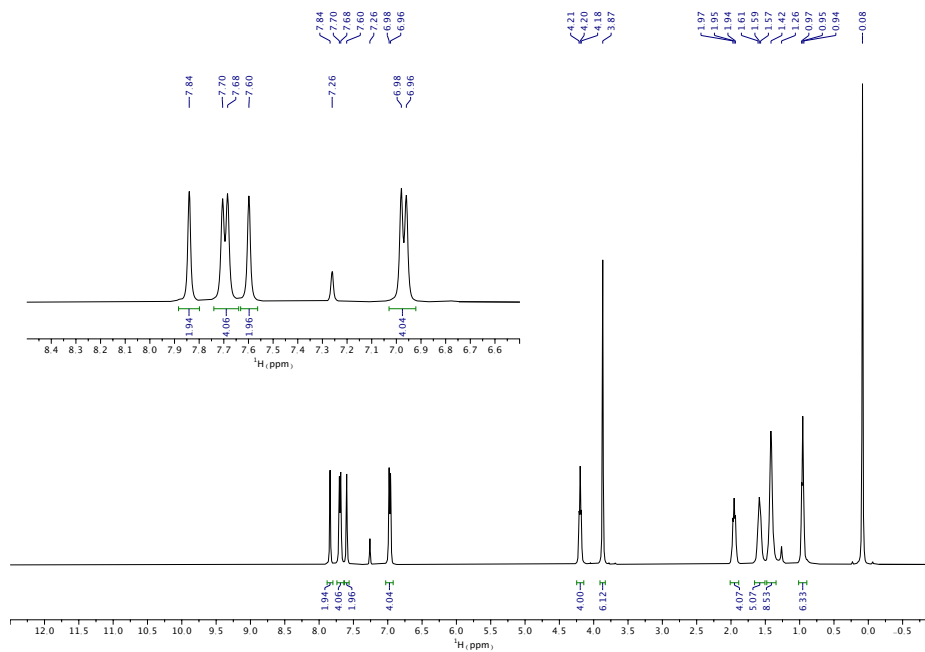


Figure 19. ^1H NMR spectrum of $\alpha(\text{OHex})(\text{PhOMe})_2$ (CDCl_3 , 400 MHz, 298 K).

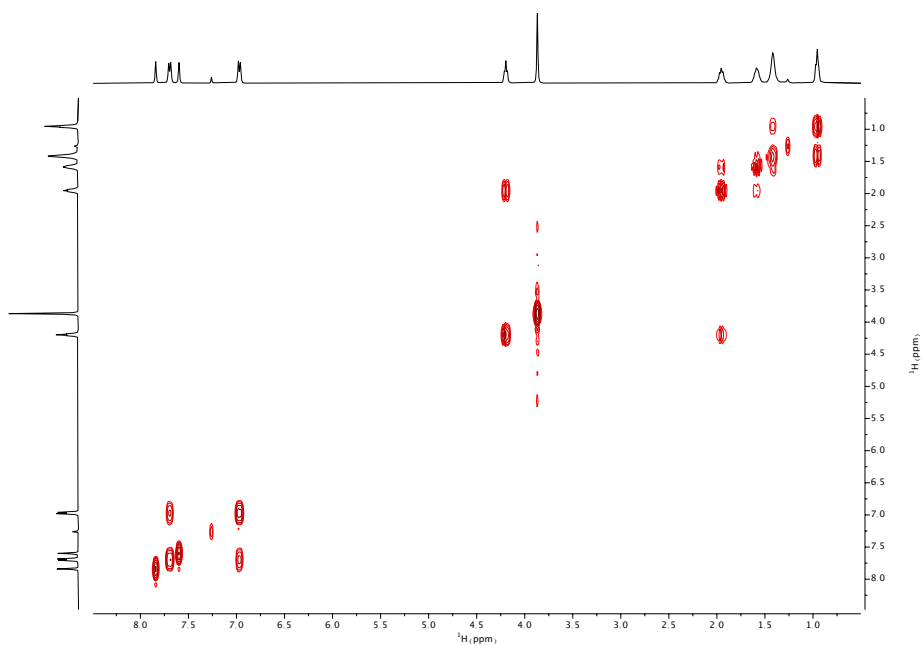


Figure 20. ^1H - ^1H COSY spectrum of $\alpha(\text{OHex})(\text{PhOMe})_2$ (CDCl_3 , 400 MHz, 298 K).

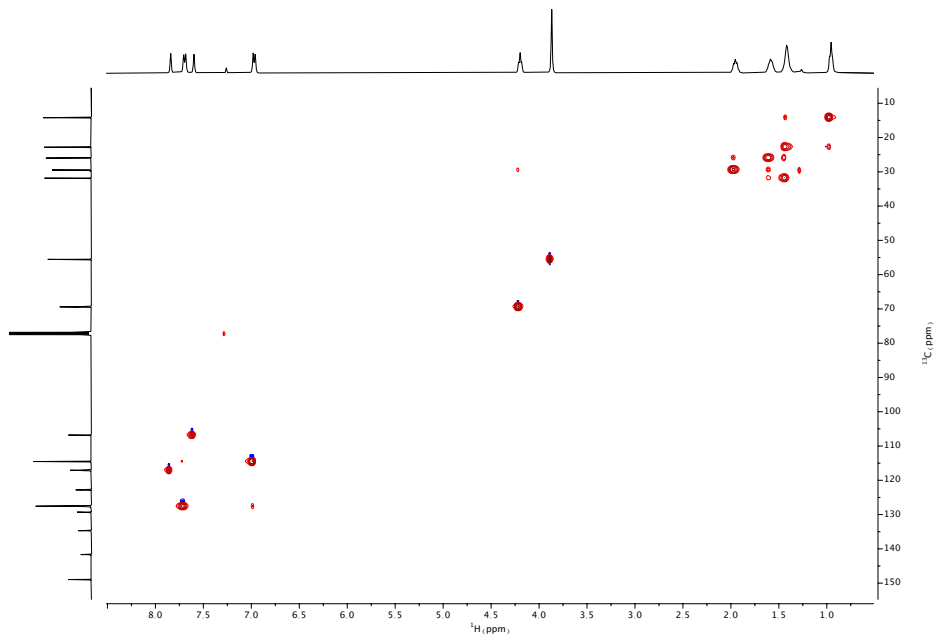


Figure 21. ^1H - ^{13}C HSQC spectrum of $\alpha(\text{OHex})(\text{PhOMe})_2$ (CDCl_3 , 400 MHz, 298 K).

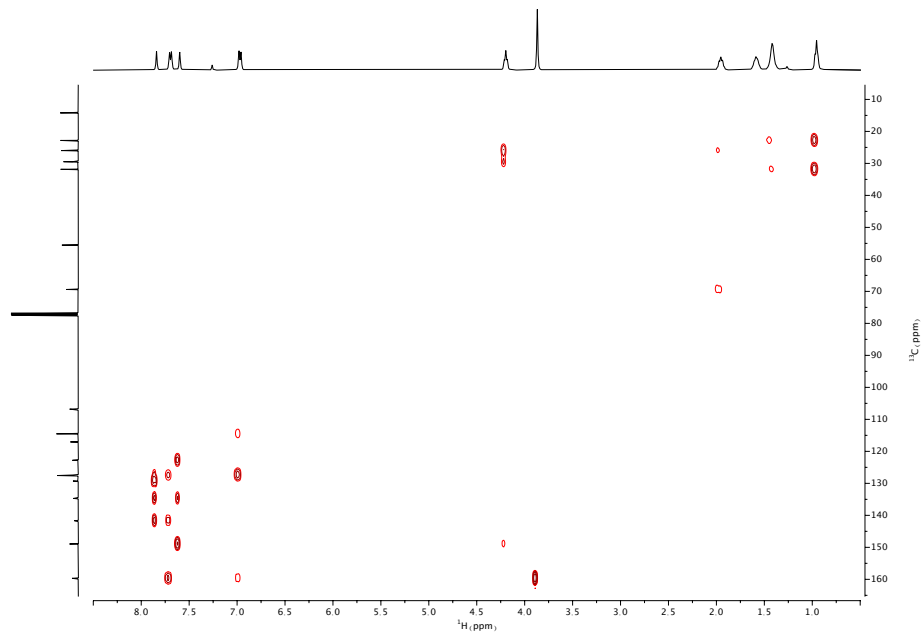


Figure 22. ^1H - ^{13}C HMBC spectrum of $\alpha(\text{OHex})(\text{PhOMe})_2$ (CDCl_3 , 400 MHz, 298 K).

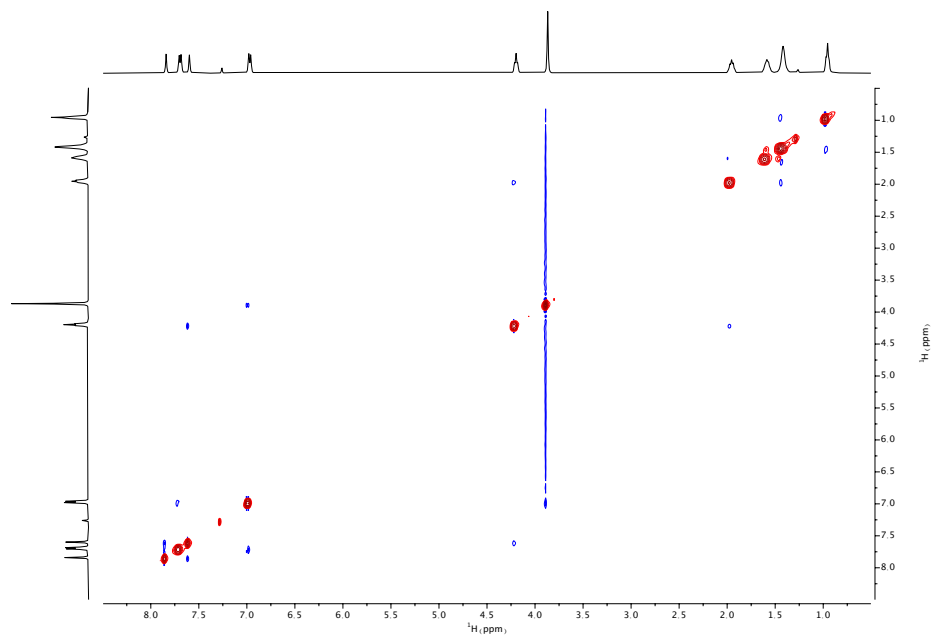


Figure 23. ^1H - ^1H NOESY spectrum of $\alpha(\text{OHex})(\text{PhOMe})_2$ (CDCl_3 , 400 MHz, 298 K).

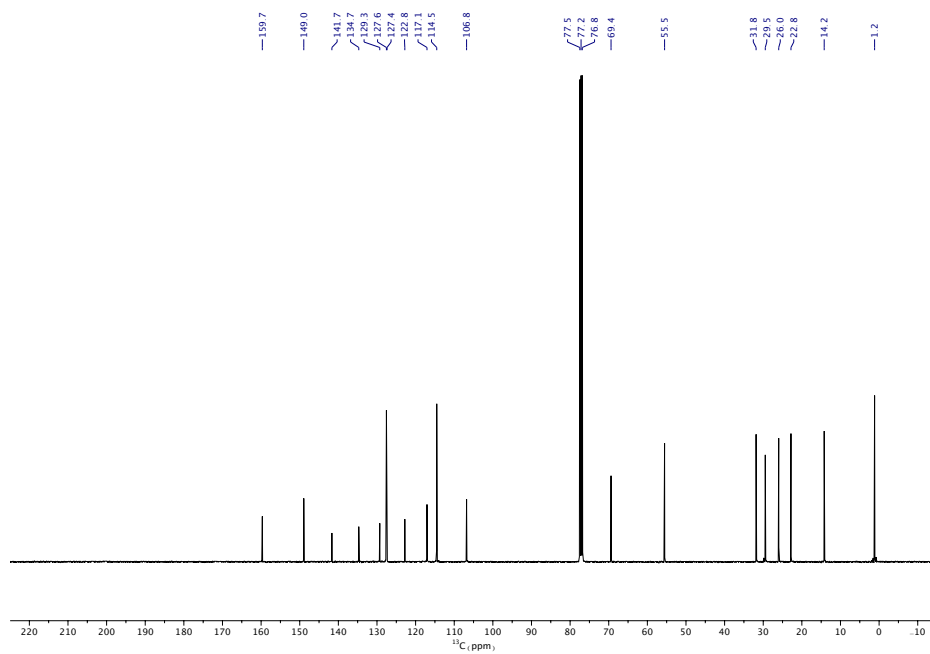


Figure 24. $^{13}\text{C}\{^1\text{H}\}$ NMR spectrum of $\alpha(\text{OHex})(\text{PhOMe})_2$ (CDCl_3 , 101 MHz, 298 K).

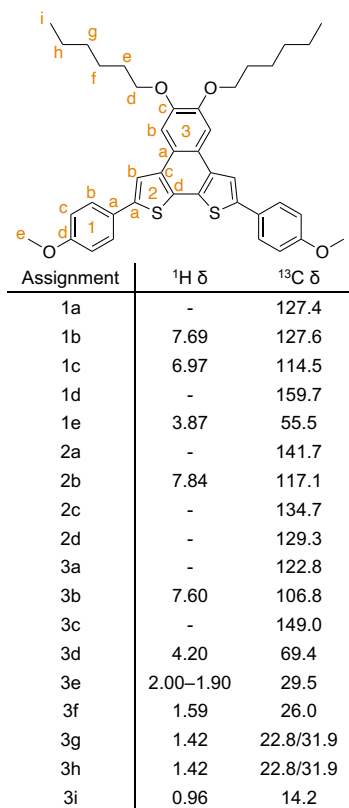


Figure 25. $\alpha(\text{OHex})(\text{PhOMe})_2$ with assignment of ¹H and ¹³C resonances.

5,6-bis(hexyloxy)-2,9-di(4-trifluoromethylphenyl)naphtho[2,1-*b*:3,4-*b'*]dithiophene, $\alpha(\text{OHex})(\text{PhCF}_3)_2$

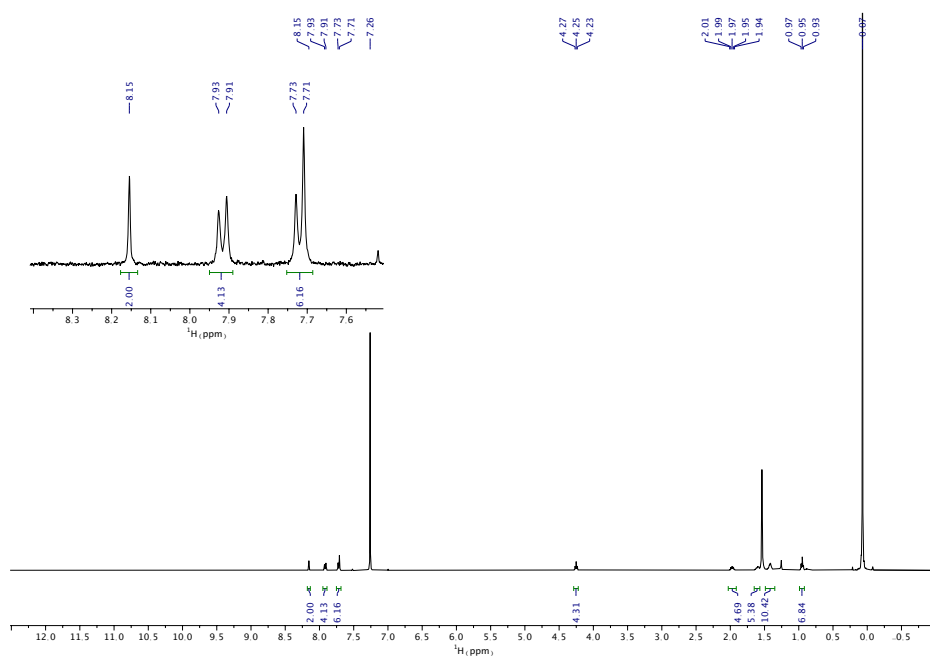


Figure 26. ¹H NMR spectrum of $\alpha(\text{OHex})(\text{PhCF}_3)_2$ (CDCl_3 , 400 MHz, 298 K).

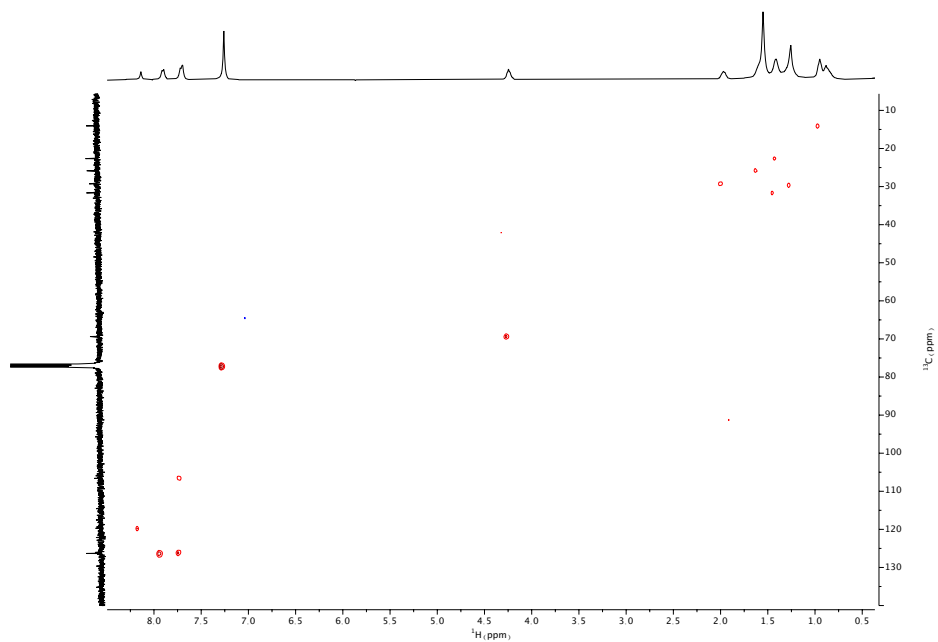


Figure 27. ^1H - ^{13}C HSQC spectrum of $\alpha(\text{OHex})(\text{PhCF}_3)_2$ (CDCl_3 , 400 MHz, 298 K).

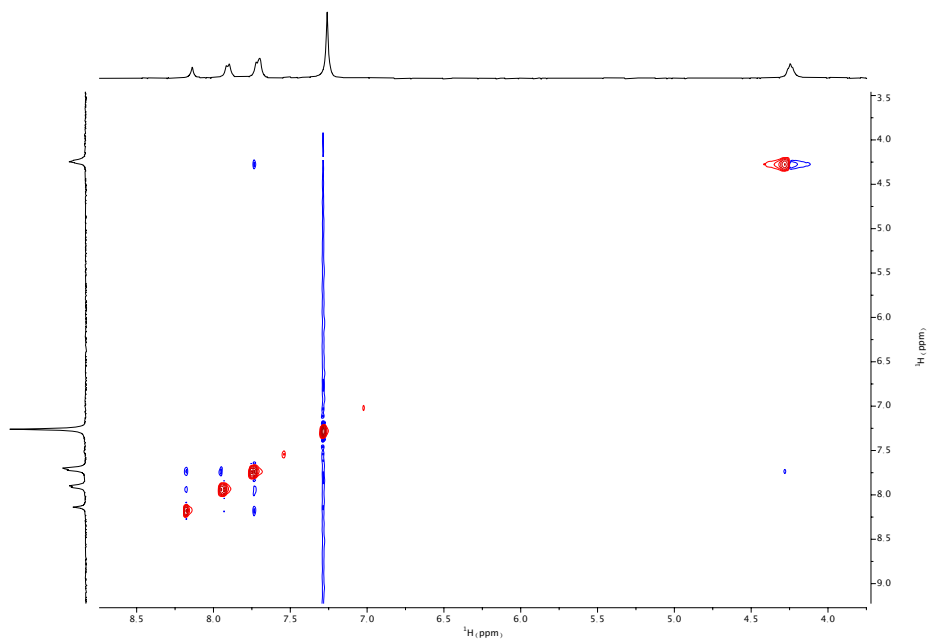


Figure 28. ^1H - ^1H NOESY spectrum of $\alpha(\text{OHex})(\text{PhCF}_3)_2$ (CDCl_3 , 400 MHz, 298 K).

| Assignment | $^1\text{H } \delta$ | $^{13}\text{C } \delta$ |
|------------|----------------------|-------------------------|
| 1a | - | - |
| 1b | 7.92 | 126.3 |
| 1c | 7.72 | 126.3 |
| 1d | - | - |
| 1e | - | - |
| 2a | - | - |
| 2b | 8.15 | 119.8 |
| 2c | - | - |
| 2d | - | - |
| 3a | - | - |
| 3b | 7.71 | 106.6 |
| 3c | - | - |
| 3d | 4.25 | 69.5 |
| 3e | 1.97 | 29.2 |
| 3f | 1.64–1.57 | 25.7 |
| 3g | 1.47–1.35 | 22.8/31.8 |
| 3h | 1.47–1.35 | 22.8/31.8 |
| 3i | 0.98–0.91 | 14.1 |

Figure 29. $\alpha(\text{OHex})(\text{PhCF}_3)_2$ with assignment of ^1H and ^{13}C resonances. ^{13}C resonances extracted from HSQC.

5,6-bis(methoxy)-2,9-diphenylnaphtho[2,1-*b*:3,4-*b'*]dithiophene, **a(OMe)Ph₂**

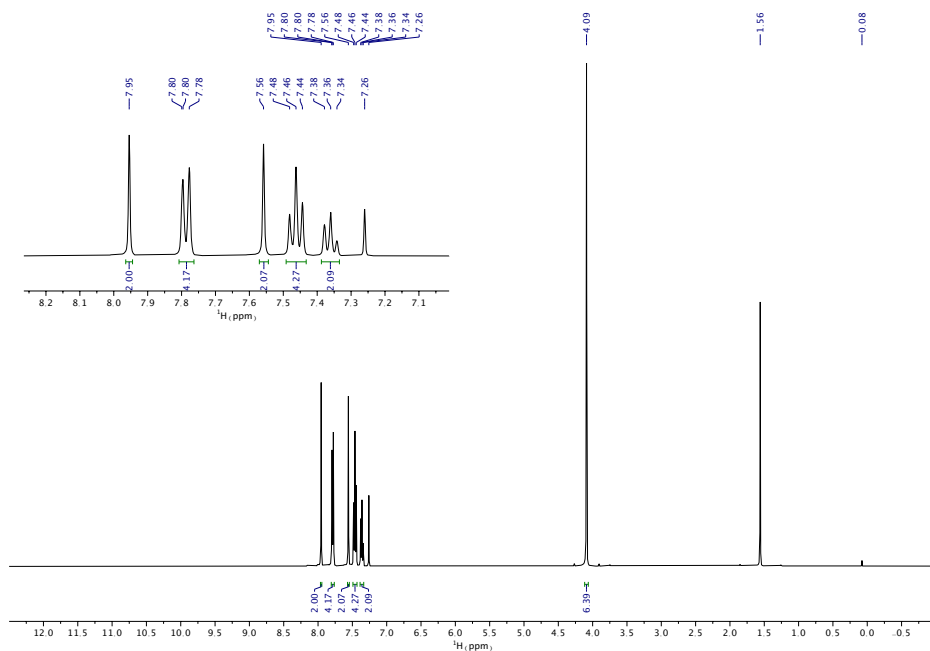


Figure 30. ¹H NMR spectrum of **a(OMe)Ph₂** (CDCl₃, 400 MHz, 298 K).

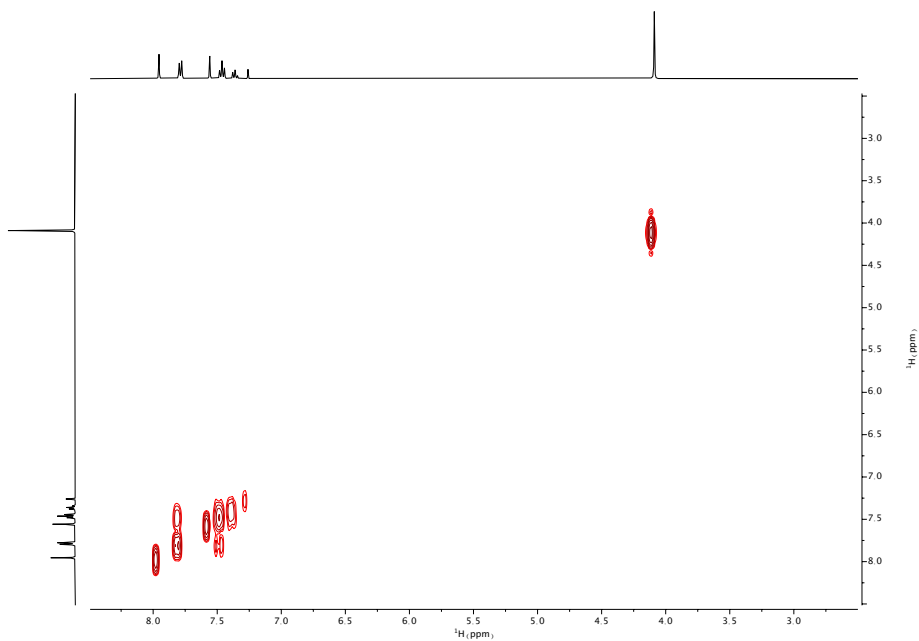


Figure 31. ¹H-¹H COSY spectrum of **a(OMe)Ph₂** (CDCl₃, 400 MHz, 298 K).

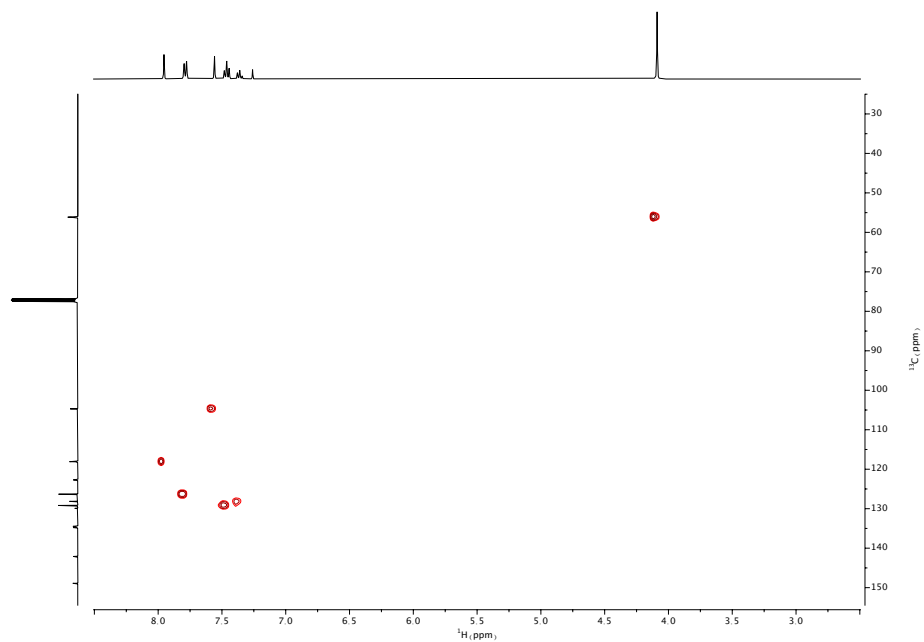


Figure 32. ^1H - ^{13}C HSQC spectrum of $\alpha(\text{OMe})\text{Ph}_2$ (CDCl_3 , 400 MHz, 298 K).

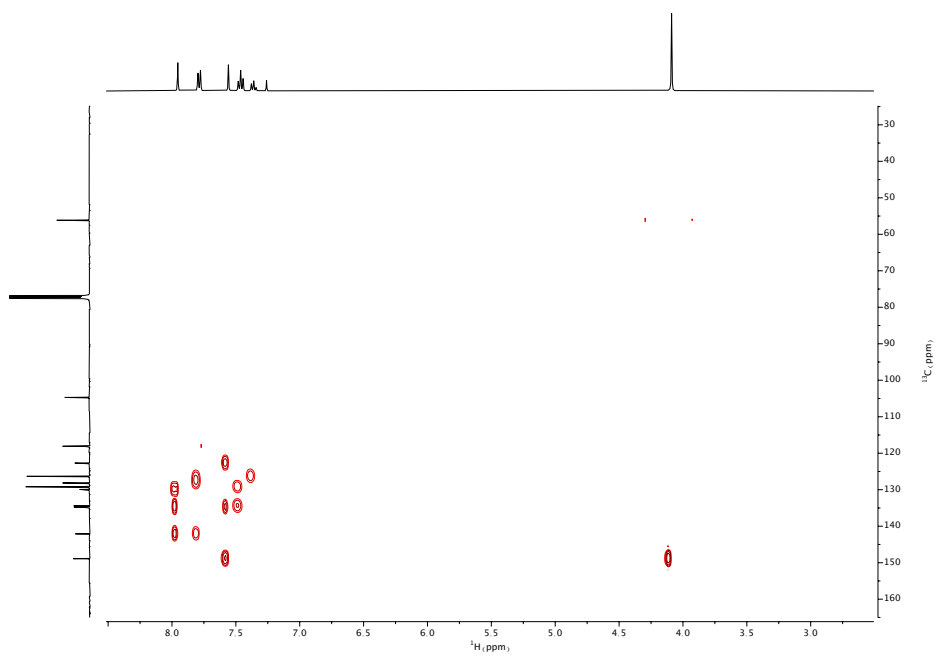


Figure 33. ^1H - ^{13}C HMBC spectrum of $\alpha(\text{OMe})\text{Ph}_2$ (CDCl_3 , 400 MHz, 298 K).

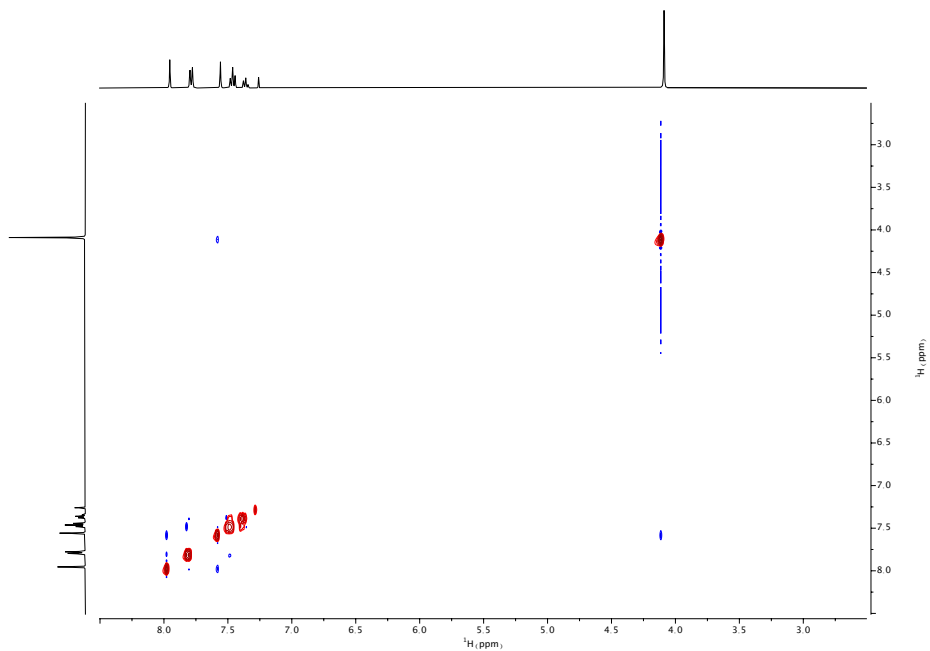


Figure 34. ^1H - ^1H NOESY spectrum of $\alpha(\text{OMe})\text{Ph}_2$ (CDCl_3 , 400 MHz, 298 K).

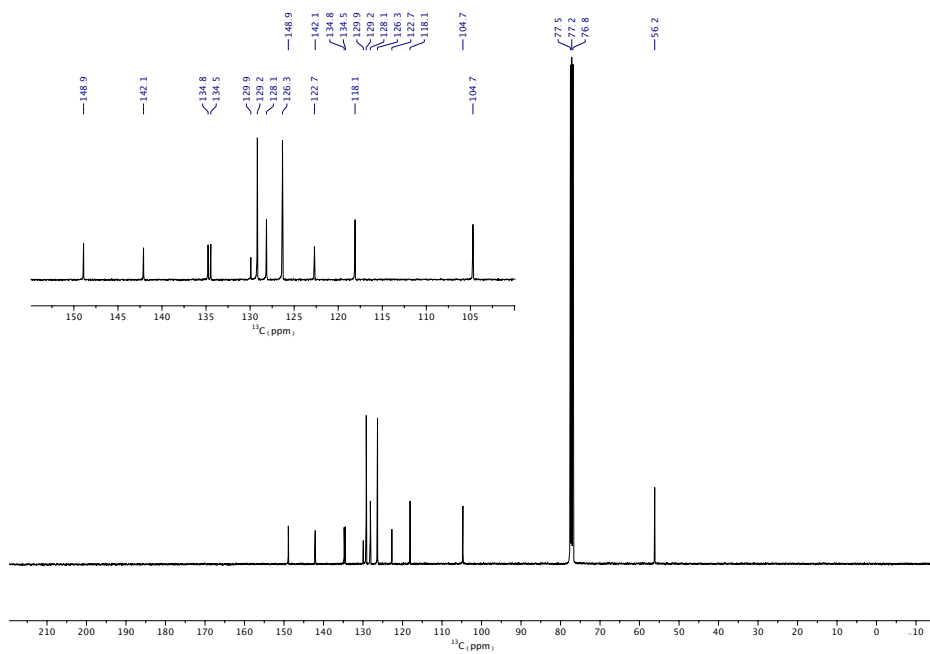


Figure 35. $^{13}\text{C}\{^1\text{H}\}$ NMR spectrum of $\alpha(\text{OMe})\text{Ph}_2$ (CDCl_3 , 101 MHz, 298 K).

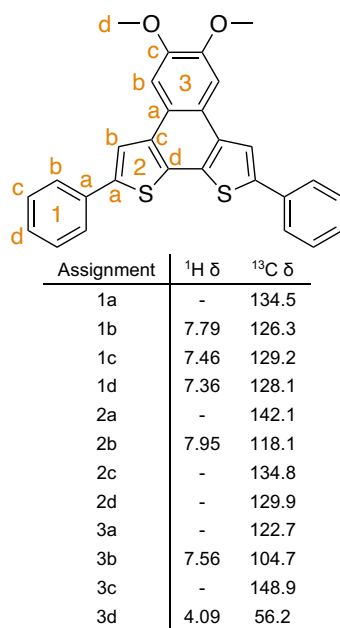


Figure 36. $\alpha(\text{OMe})\text{Ph}_2$ with assignment of ^1H and ^{13}C resonances.

5,6-bis(methoxy)-2,9-di-*p*-tolynaphtho[2,1-*b*:3,4-*b'*]dithiophene, $\alpha(\text{OMe})\text{ToI}_2$

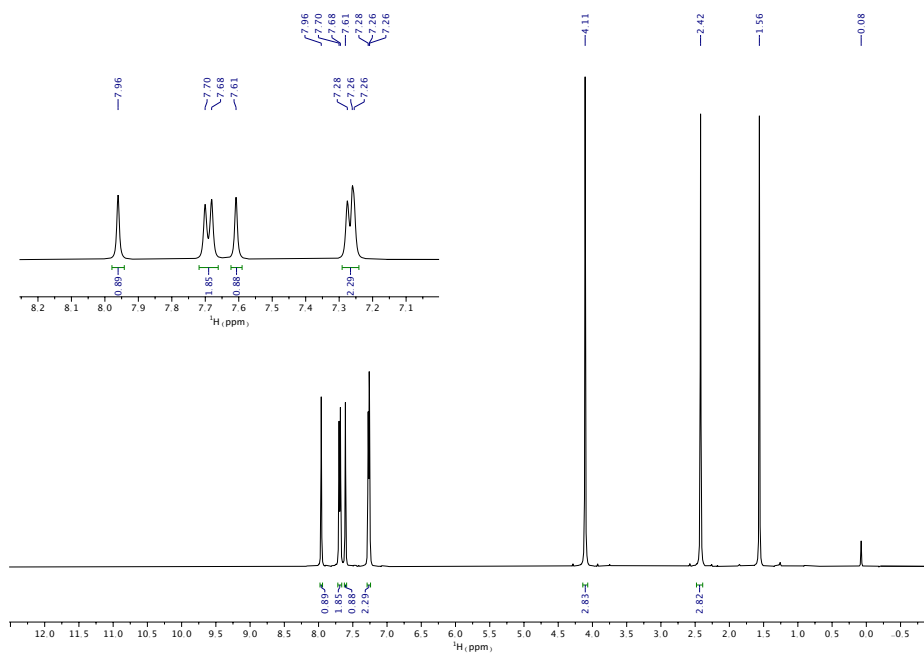


Figure 37. ^1H NMR spectrum of $\alpha(\text{OMe})\text{ToI}_2$ (CDCl₃, 400 MHz, 298 K).

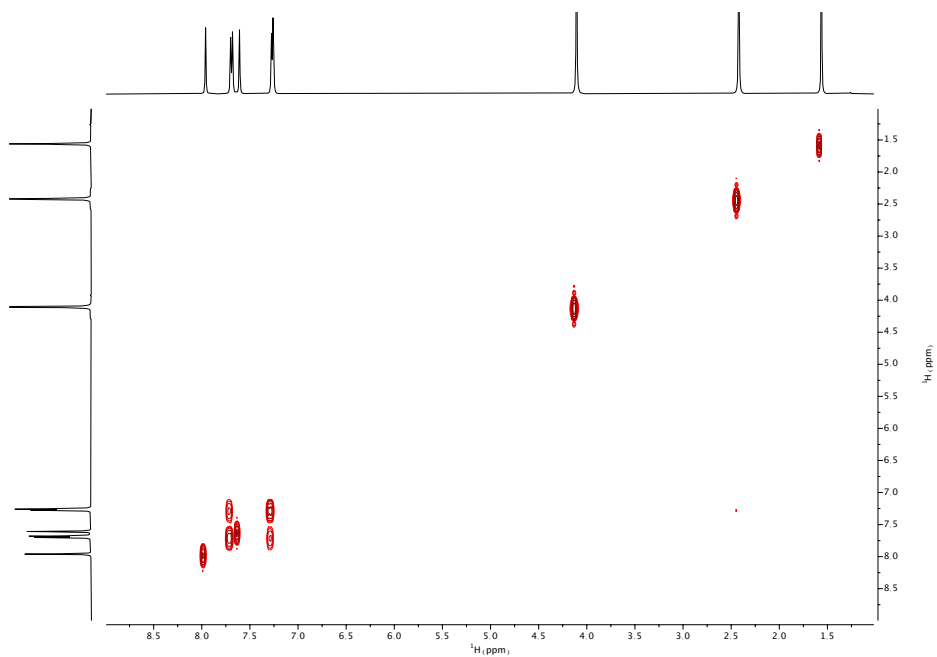


Figure 38. ^1H - ^1H COSY spectrum of $\alpha(\text{OMe})\text{Tol}_2$ (CDCl_3 , 400 MHz, 298 K).

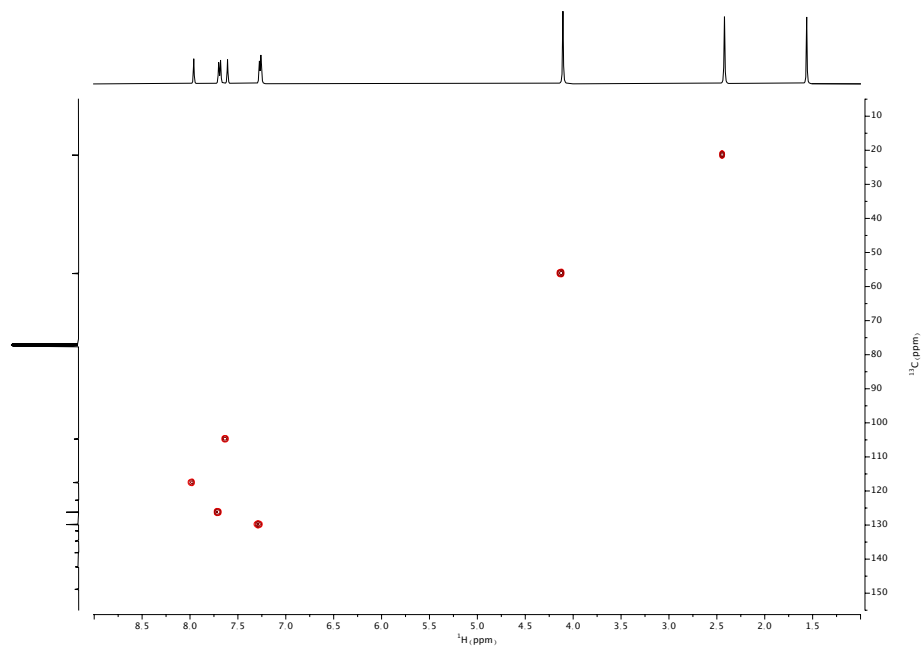


Figure 39. ^1H - ^{13}C HSQC spectrum of $\alpha(\text{OMe})\text{Tol}_2$ (CDCl_3 , 400 MHz, 298 K).

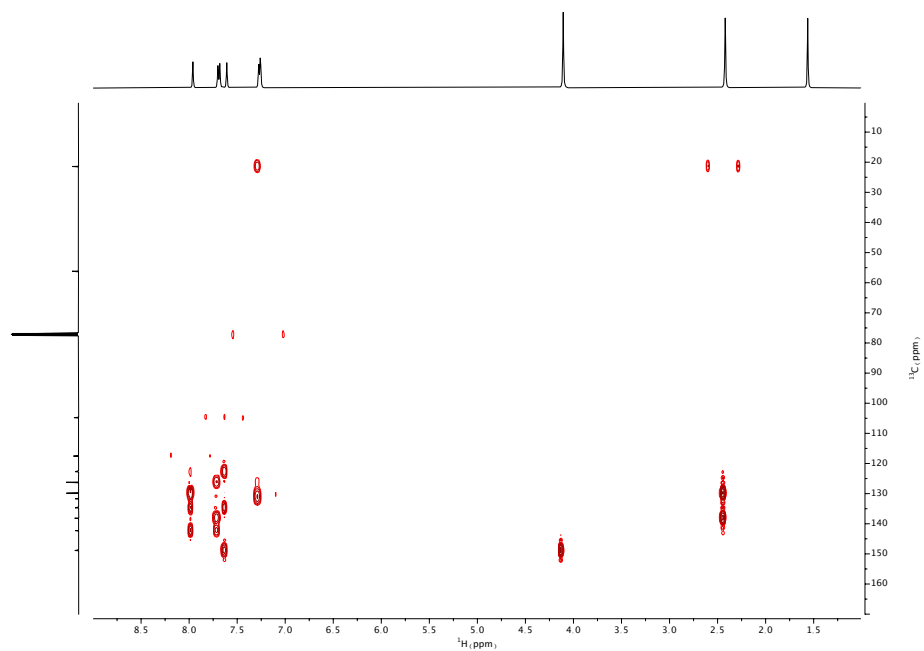


Figure 40. ¹H-¹³C HMBC spectrum of $\alpha(\text{OMe})\text{Tol}_2$ (CDCl_3 , 400 MHz, 298 K).

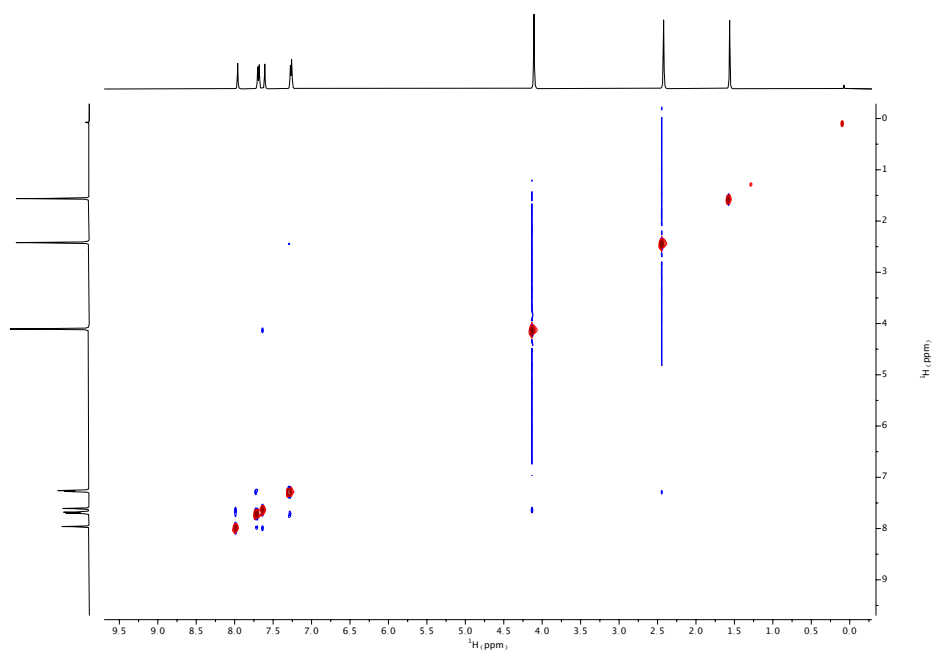


Figure 41. ¹H-¹H NOESY spectrum of $\alpha(\text{OMe})\text{Tol}_2$ (CDCl_3 , 400 MHz, 298 K).

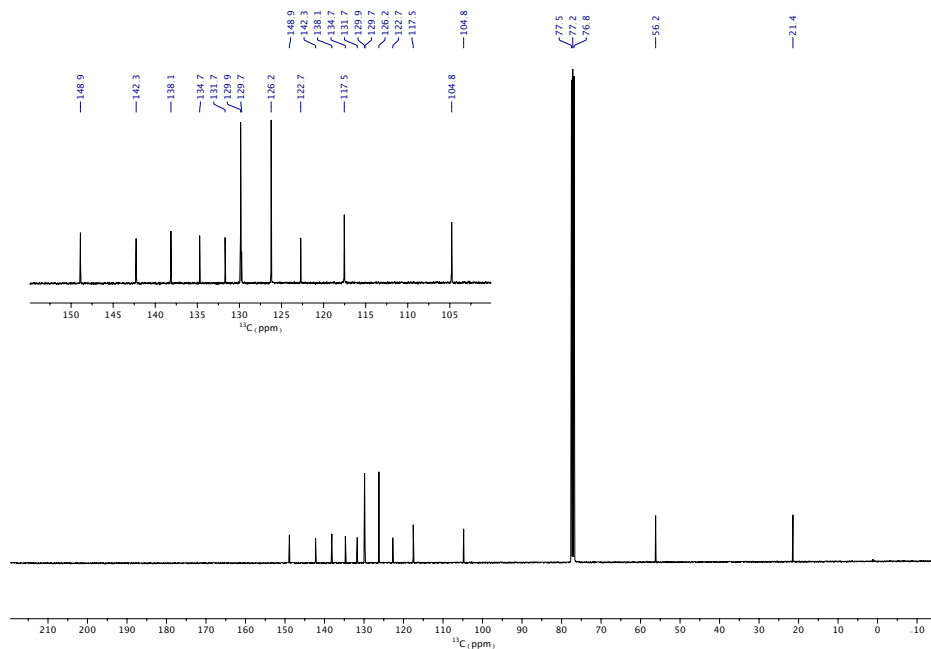


Figure 42. $^{13}\text{C}\{^1\text{H}\}$ NMR spectrum of $\alpha(\text{OMe})\text{Tol}_2$ (CDCl_3 , 101 MHz, 298 K).

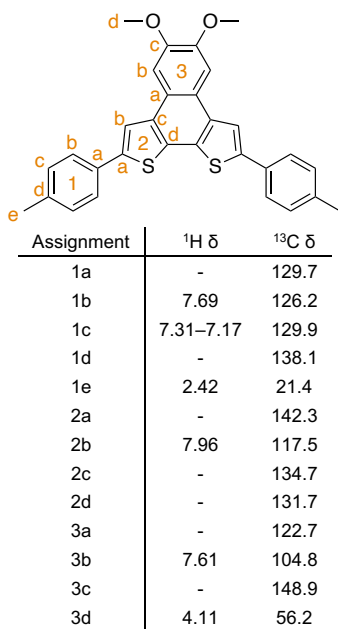


Figure 43. $\alpha(\text{OMe})\text{Tol}_2$ with assignment of ^1H and ^{13}C resonances.

5,6-bis(methoxy)-2,9-di(4-methoxyphenyl)naphtho[2,1-*b*:3,4-*b'*]dithiophene, $\alpha(\text{OMe})(\text{PhOMe})_2$

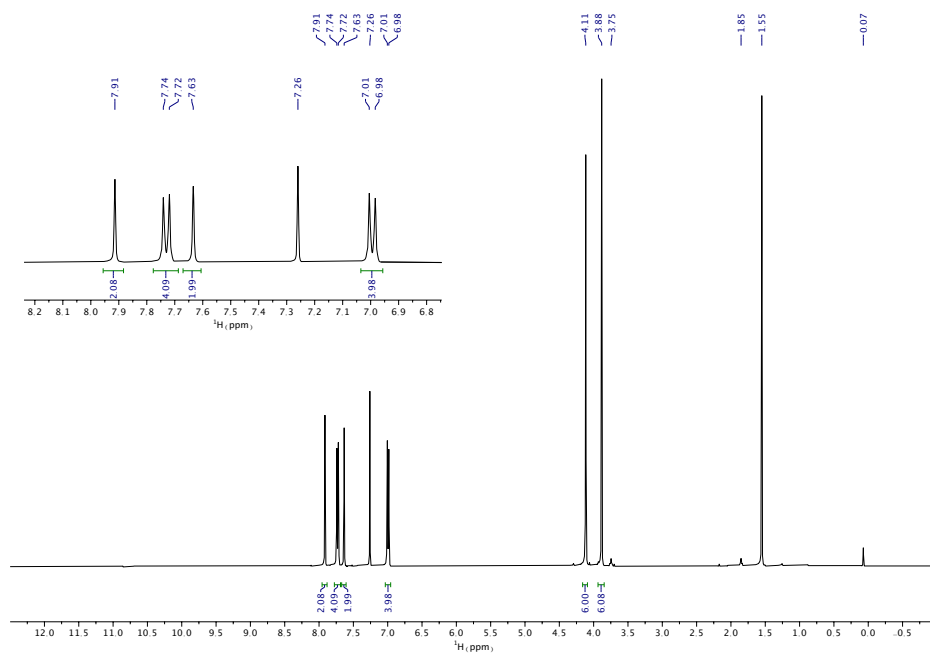


Figure 44. ^1H NMR spectrum of $\alpha(\text{OMe})(\text{PhOMe})_2$ (CDCl_3 , 400 MHz, 298 K).

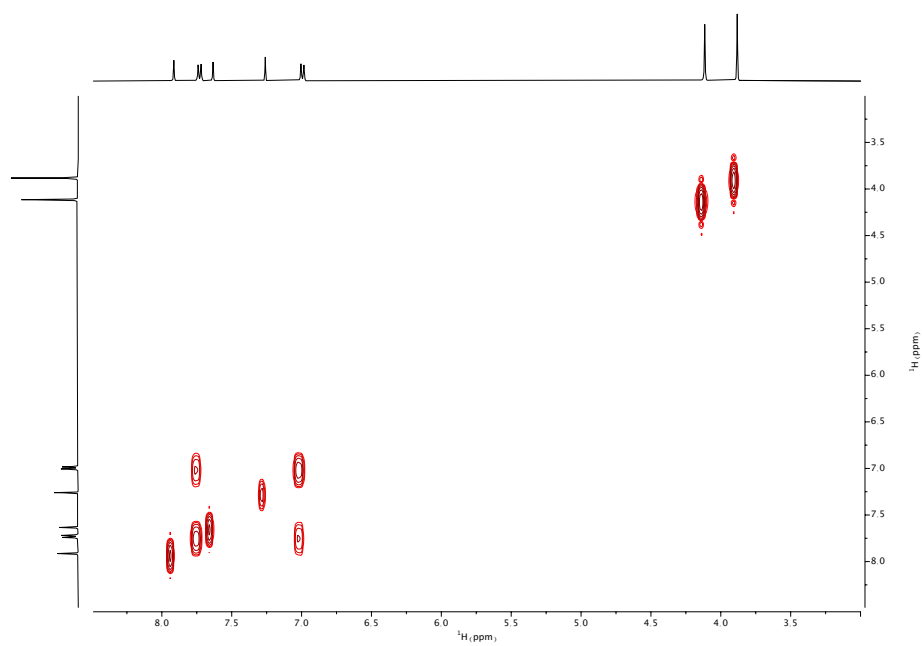


Figure 45. ^1H - ^1H COSY spectrum of $\alpha(\text{OMe})(\text{PhOMe})_2$ (CDCl_3 , 400 MHz, 298 K).

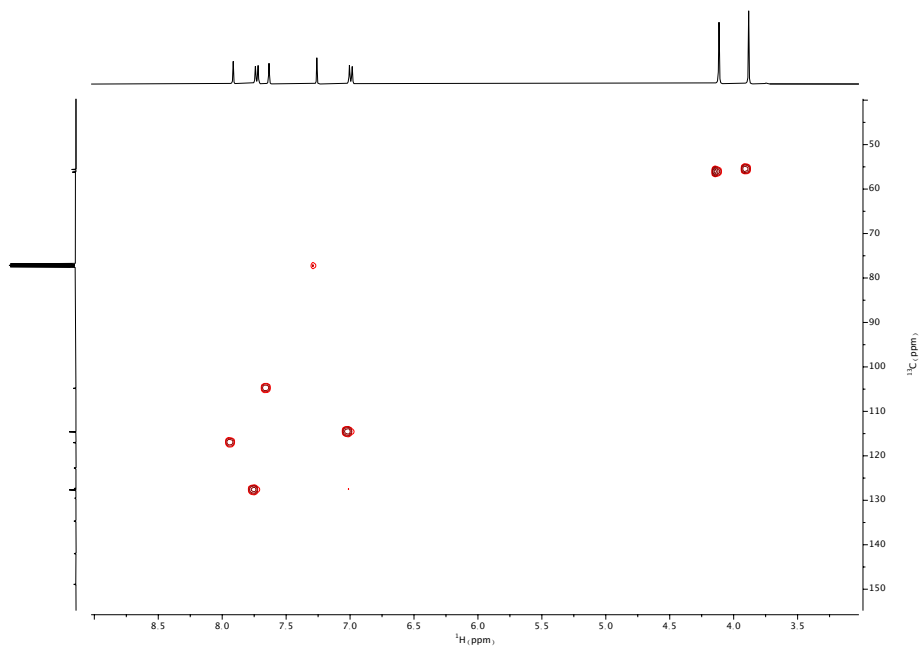


Figure 46. ^1H - ^{13}C HSQC spectrum of $\alpha(\text{OMe})(\text{PhOMe})_2$ (CDCl_3 , 400 MHz, 298 K).

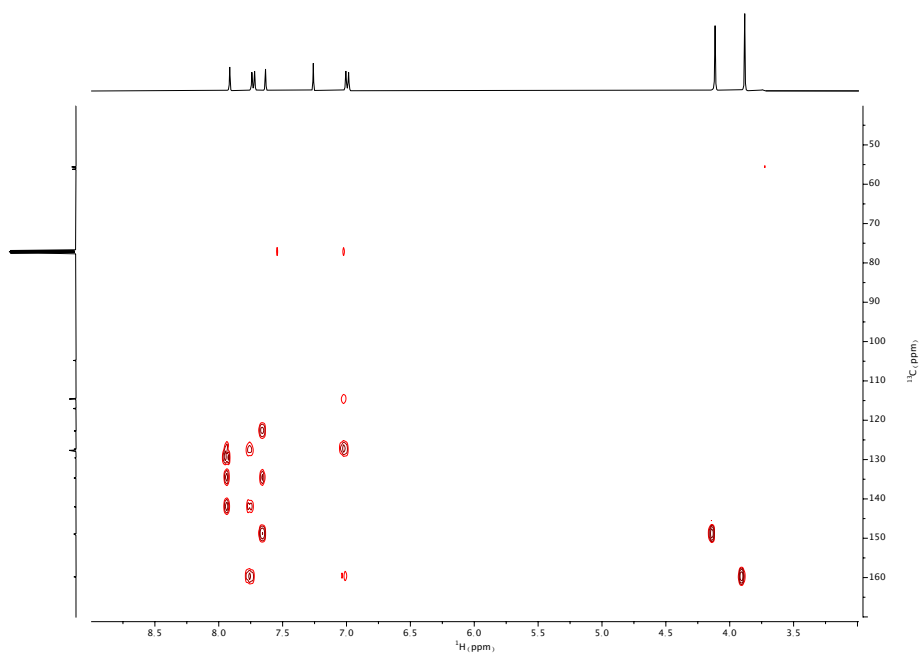


Figure 47. ^1H - ^{13}C HMBC spectrum of $\alpha(\text{OMe})(\text{PhOMe})_2$ (CDCl_3 , 400 MHz, 298 K).

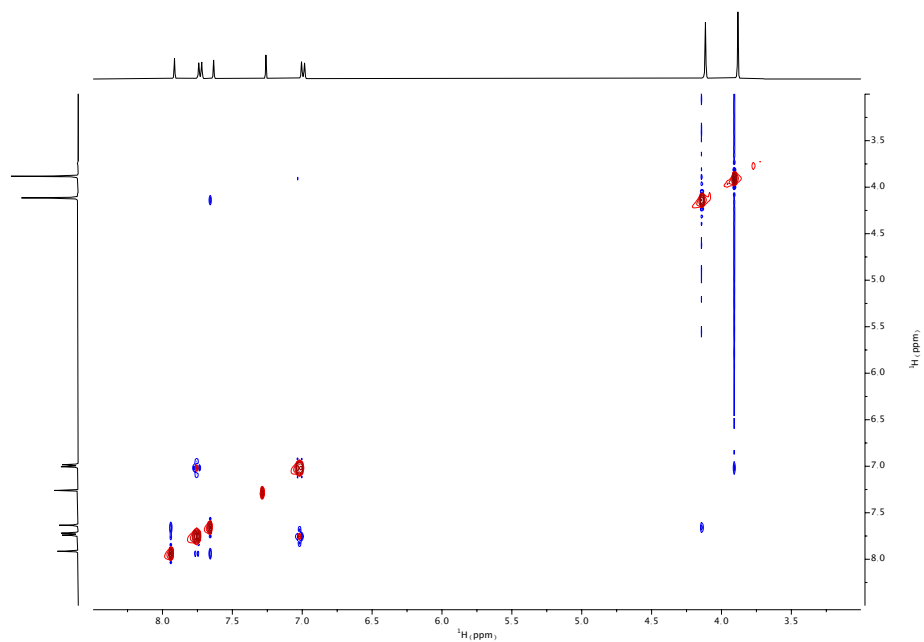


Figure 48. ^1H - ^1H NOESY spectrum of $\alpha(\text{OMe})(\text{PhOMe})_2$ (CDCl_3 , 400 MHz, 298 K).

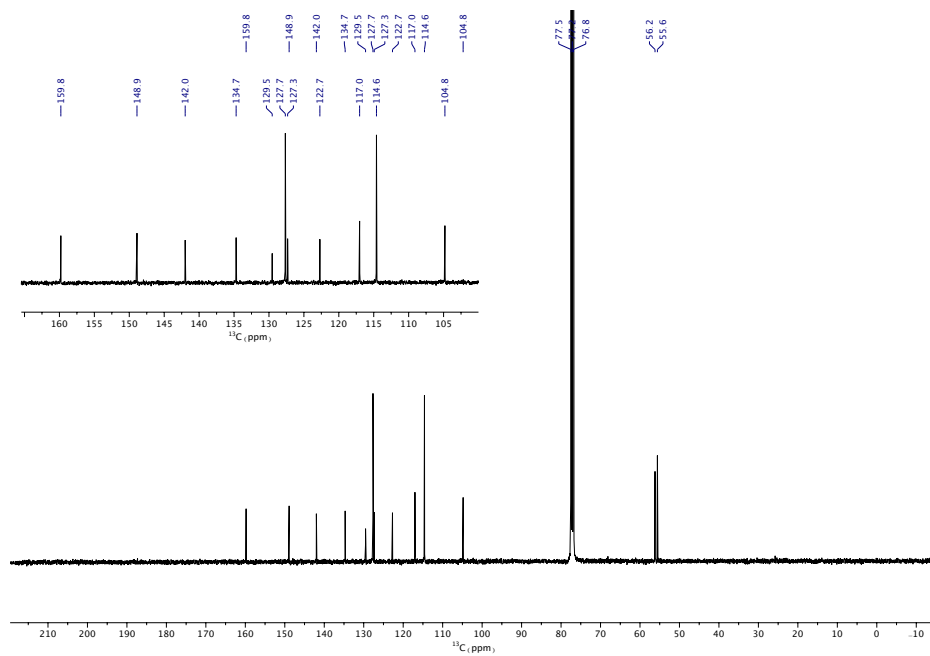


Figure 49. $^{13}\text{C}\{^1\text{H}\}$ NMR spectrum of $\alpha(\text{OMe})(\text{PhOMe})_2$ (CDCl_3 , 101 MHz, 298 K).

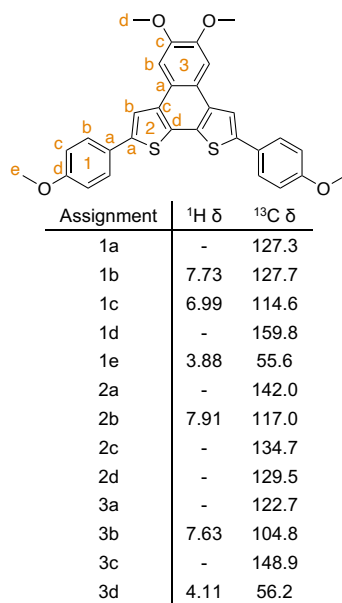


Figure 50. $\alpha(\text{OMe})(\text{PhOMe})_2$ with assignment of ^1H and ^{13}C resonances.

5,6-bis(methoxy)-2,9-di(4-trifluoromethylphenyl)naphtho[2,1-*b*:3,4-*b'*]dithiophene, $\alpha(\text{OMe})(\text{PhCF}_3)_2$

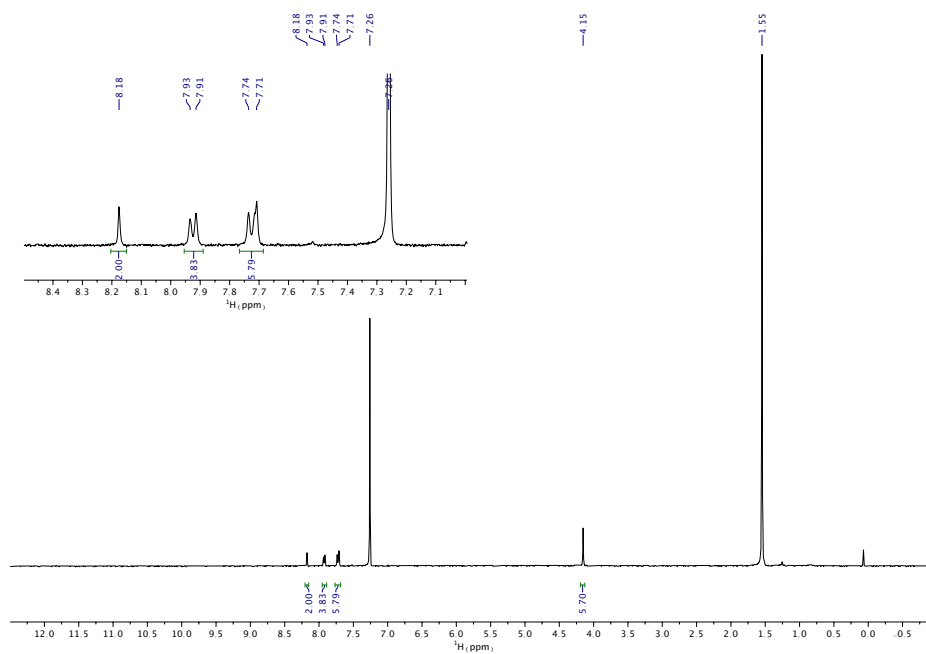


Figure 51. ^1H NMR spectrum of $\alpha(\text{OMe})(\text{PhCF}_3)_2$ (CDCl_3 , 400 MHz, 298 K).

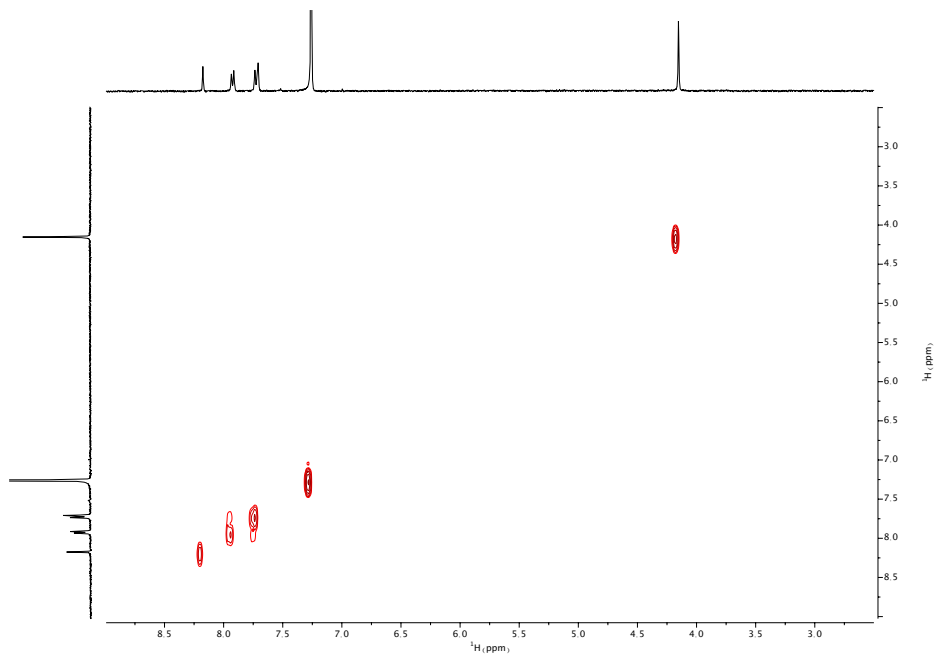


Figure 52. ^1H - ^1H COSY spectrum of $\alpha(\text{OMe})(\text{PhCF}_3)_2$ (CDCl_3 , 400 MHz, 298 K).

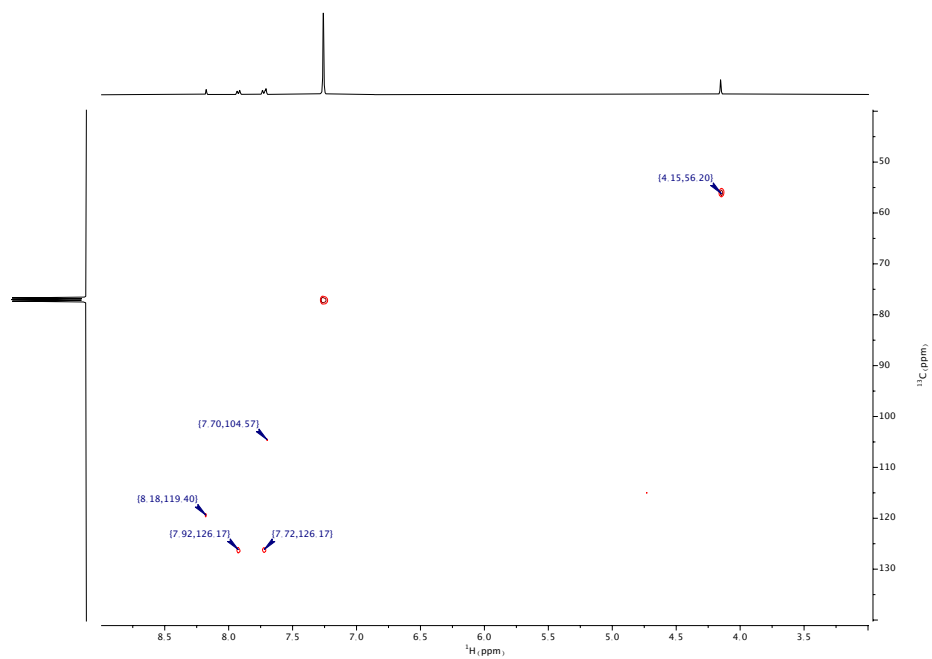


Figure 53. ^1H - ^{13}C HSQC spectrum of $\alpha(\text{OMe})(\text{PhCF}_3)_2$ (CDCl_3 , 400 MHz, 298 K).

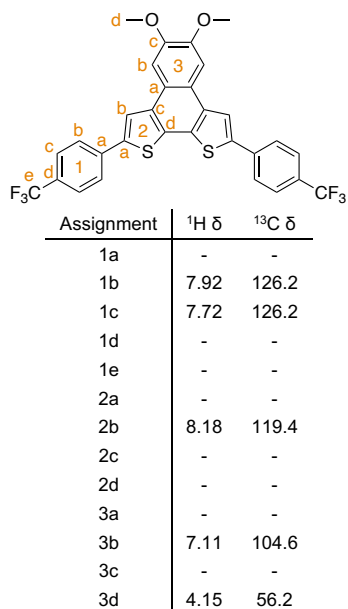


Figure 54. $\alpha(\text{OMe})(\text{PhCF}_3)_2$ with assignment of ^1H and ^{13}C resonances. ^{13}C resonances extracted from HSQC.

1,2-dibromo-4,5-di-isopentyloxybenzene, **1(Oi-Pent)**

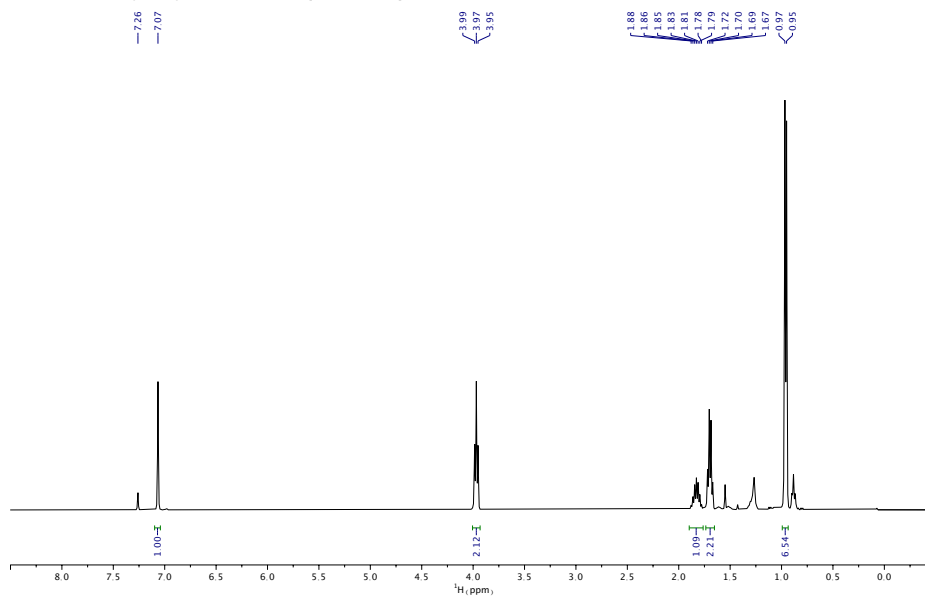


Figure 55. ^1H NMR spectrum of **1(Oi-Pent)** (CDCl_3 , 400 MHz, 298 K).

1,2-di(2-thienyl)-4,5-di-isopentyloxybenzene, **3(Oi-Pent)**

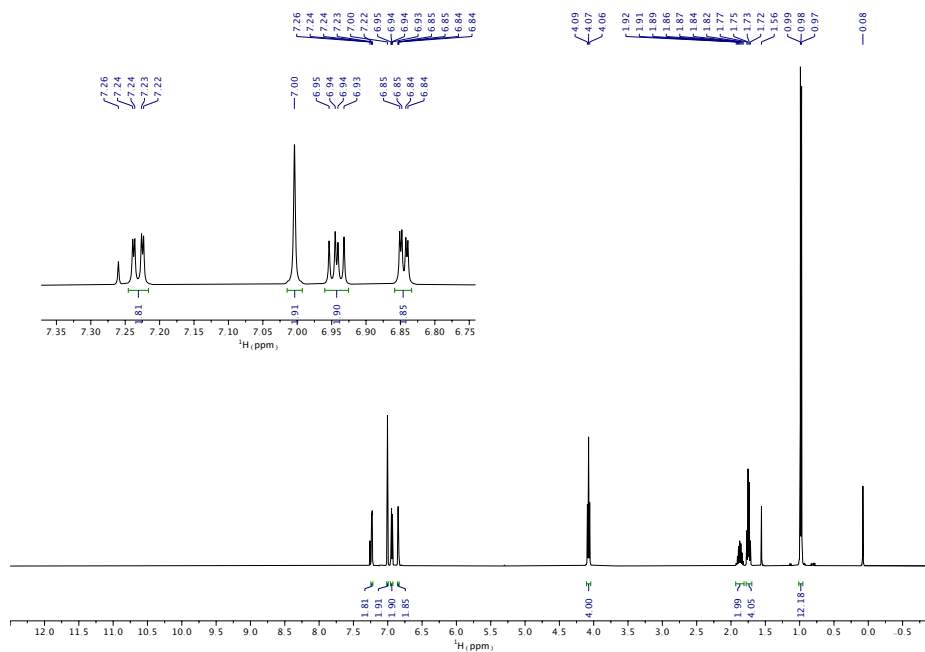


Figure 56. ^1H NMR spectrum of **3(Oi-Pent)** (CDCl_3 , 400 MHz, 298 K).

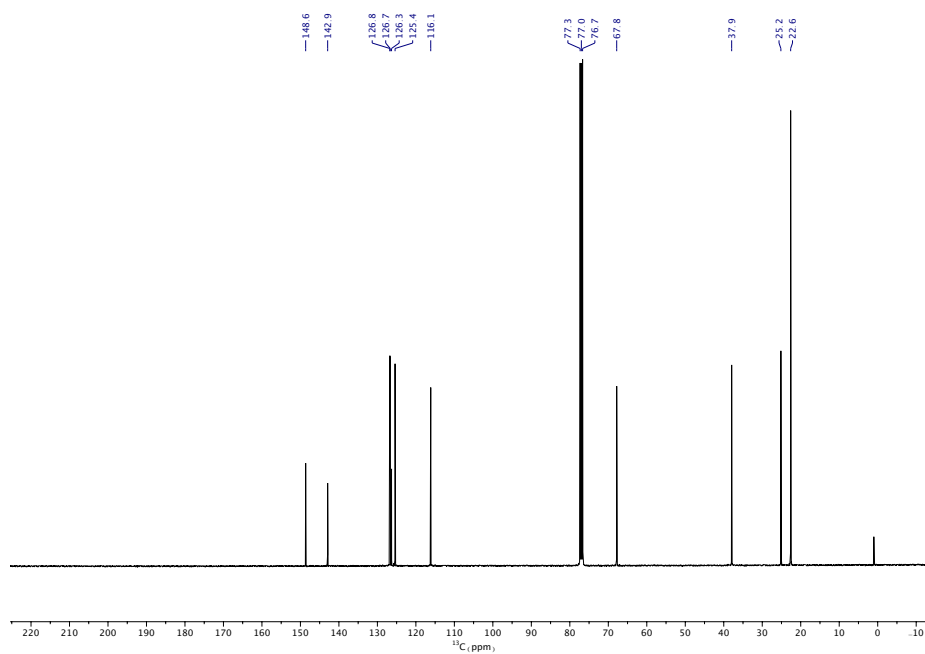


Figure 57. $^{13}\text{C}\{^1\text{H}\}$ NMR spectrum of **3(Oi-Pent)** (CDCl_3 , 101 MHz, 298 K).

1,2-di(2-(5-bromothieryl))-4,5-di-isopentyloxybenzene, **4(Oi-Pent)**

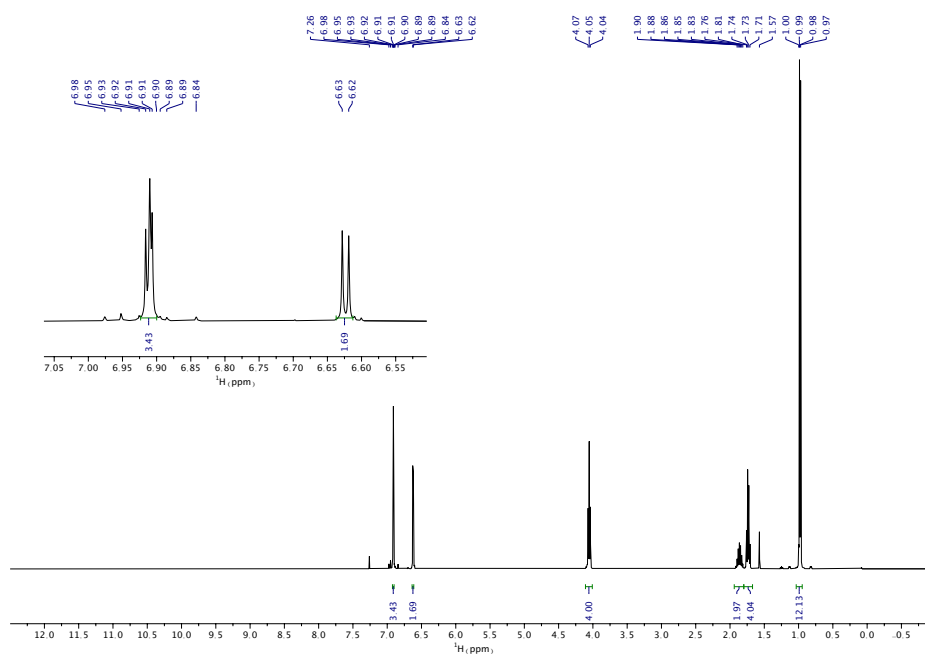


Figure 58. ¹H NMR spectrum of **4(Oi-Pent)** (CDCl₃, 400 MHz, 298 K).

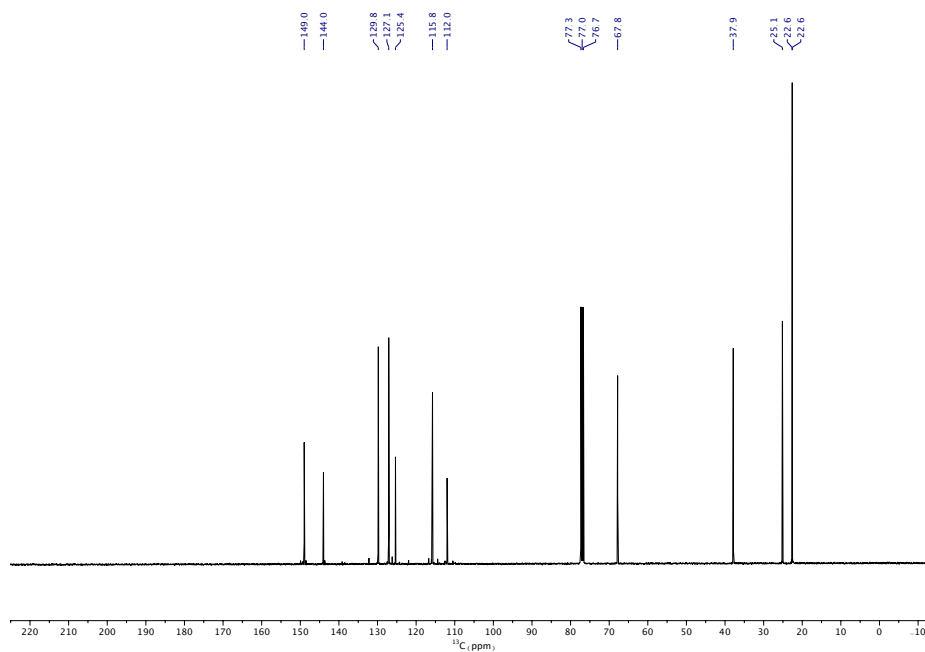


Figure 59. ¹³C{¹H} NMR spectrum of **4(Oi-Pent)** (CDCl₃, 101 MHz, 298 K).

2,5-dibromo-8,9-bis(isopentyloxy)naphtho[1,2-b:4,3-b']dithiophene, $\beta(\text{O}i\text{-Pent})\text{Br}_2$

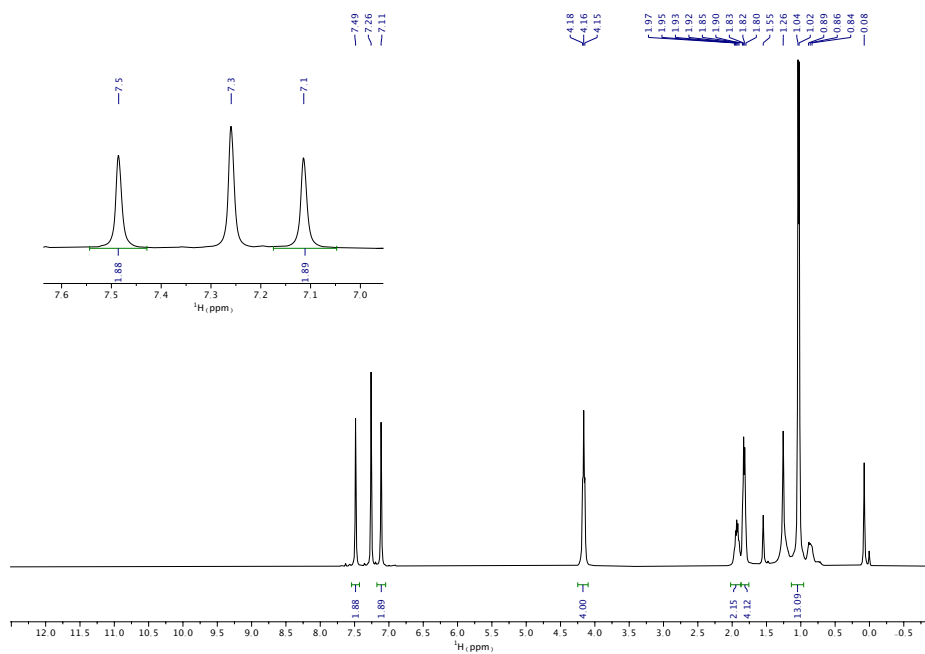


Figure 60. ^1H NMR spectrum of $\beta(\text{O}i\text{-Pent})\text{Br}_2$ (CDCl_3 , 400 MHz, 298 K).

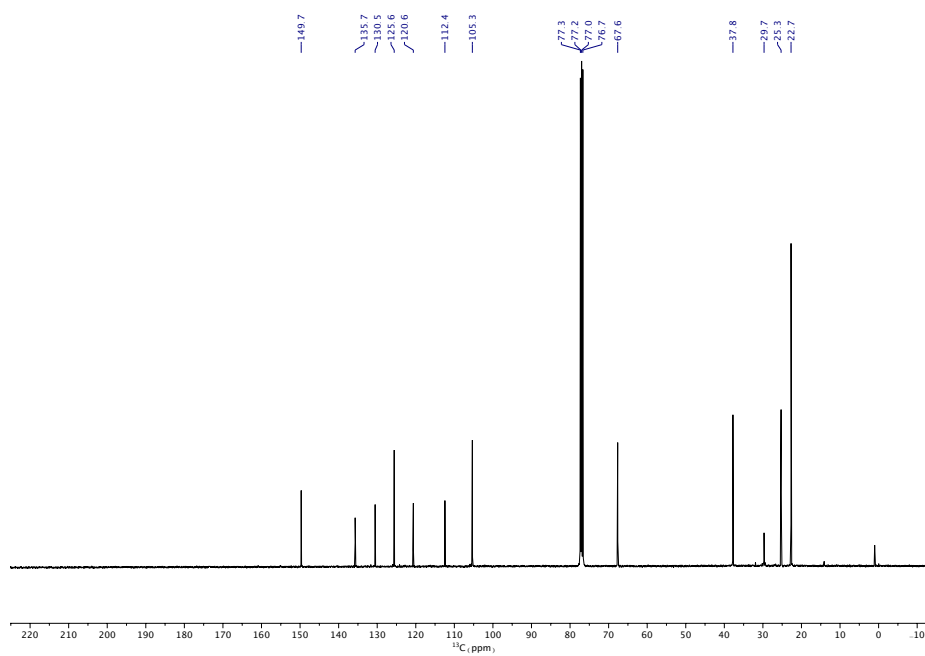


Figure 61. $^{13}\text{C}\{^1\text{H}\}$ NMR spectrum of $\beta(\text{O}i\text{-Pent})\text{Br}_2$ (CDCl_3 , 101 MHz, 298 K).

8,9-bis(isopentyloxy)-2,5-diphenylnaphtho[1,2-*b*:4,3-*b'*]dithiophene, $\beta(\text{O}i\text{-Pent})\text{Ph}_2$

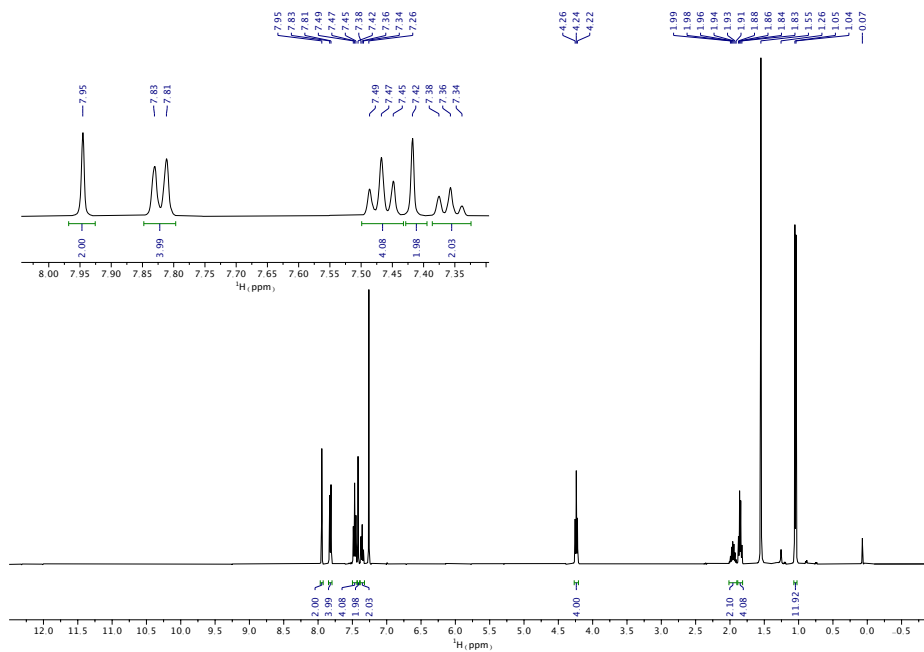


Figure 62. ^1H NMR spectrum of $\beta(\text{O}i\text{-Pent})\text{Ph}_2$ (CDCl_3 , 400 MHz, 298 K).

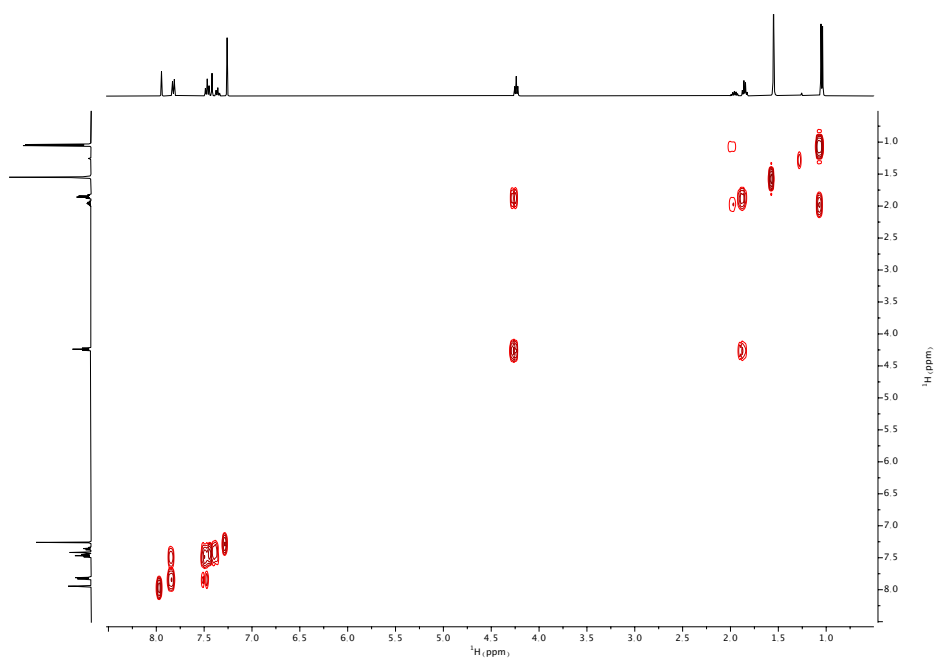


Figure 63. ^1H - ^1H COSY spectrum of $\beta(\text{O}i\text{-Pent})\text{Ph}_2$ (CDCl_3 , 400 MHz, 298 K).

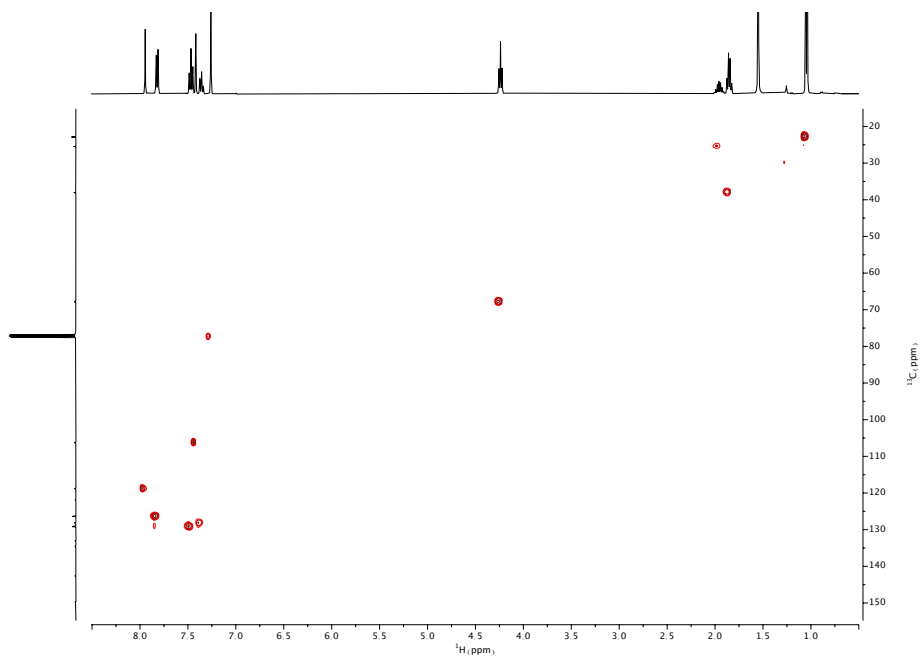


Figure 64. ^1H - ^{13}C HSQC spectrum of $\beta(\text{O}i\text{-Pent})\text{Ph}_2$ (CDCl_3 , 400 MHz, 298 K).

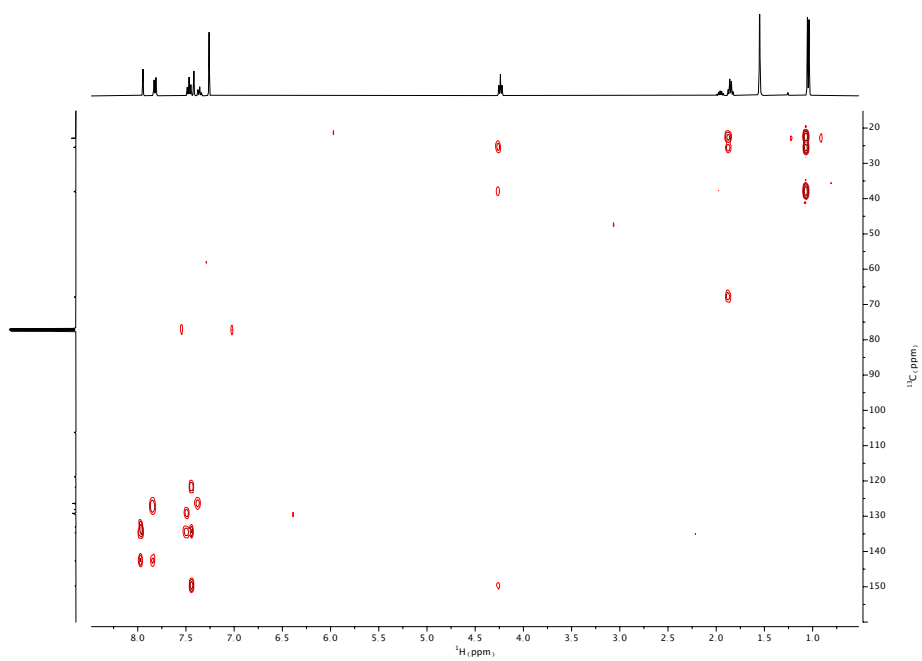


Figure 65. ^1H - ^{13}C HMBC spectrum of $\beta(\text{O}i\text{-Pent})\text{Ph}_2$ (CDCl_3 , 400 MHz, 298 K).

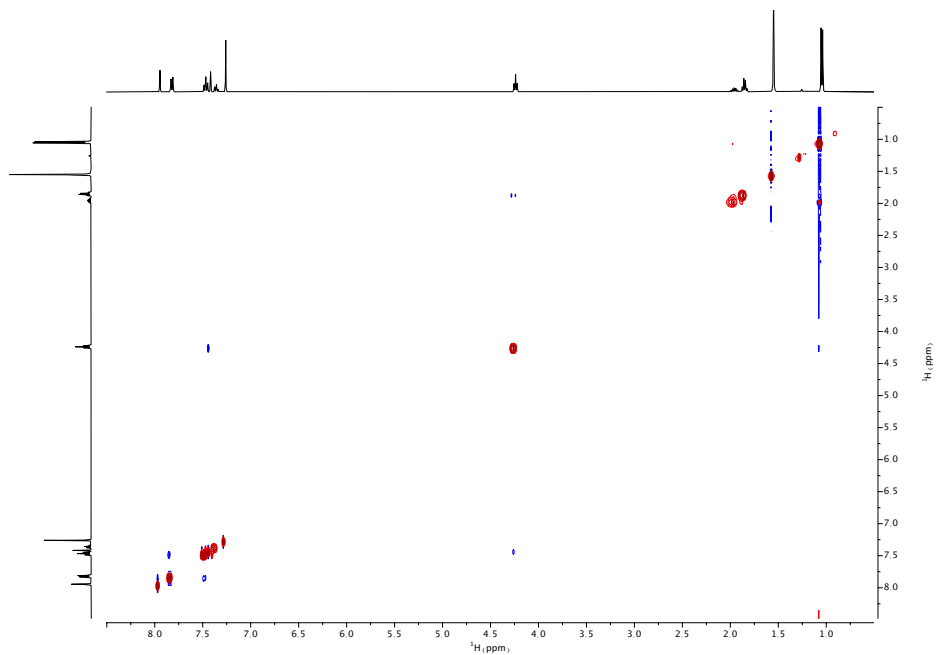


Figure 66. ^1H - ^1H NOESY spectrum of $\beta(\text{O}i\text{-Pent})\text{Ph}_2$ (CDCl_3 , 400 MHz, 298 K).

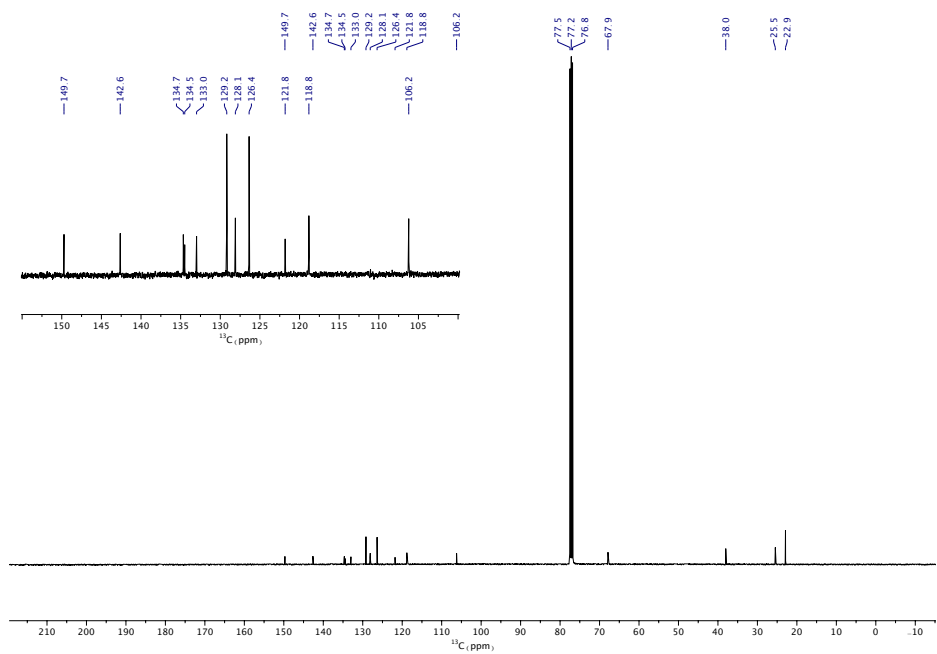
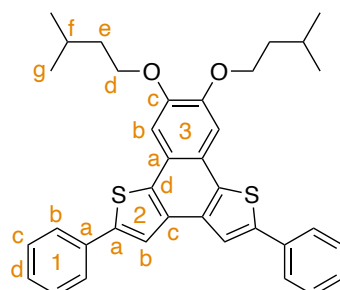


Figure 67. $^{13}\text{C}\{^1\text{H}\}$ NMR spectrum of $\beta(\text{O}i\text{-Pent})\text{Ph}_2$ (CDCl_3 , 101 MHz, 298 K).



| Assignment | $^1\text{H } \delta$ | $^{13}\text{C } \delta$ |
|------------|----------------------|-------------------------|
| 1a | - | 133.0 |
| 1b | 7.82 | 126.4 |
| 1c | 7.47 | 129.2 |
| 1d | 7.36 | 128.1 |
| 2a | - | 142.6 |
| 2b | 7.95 | 118.8 |
| 2c | - | 134.7 |
| 2d | - | 134.5 |
| 3a | - | 121.8 |
| 3b | 7.42 | 106.2 |
| 3c | - | 149.7 |
| 3d | 4.24 | 67.9 |
| 3e | 1.85 | 38.0 |
| 3f | 1.95 | 25.5 |
| 3g | 1.05 | 22.9 |

Figure 68. $\beta(\text{Oi-Pent})\text{Ph}_2$ with assignment of ^1H and ^{13}C resonances.

8,9-bis(isopentyloxy)-2,5-di-*p*-tolynaphtho[1,2-*b*:4,3-*b'*]dithiophene, $\beta(\text{Oi-Pent})\text{Tol}_2$

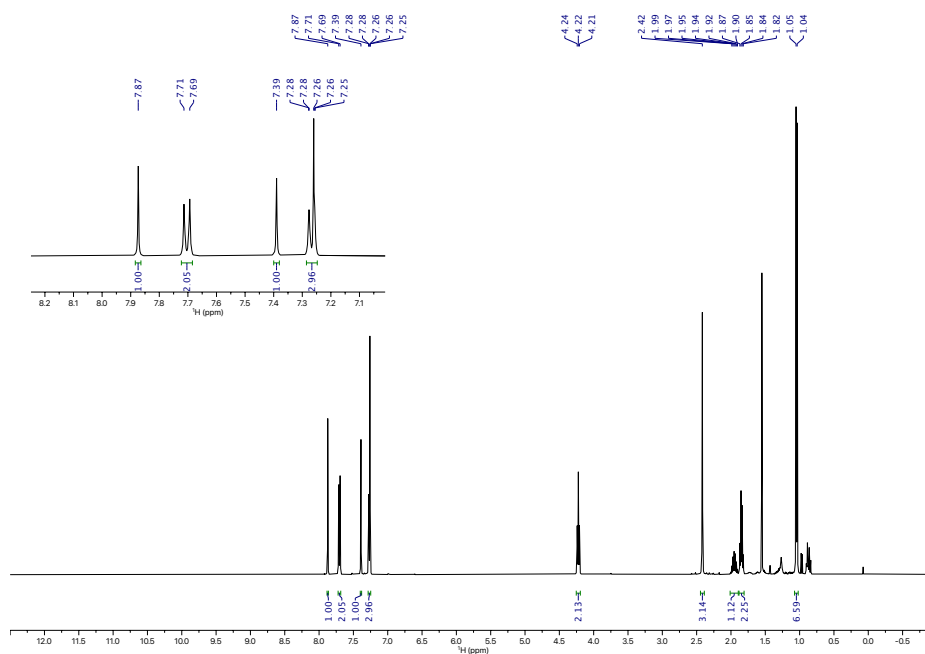


Figure 69. ^1H NMR spectrum of $\beta(\text{Oi-Pent})\text{Tol}_2$ (CDCl_3 , 400 MHz, 298 K).

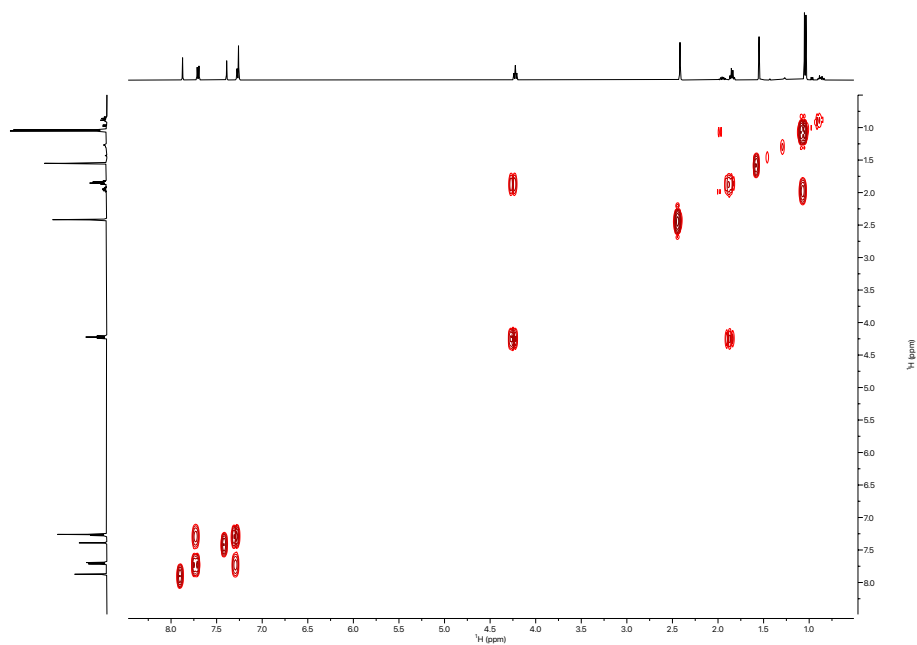


Figure 70. ^1H - ^1H COSY spectrum of $\beta(\text{O}i\text{-Pent})\text{ToI}_2$ (CDCl_3 , 400 MHz, 298 K).

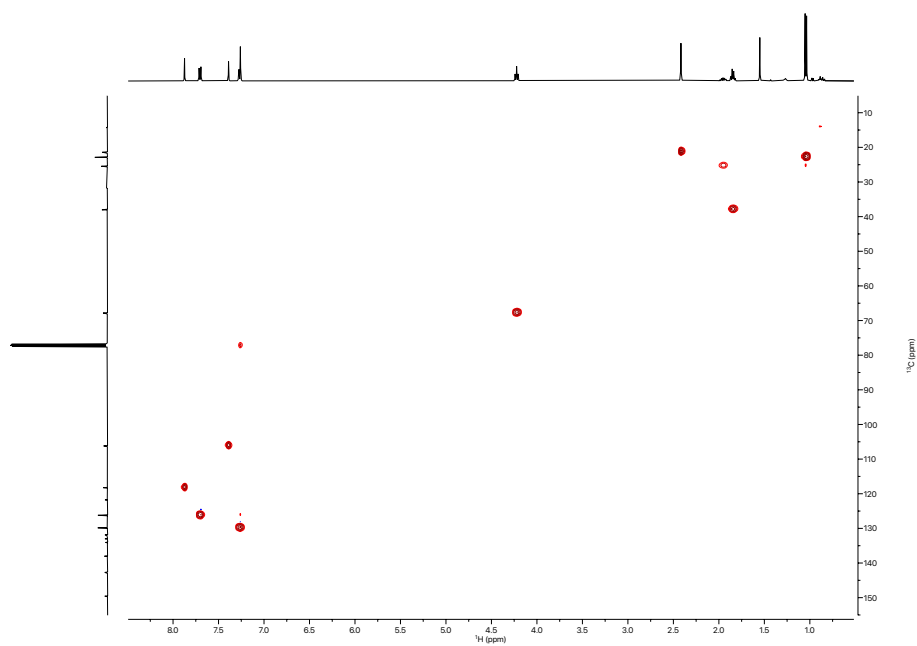


Figure 71. ^1H - ^{13}C HSQC spectrum of $\beta(\text{O}i\text{-Pent})\text{ToI}_2$ (CDCl_3 , 400 MHz, 298 K).

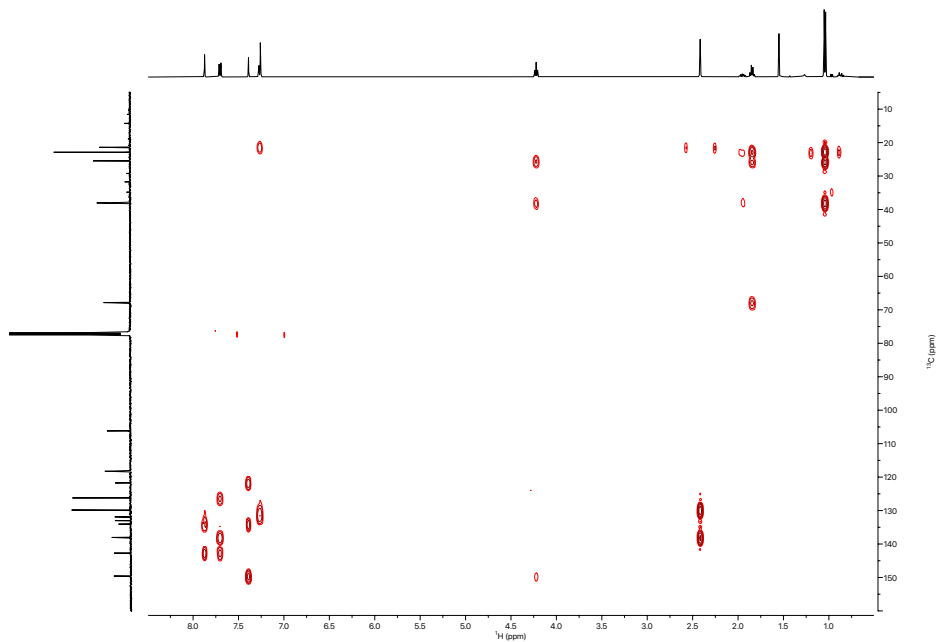


Figure 72. ¹H-¹³C HMBC spectrum of $\beta(\text{O}i\text{-Pent})\text{Tol}_2$ (CDCl₃, 400 MHz, 298 K).

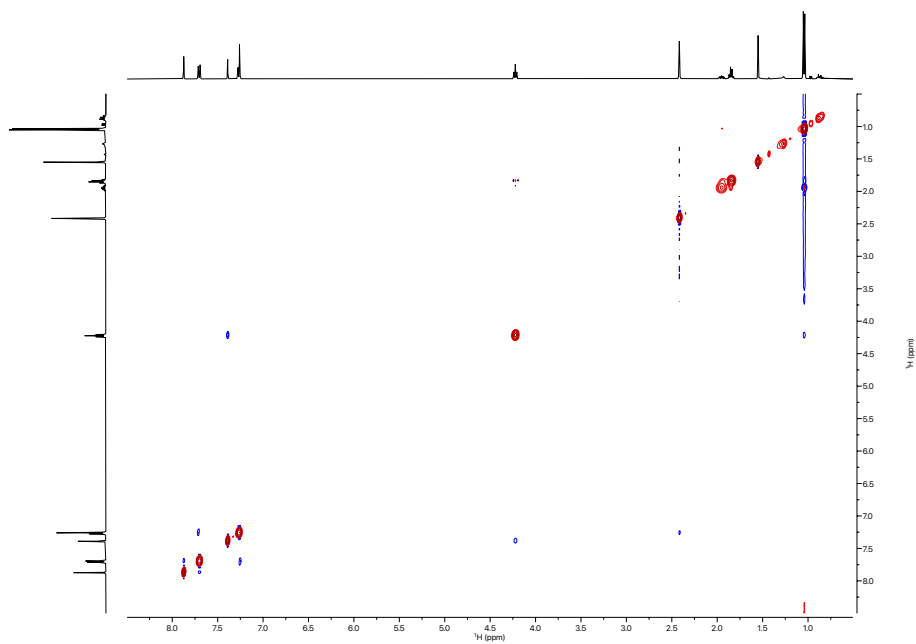


Figure 73. ¹H-¹H NOESY spectrum of $\beta(\text{O}i\text{-Pent})\text{Tol}_2$ (CDCl₃, 400 MHz, 298 K).

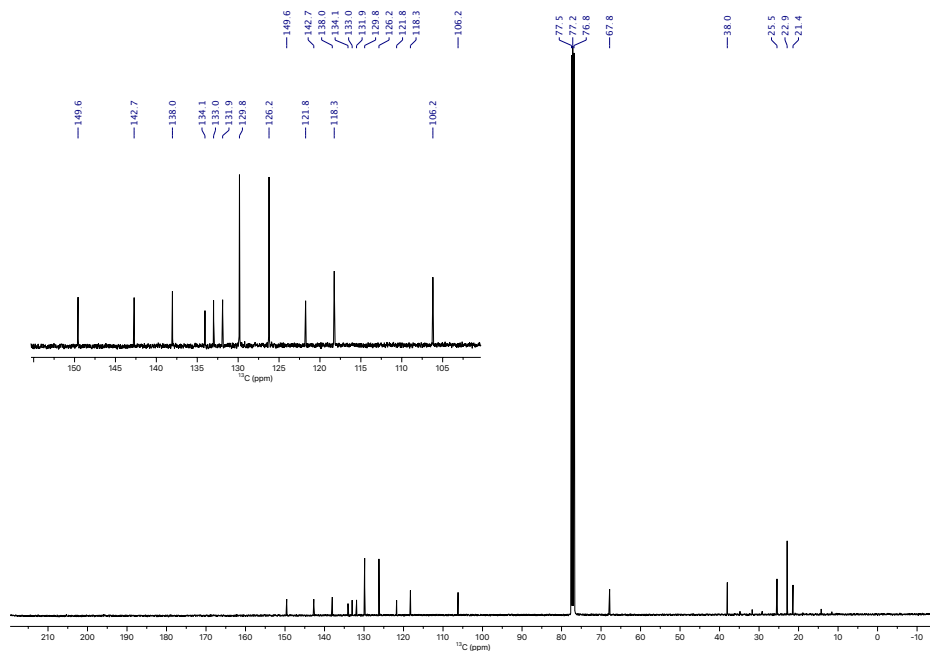
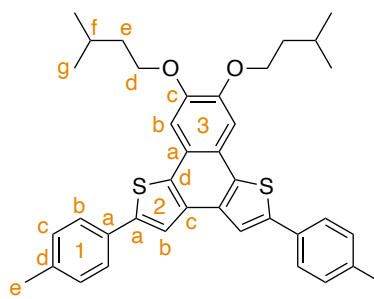


Figure 74. $^{13}\text{C}\{^1\text{H}\}$ NMR spectrum of $\beta(\text{O}i\text{-Pent})\text{Tol}_2$ (CDCl_3 , 101 MHz, 298 K).



| Assignment | $^1\text{H } \delta$ | $^{13}\text{C } \delta$ |
|------------|----------------------|-------------------------|
| 1a | - | 131.9 |
| 1b | 7.70 | 126.2 |
| 1c | 7.29–7.23 | 129.8 |
| 1d | - | 138.0 |
| 1e | 2.42 | 21.4 |
| 2a | - | 142.7 |
| 2b | 7.87 | 118.3 |
| 2c | - | 133.0 |
| 2d | - | 134.1 |
| 3a | - | 121.8 |
| 3b | 7.39 | 106.2 |
| 3c | - | 149.6 |
| 3d | 4.22 | 67.8 |
| 3e | 1.85 | 38.0 |
| 3f | 1.95 | 25.5 |
| 3g | 1.04 | 22.9 |

Figure 75. $\beta(\text{O}i\text{-Pent})\text{Tol}_2$ with assignment of ^1H and ^{13}C resonances.

8,9-bis(isopentyloxy)-2,5-di(4-methoxyphenyl)naphtho[1,2-*b*:4,3-*b'*]dithiophene, β (*O*-Pent)(PhOMe)₂

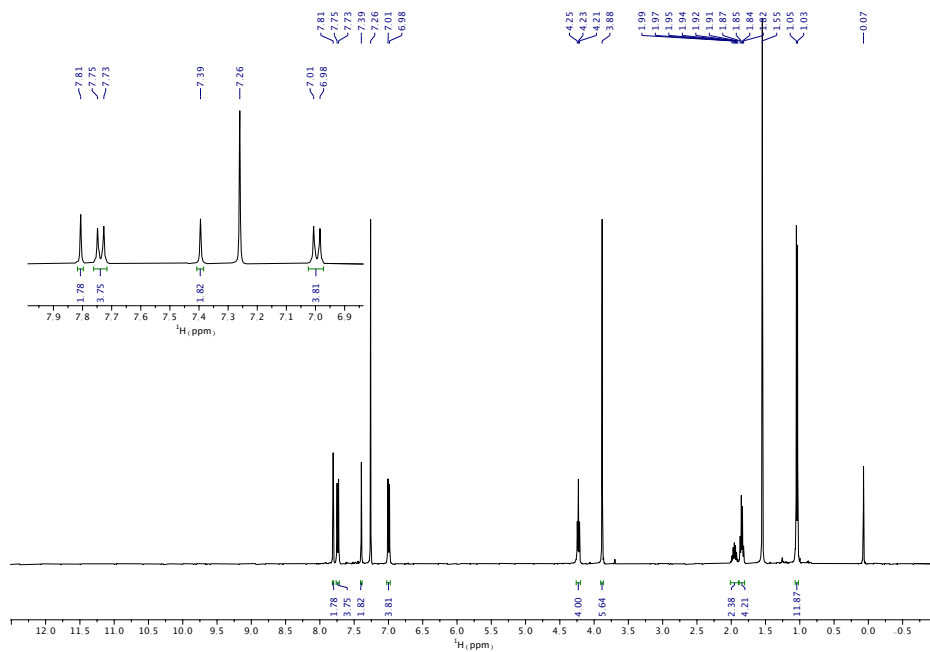


Figure 76. ¹H NMR spectrum of β (*O*-Pent)(PhOMe)₂ (CDCl₃, 400 MHz, 298 K).

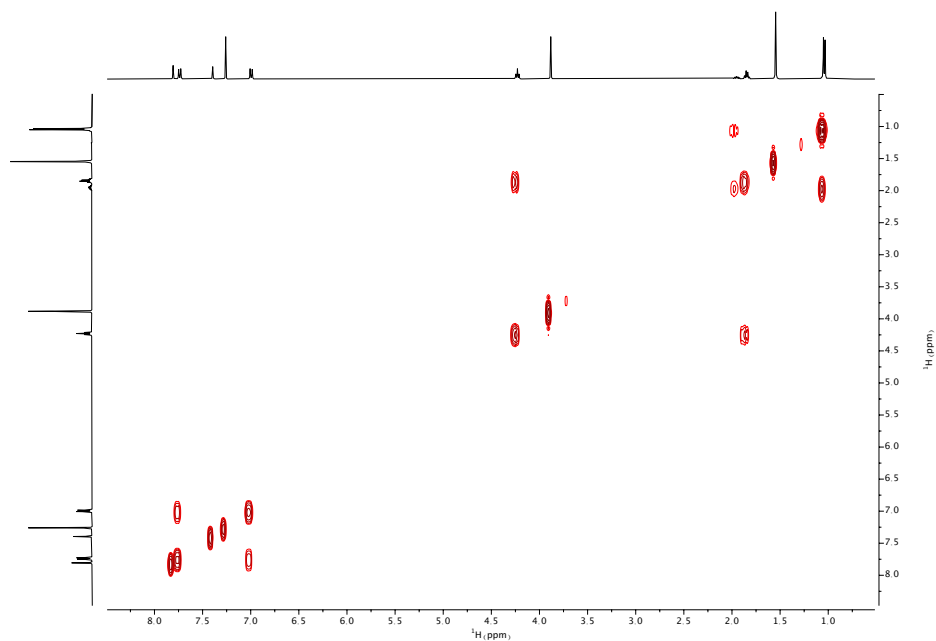


Figure 77. ¹H-¹H COSY spectrum of β (*O*-Pent)(PhOMe)₂ (CDCl₃, 400 MHz, 298 K).

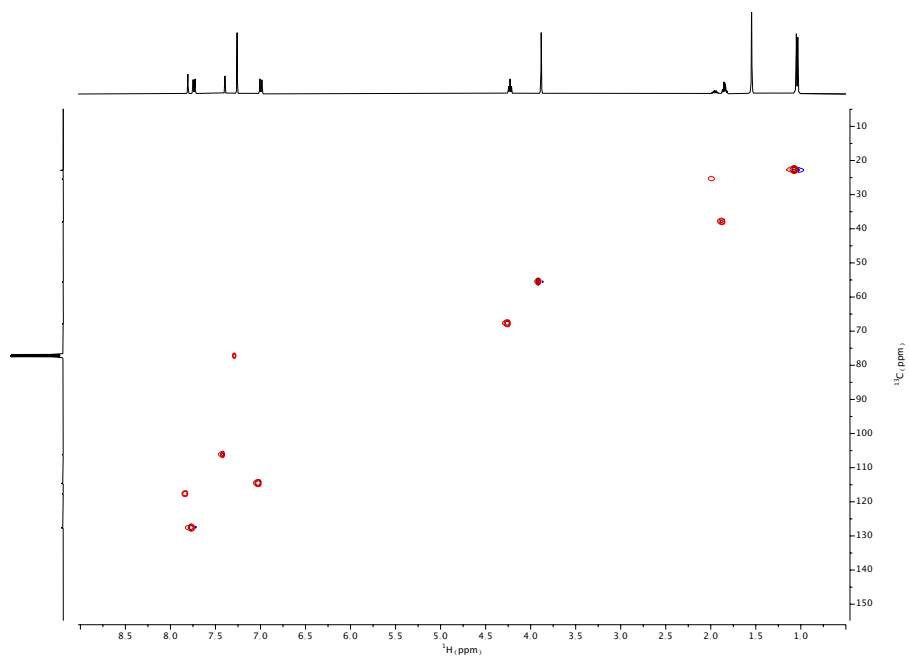


Figure 78. ^1H - ^{13}C HSQC spectrum of $\beta(\text{O}i\text{-Pent})(\text{PhOMe})_2$ (CDCl_3 , 400 MHz, 298 K).

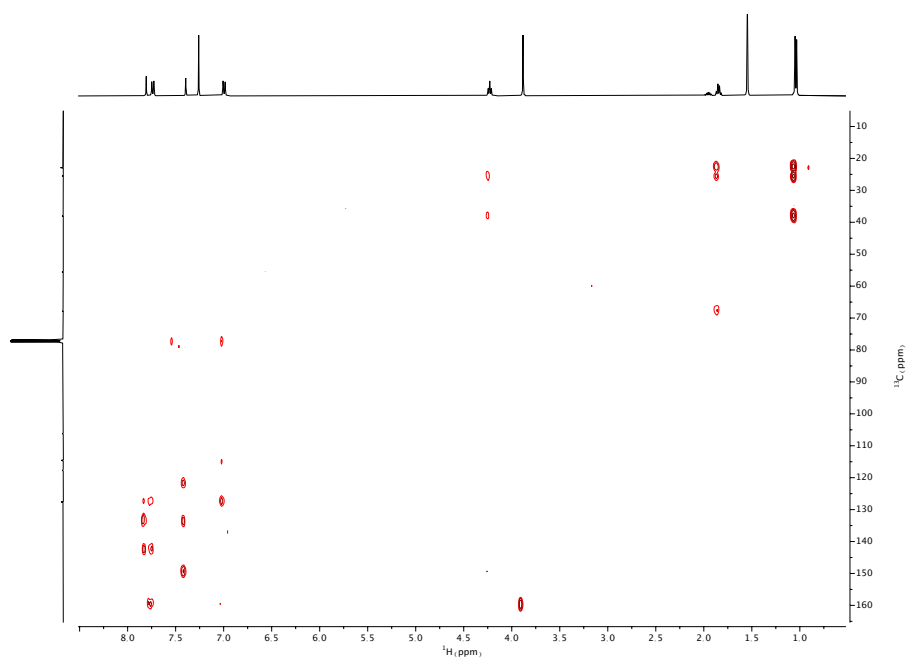


Figure 79. ^1H - ^{13}C HMBC spectrum of $\beta(\text{O}i\text{-Pent})(\text{PhOMe})_2$ (CDCl_3 , 400 MHz, 298 K).

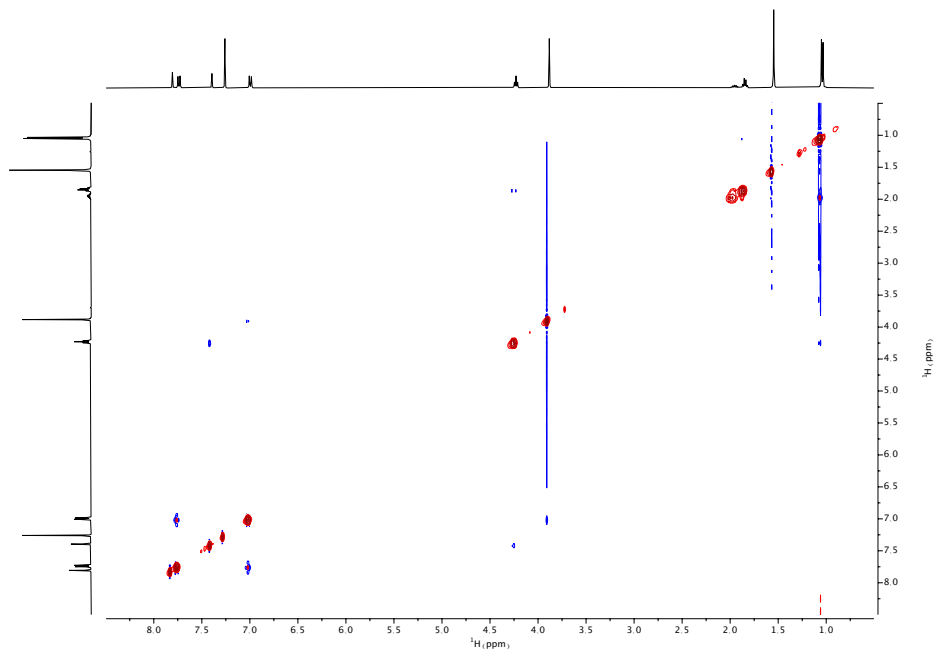


Figure 80. ^1H - ^1H NOESY spectrum of $\beta(\text{O}i\text{-Pent})(\text{PhOMe})_2$ (CDCl_3 , 400 MHz, 298 K).

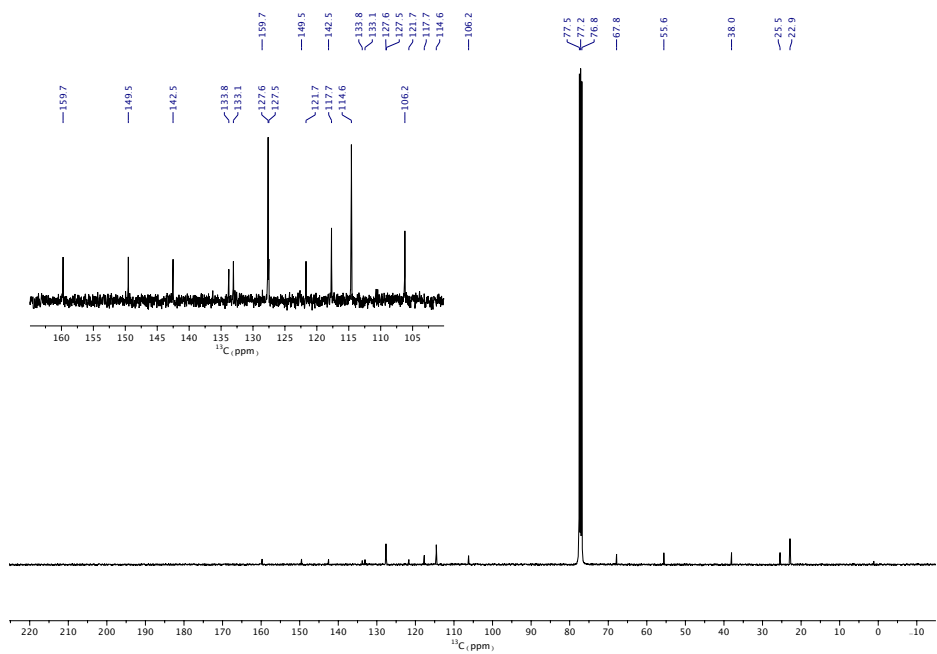
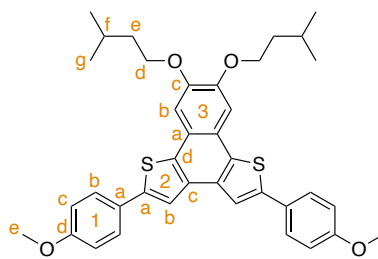


Figure 81. $^{13}\text{C}\{^1\text{H}\}$ NMR spectrum of $\beta(\text{O}i\text{-Pent})(\text{PhOMe})_2$ (CDCl_3 , 101 MHz, 298 K).



| Assignment | $^1\text{H } \delta$ | $^{13}\text{C } \delta$ |
|------------|----------------------|-------------------------|
| 1a | - | 127.5 |
| 1b | 7.74 | 127.6 |
| 1c | 7.00 | 114.6 |
| 1d | - | 159.8 |
| 1e | 3.88 | 55.6 |
| 2a | - | 142.5 |
| 2b | 7.81 | 117.7 |
| 2c | - | 133.1 |
| 2d | - | 133.8 |
| 3a | - | 121.7 |
| 3b | 7.39 | 106.2 |
| 3c | - | 149.5 |
| 3d | 4.23 | 67.9 |
| 3e | 1.84 | 38.0 |
| 3f | 1.95 | 25.5 |
| 3g | 1.04 | 22.9 |

Figure 82. $\beta(\text{O}i\text{-Pent})(\text{PhOMe})_2$ with assignment of ^1H and ^{13}C resonances.

8,9-bis(isopentyloxy)-2,5-di(4-trifluoromethylphenyl)naphtho[1,2-*b*:4,3-*b'*]dithiophene, $\beta(\text{O}i\text{-Pent})(\text{PhCF}_3)_2$

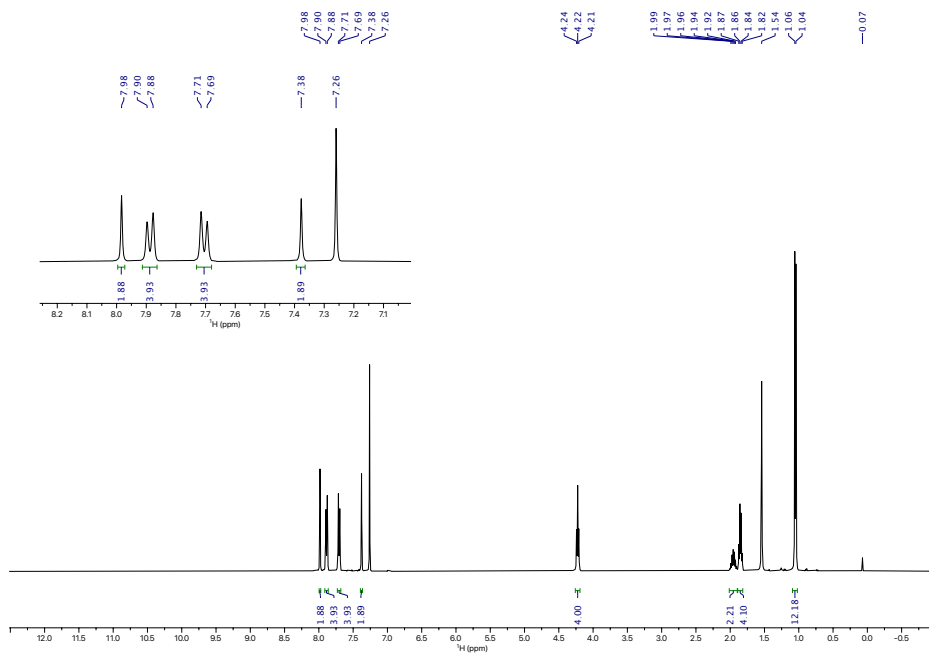


Figure 83. ^1H NMR spectrum of $\beta(\text{O}i\text{-Pent})(\text{PhCF}_3)_2$ (CDCl_3 , 400 MHz, 298 K).

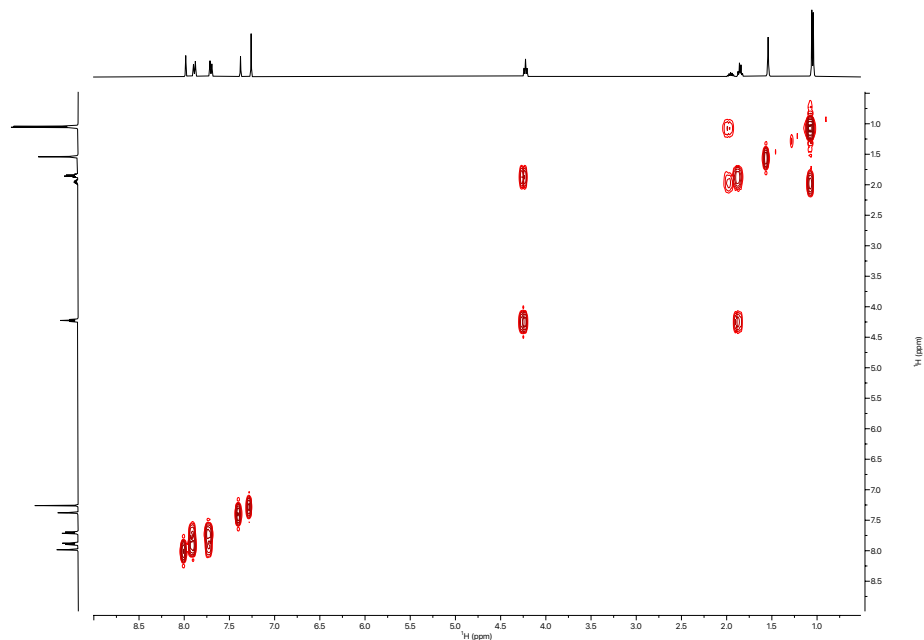


Figure 84. ^1H - ^1H COSY spectrum of $\beta(\text{O}i\text{-Pent})(\text{PhCF}_3)_2$ (CDCl_3 , 400 MHz, 298 K).

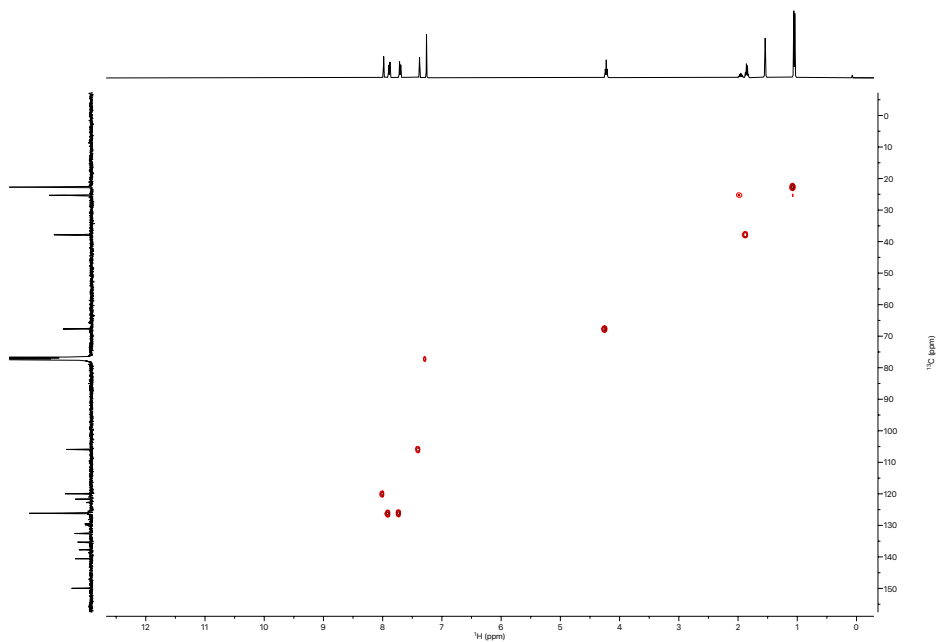


Figure 85. ^1H - ^{13}C HSQC spectrum of $\beta(\text{O}i\text{-Pent})(\text{PhCF}_3)_2$ (CDCl_3 , 400 MHz, 298 K).

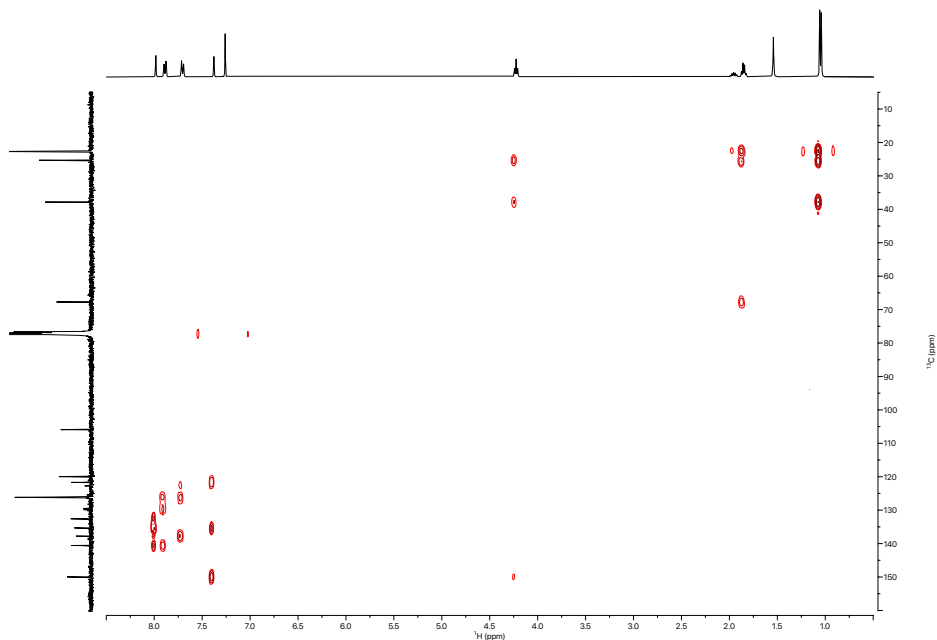


Figure 86. ¹H-¹³C HMBC spectrum of $\beta(\text{O-}i\text{-Pent})(\text{PhCF}_3)_2$ (CDCl_3 , 400 MHz, 298 K).

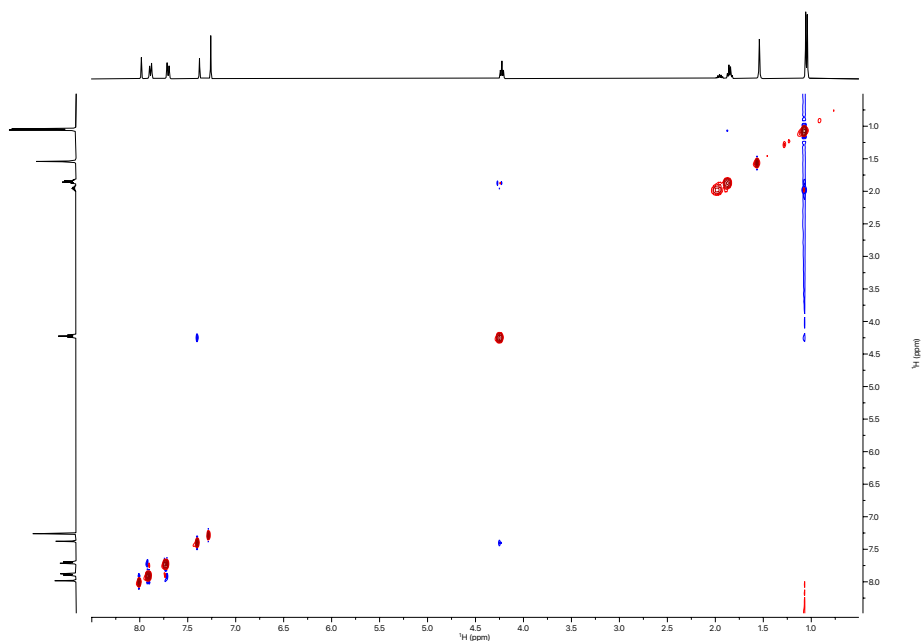


Figure 87. ¹H-¹H NOESY spectrum of $\beta(\text{O-}i\text{-Pent})(\text{PhCF}_3)_2$ (CDCl_3 , 400 MHz, 298 K).

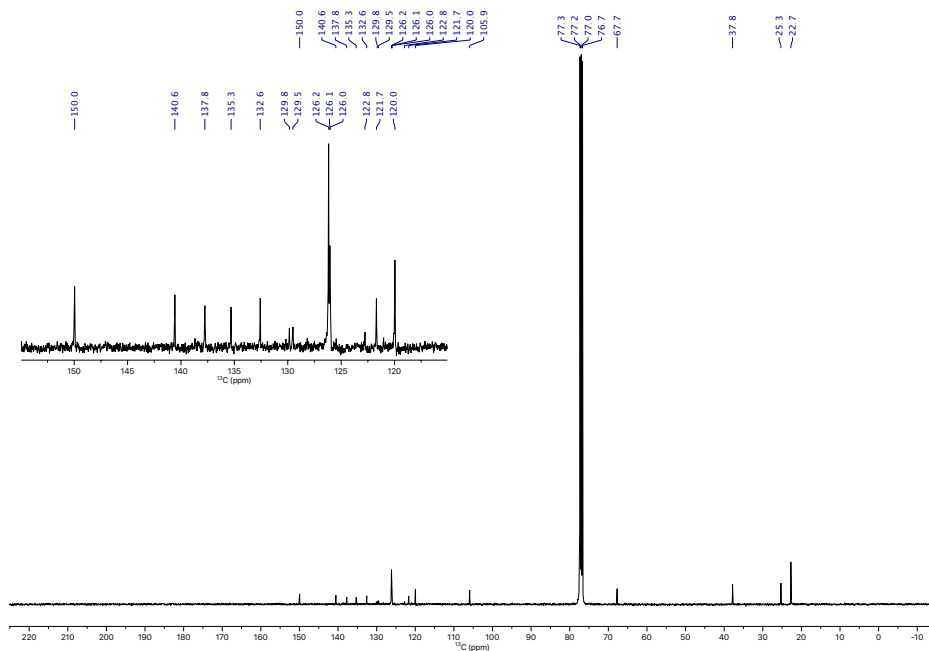


Figure 88. $^{13}\text{C}\{^1\text{H}\}$ NMR spectrum of $\beta(\text{O}i\text{-Pent})(\text{PhCF}_3)_2$ (CDCl_3 , 101 MHz, 298 K).

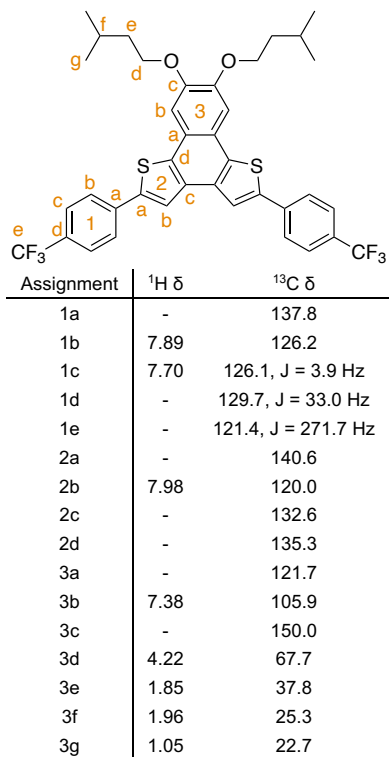


Figure 89. $\beta(\text{O}i\text{-Pent})(\text{PhCF}_3)_2$ with assignment of ^1H and ^{13}C resonances.

3) Photophysical Properties of $\alpha(\text{OHex})\text{R}_2$ and $\beta(\text{O}i\text{-Pent})\text{R}_2$

Absorbance spectra were collected on an Agilent Cary Bio100 spectrophotometer and corrected for solvent background absorbance and instrument drift. Emission spectra were recorded on a Horiba Jon-Yvon Fluorolog-3 with excitation and emission slit widths set at 2 nm. Both series, $\alpha(\text{OHex})\text{R}_2$ and $\beta(\text{O}i\text{-Pent})\text{R}_2$, were prepared under inert atmosphere, sealed in 1 cm path length quartz cuvettes, and were analyzed at $\lambda_{\text{ex}} = 365$ nm (for emission spectra). Fluorescence quantum yields were determined by reference to 9,10-diphenylanthracene in cyclohexane ($\phi = 0.91$) which was cross-checked with quinine bisulfate in 0.5 M H_2SO_4 (aq) ($\phi = 0.54$). Five solutions of varying concentration were prepared for each sample and good fits ($R^2 \geq 0.99$) were obtained in all cases. The absorbance of all sample solutions was kept below 0.10 to avoid the inner-filter effect. Measurements were performed at room temperature with both sample and standard excited at the same wavelength (365 nm). Plots are given below with UV-visible spectra as solid lines and emission spectra as dashed lines. UV-visible spectra are plotted as either molar absorptivity or normalized absorption (left vertical axis) vs wavelength (horizontal axis). Emission spectra are plotted as normalized intensities (right vertical axis) vs wavelength (horizontal axis).

$\alpha(\text{OHex})\text{Ph}_2$ and $\beta(\text{O}i\text{-Pent})\text{Ph}_2$

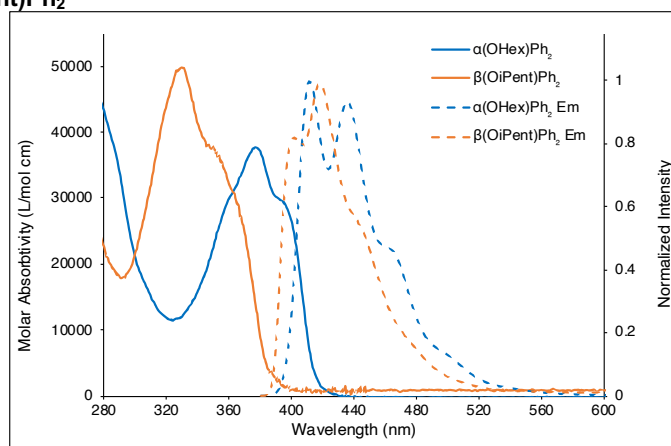


Figure 90. Absorbance and emission spectra for $\alpha(\text{OHex})\text{Ph}_2$ and $\beta(\text{O}i\text{-Pent})\text{Ph}_2$ in THF.

$\alpha(\text{OHex})\text{Tol}_2$ and $\beta(\text{O}i\text{-Pent})\text{Tol}_2$

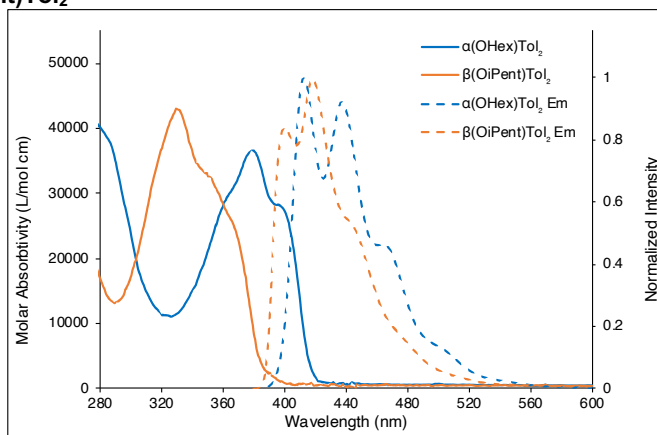


Figure 91. Absorbance and emission spectra for $\alpha(\text{OHex})\text{Tol}_2$ and $\beta(\text{O}i\text{-Pent})\text{Tol}_2$ in THF.

$\alpha(\text{OHex})(\text{PhOMe})_2$ and $\beta(\text{Oi-Pent})(\text{PhOMe})_2$

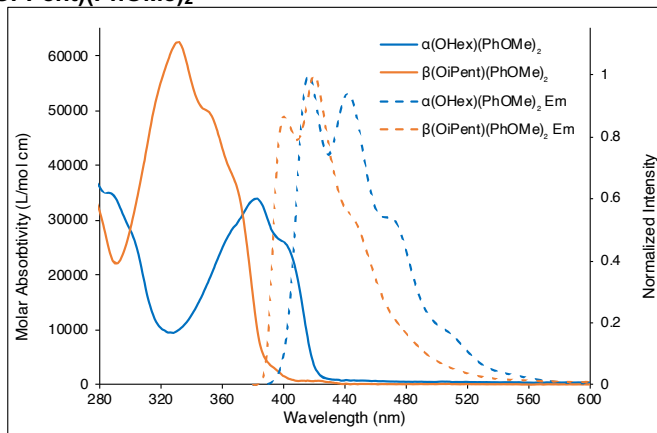


Figure 92. Absorbance and emission spectra for $\alpha(\text{OHex})(\text{PhOMe})_2$ and $\beta(\text{Oi-Pent})(\text{PhOMe})_2$ in THF.

$\alpha(\text{OHex})(\text{PhCF}_3)_2$ and $\beta(\text{Oi-Pent})(\text{PhCF}_3)_2$

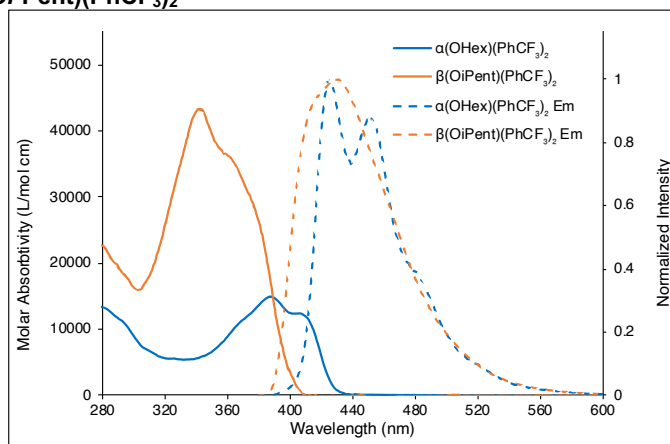


Figure 93. Absorbance and emission spectra for $\alpha(\text{OHex})(\text{PhCF}_3)_2$ and $\beta(\text{Oi-Pent})(\text{PhCF}_3)_2$ in THF.

$\alpha(\text{OHex})\text{R}_2$ Series

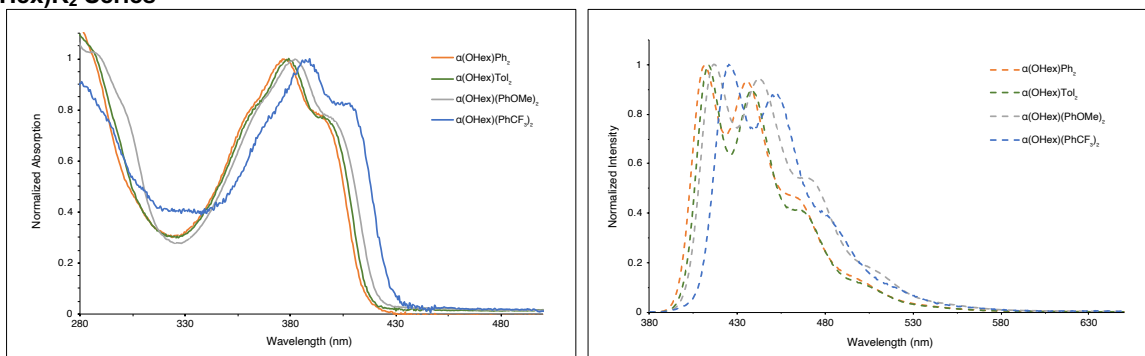


Figure 94. Normalised absorbance and emission spectra for $\alpha(\text{OHex})\text{R}_2$ Series in THF.

$\beta(\text{O}i\text{-Pent})\text{R}_2$ Series

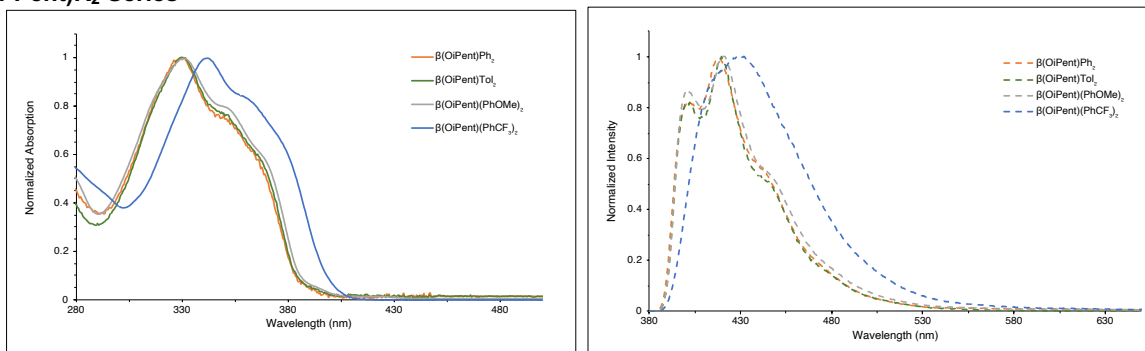


Figure 95. Normalised absorbance and emission spectra for $\beta(\text{O}i\text{-Pent})\text{R}_2$ Series in THF.

Solvatochromism Analysis, $\beta(\text{O}i\text{-Pent})(\text{PhCF}_3)_2$

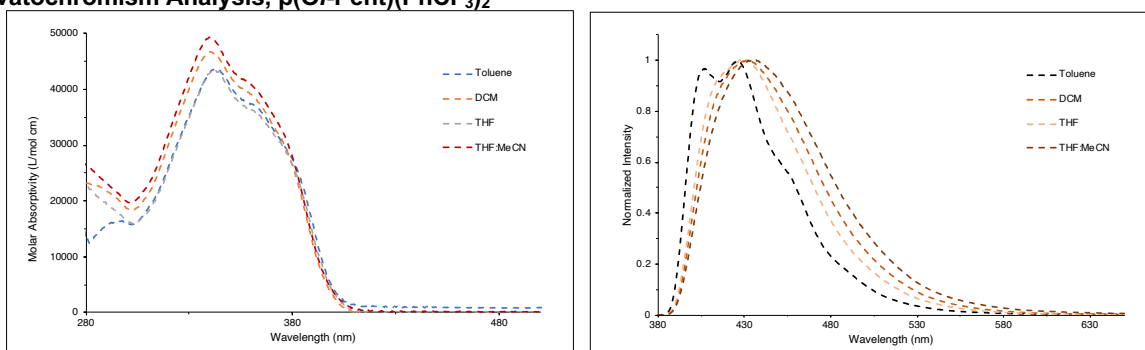


Figure 96. Absorbance and emission spectra for $\beta(\text{O}i\text{-Pent})(\text{PhCF}_3)_2$ in: THF, toluene, DCM, and THF·MeCN (1:1).

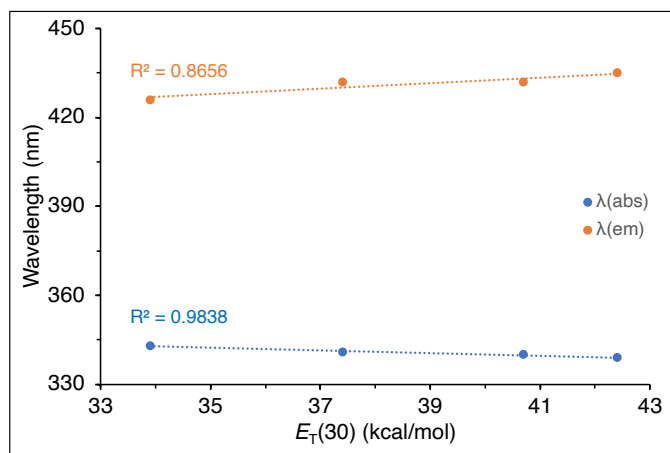


Figure 97. Plot of absorbance and emission normalized maxima λ vs $E_T(30)$ parameter for $\beta(\text{O}i\text{-Pent})(\text{PhCF}_3)_2$ in THF, toluene, DCM, and THF·MeCN (1:1).

4) Solution-State Analysis

Concentration dependent ^1H NMR analysis

A series of $\alpha(\text{OHex})\text{R}_2$ and $\beta(\text{Oi-Pent})\text{R}_2$ solutions in CDCl_3 were probed via ^1H NMR spectroscopy to determine the extent of solution-state aggregation. Over the concentration range probed (50-1 mM, actual concentrations see Table S1) only minor ($\Delta\delta$) are observed across aromatic and alkoxy resonances ($\Delta\delta < 0.15$ ppm for all resonances). Chemical shifts with $\Delta\delta \geq 0.05$ ppm were fit over the concentration range with the NMR aggregation model in Bindfit.⁷

Aggregation Analysis, $\alpha(\text{OHex})\text{Ph}_2$

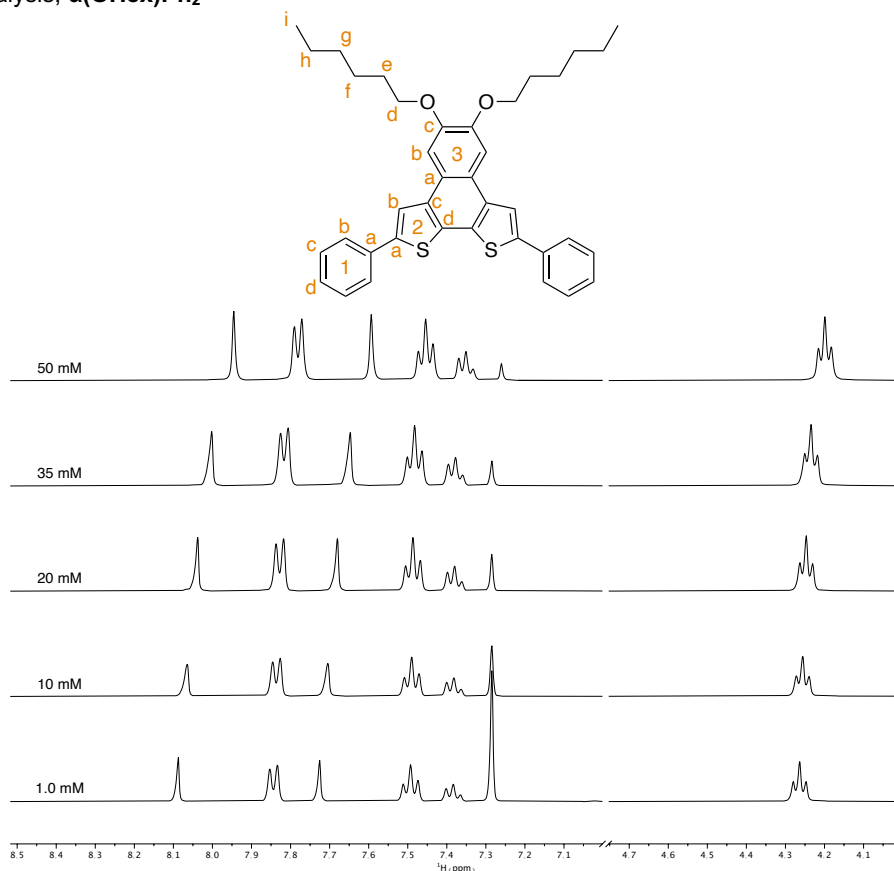


Figure 98. Partial ^1H NMR spectra of $\alpha(\text{OHex})\text{Ph}_2$ (50–1 mM, CDCl_3 , 400 MHz, 298K), $K_d = 3.2 \times 10^{-4} \pm 1.6 \times 10^{-4}$ M.

| Conc. (mM) | 1b | 1c | 1d | 2b | 3b | 3d |
|------------------|--------|--------|--------|--------|--------|--------|
| 50 | 7.781 | 7.454 | 7.351 | 7.945 | 7.593 | 4.119 |
| 35 | 7.792 | 7.458 | 7.353 | 7.977 | 7.623 | 4.21 |
| 20 | 7.803 | 7.462 | 7.355 | 8.014 | 7.657 | 4.222 |
| 10 | 7.812 | 7.465 | 7.357 | 8.041 | 7.681 | 4.232 |
| 1.0 | 7.819 | 7.468 | 7.359 | 8.063 | 7.701 | 4.239 |
| $\Delta\delta =$ | -0.038 | -0.014 | -0.008 | -0.118 | -0.108 | -0.120 |

Table 1. ^1H chemical shifts for $\alpha(\text{OHex})\text{Ph}_2$ (50–1 mM, CDCl_3 , 400 MHz, 298K) used in analysis.

Aggregation Analysis, $\alpha(\text{OHex})(\text{PhOMe})_2$

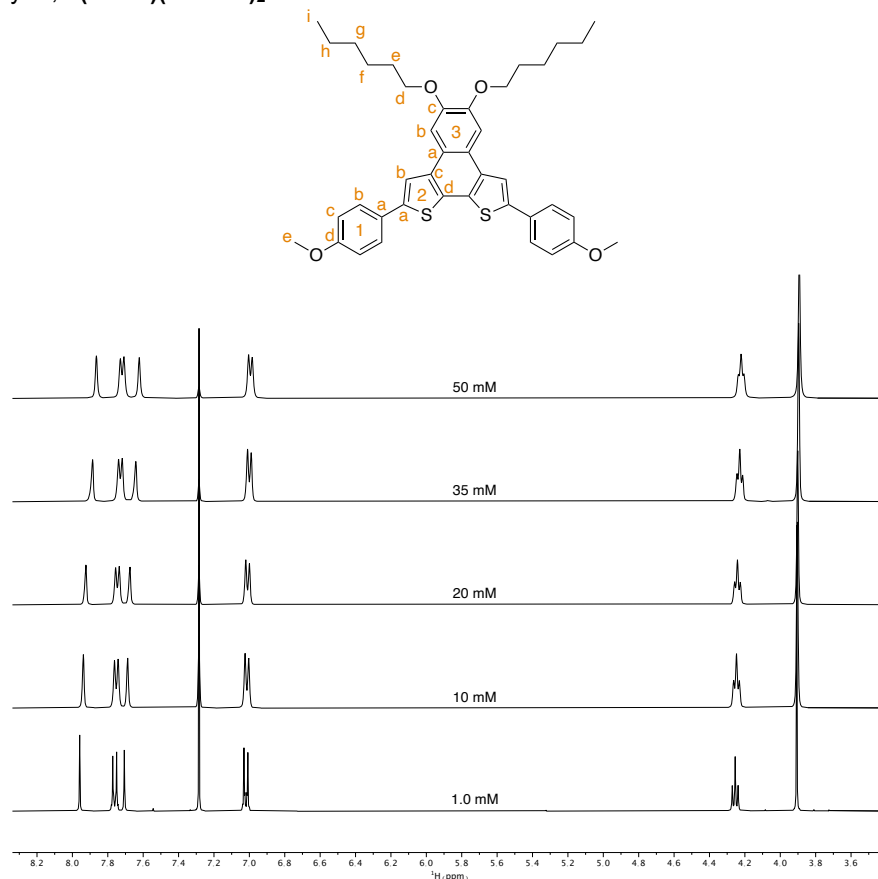


Figure 99. Partial ^1H NMR spectra of $\alpha(\text{OHex})(\text{PhOMe})_2$ (50–1 mM, CDCl_3 , 400 MHz, 298K), $K_d = 1.2 \pm 0.6$ M.

| Conc. (mM) | 1b | 1c | 1e | 2b | 3b | 3d |
|------------------|--------|--------|--------|--------|--------|--------|
| 50 | 7.719 | 6.994 | 3.892 | 7.864 | 7.622 | 4.221 |
| 35 | 7.729 | 7.000 | 3.896 | 7.886 | 7.642 | 4.229 |
| 20 | 7.745 | 7.010 | 3.902 | 7.924 | 7.675 | 4.242 |
| 10 | 7.752 | 7.011 | 3.904 | 7.939 | 7.688 | 4.247 |
| 1.0 | 7.761 | 7.019 | 3.907 | 7.959 | 7.707 | 4.255 |
| $\Delta\delta =$ | -0.042 | -0.025 | -0.015 | -0.095 | -0.085 | -0.034 |

Table 2. ^1H chemical shifts for $\alpha(\text{OHex})(\text{PhOMe})_2$ (50–1 mM, CDCl_3 , 400 MHz, 298K) used in analysis.

Aggregation Analysis, $\beta(\text{O}i\text{-Pent})\text{Tol}_2$

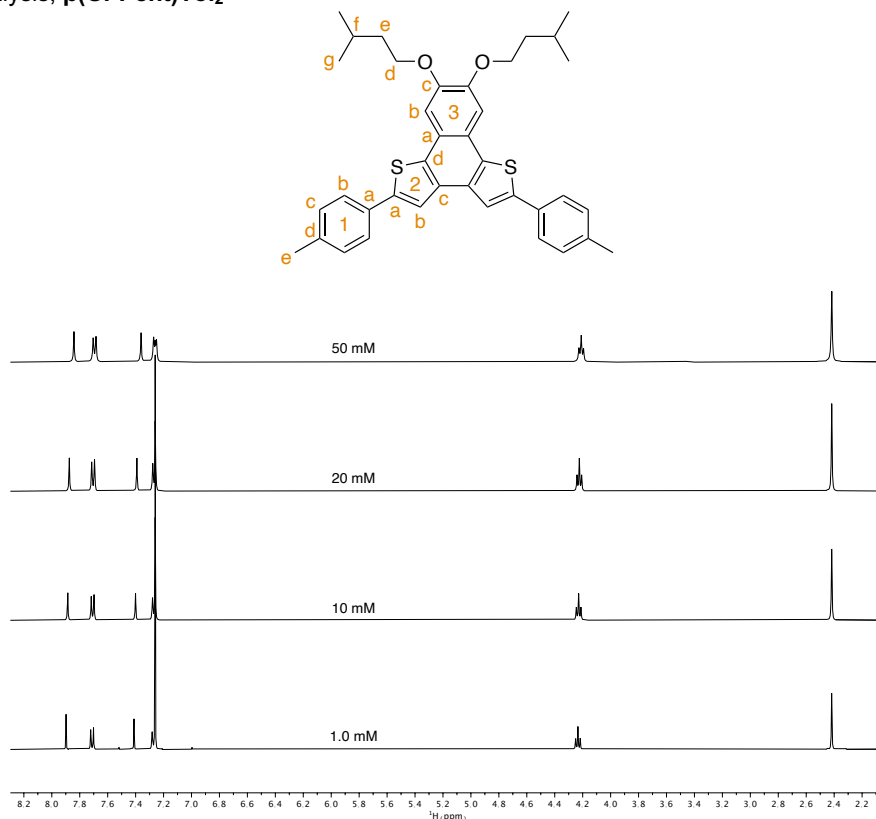


Figure 100. Partial ^1H NMR spectra of $\beta(\text{O}i\text{-Pent})\text{Tol}_2$ (50–1 mM, CDCl_3 , 400 MHz, 298K), $K_d = 1.1 \pm 0.6$ M.

| Conc. (mM) | 1b | 1c | 1e | 2b | 3b | 3d |
|------------------|--------|-------|--------|--------|--------|--------|
| 50 | 7.694 | 7.261 | 2.417 | 7.841 | 7.361 | 4.210 |
| 20 | 7.704 | 7.269 | 2.418 | 7.875 | 7.391 | 4.224 |
| 10 | 7.708 | 7.260 | 2.418 | 7.886 | 7.401 | 4.229 |
| 1.0 | 7.712 | 7.260 | 2.418 | 7.898 | 7.412 | 4.234 |
| $\Delta\delta =$ | -0.018 | 0.001 | -0.001 | -0.057 | -0.051 | -0.024 |

Table 3. ^1H chemical shifts for $\beta(\text{O}i\text{-Pent})\text{Tol}_2$ (50–1 mM, CDCl_3 , 400 MHz, 298K) used in analysis.

Aggregation Analysis, $\beta(\text{O}i\text{-Pent})(\text{PhOMe})_2$

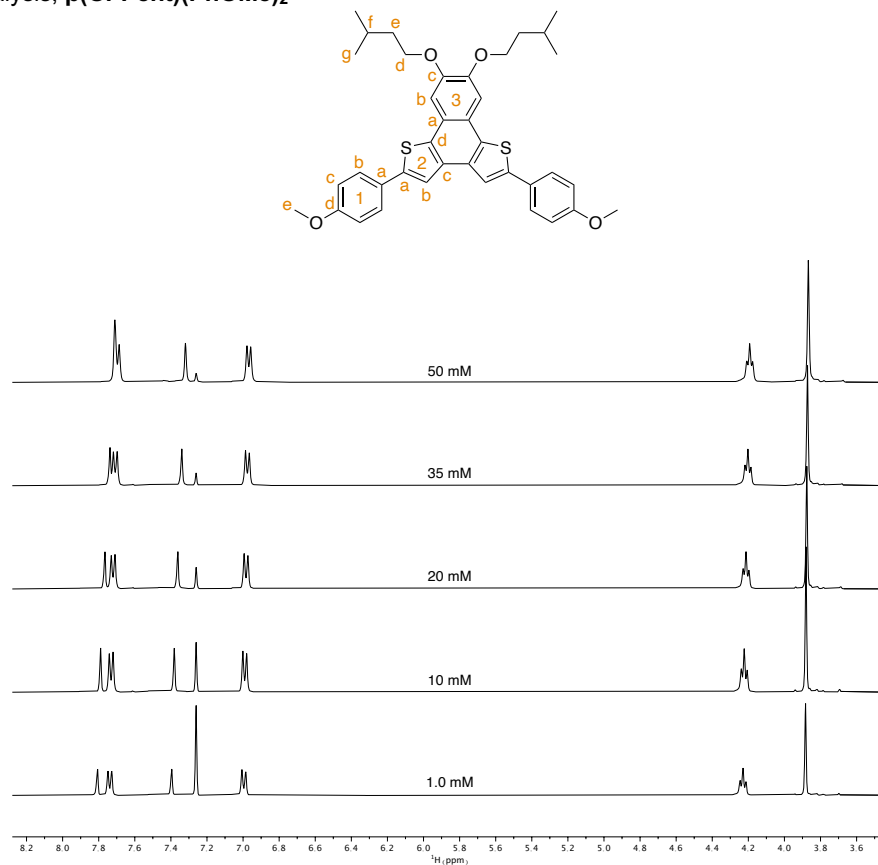


Figure 101. Partial ^1H NMR spectra of $\beta(\text{O}i\text{-Pent})(\text{PhOMe})_2$ (50–1 mM, CDCl_3 , 400 MHz, 298K), $K_d = 1.5 \pm 0.8$ M.

| Conc. (mM) | 1b | 1c | 1d | 2b | 3b | 3d |
|------------------|--------|--------|--------|--------|--------|--------|
| 50 | 7.702 | 6.968 | 3.868 | 7.710 | 7.319 | 4.192 |
| 35 | 7.708 | 6.976 | 3.872 | 7.738 | 7.340 | 4.202 |
| 20 | 7.720 | 6.984 | 3.876 | 7.766 | 7.362 | 4.213 |
| 10 | 7.731 | 6.991 | 3.880 | 7.790 | 7.381 | 4.223 |
| 1.0 | 7.738 | 6.996 | 3.883 | 7.807 | 7.396 | 4.230 |
| $\Delta\delta =$ | -0.036 | -0.028 | -0.015 | -0.097 | -0.077 | -0.038 |

Table 4. ^1H chemical shifts for $\beta(\text{O}i\text{-Pent})(\text{PhOMe})_2$ (50–1 mM, CDCl_3 , 400 MHz, 298K) used in analysis.

Comparison of remote chemical shifts in ^1H and ^{13}C

The chemical shifts of interior 2b ^1H and ^{13}C shift upfield for electron donating groups and downfield for electron. The Hammett parameters (σ) for both para and meta can be contrasted against these 2b resonances. The fits are presented, wherein σ_{para} provides quality fits (given in blue) while σ_{meta} (shown in orange) yields poor fits.

$\alpha(\text{OHex})\text{R}_2$ Series

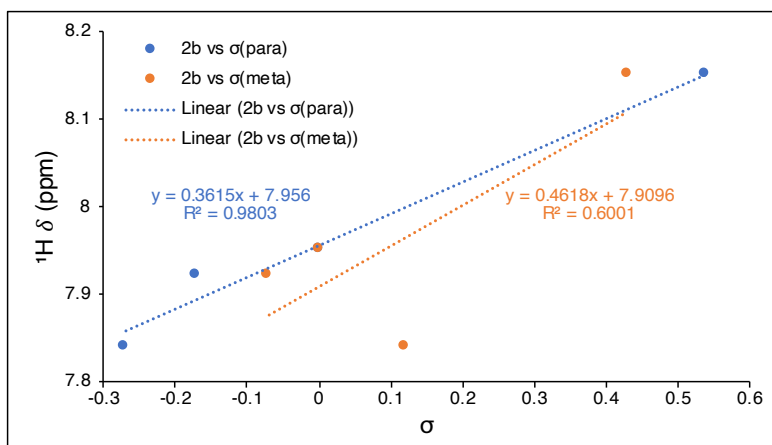


Figure 102. Plot of $\alpha(\text{OHex})\text{R}_2$ ^1H δ (ppm) vs σ .

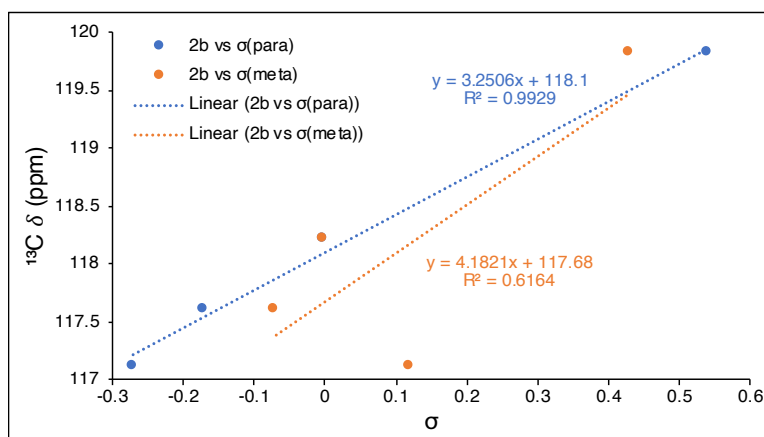


Figure 103. Plot of $\alpha(\text{OHex})\text{R}_2$ ^{13}C δ (ppm) vs σ .

| $\alpha(\text{OHex})\text{R}_2$ | 2b resonances | | | |
|--|-----------------------------|--------------------------------|------------|------------|
| | ^1H δ (ppm) | ^{13}C δ (ppm) | σ_m | σ_p |
| $\alpha(\text{OHex})\text{Ph}_2$ | 7.95 | 118.2 | 0.00 | 0.00 |
| $\alpha(\text{OHex})\text{ToI}_2$ | 7.92 | 117.6 | -0.07 | -0.17 |
| $\alpha(\text{OHex})(\text{PhOMe})_2$ | 7.84 | 117.1 | 0.12 | -0.27 |
| $\alpha(\text{OHex})(\text{PhCF}_3)_2$ | 8.15 | 119.8 | 0.43 | 0.54 |

Table 5. 2b resonances and Hammett parameters for $\alpha(\text{OHex})\text{R}_2$ Series.

$\alpha(\text{OMe})\text{R}_2$ Series

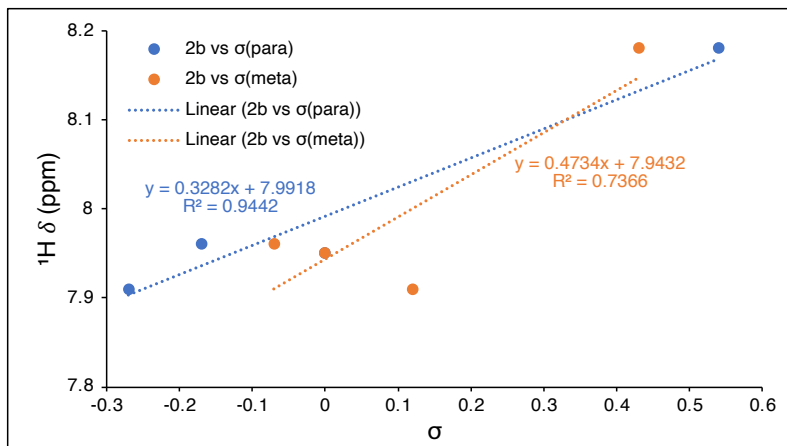


Figure 104. Plot of $\alpha(\text{OMe})\text{R}_2$ ^1H δ (ppm) vs σ .

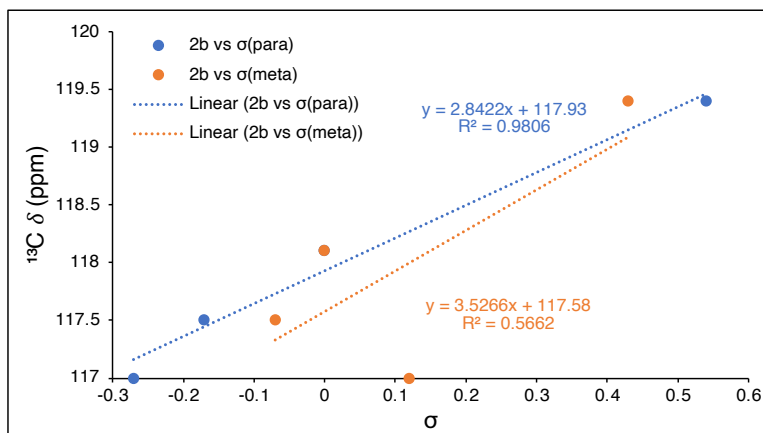


Figure 105. Plot of $\alpha(\text{OMe})\text{R}_2$ ^{13}C δ (ppm) vs σ .

| $\alpha(\text{OHex})\text{R}_2$ | 2b resonances | | | |
|--|-----------------------------|--------------------------------|------------|------------|
| | ^1H δ (ppm) | ^{13}C δ (ppm) | σ_m | σ_p |
| $\alpha(\text{OHex})\text{Ph}_2$ | 7.95 | 118.1 | 0.00 | 0.00 |
| $\alpha(\text{OHex})\text{Tol}_2$ | 7.96 | 117.5 | -0.07 | -0.17 |
| $\alpha(\text{OHex})(\text{PhOMe})_2$ | 7.91 | 117.0 | 0.12 | -0.27 |
| $\alpha(\text{OHex})(\text{PhCF}_3)_2$ | 8.18 | 119.4 | 0.43 | 0.54 |

Table 6. 2b resonances and Hammett parameters for $\alpha(\text{OMe})\text{R}_2$ Series.

$\beta(\text{O}i\text{-Pent})\text{R}_2$ Series

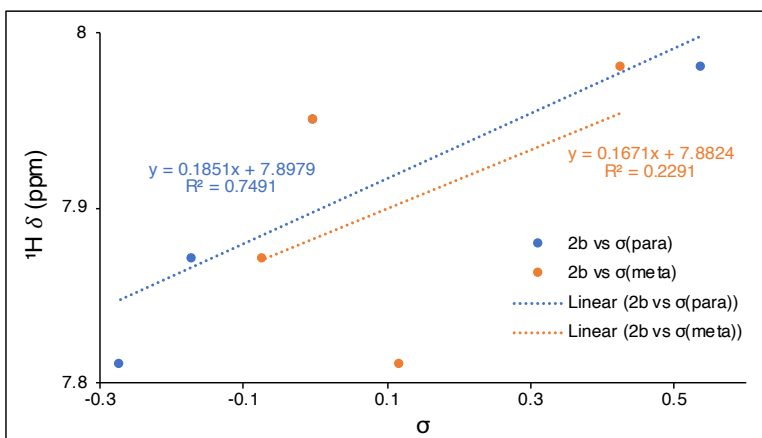


Figure 106. Plot of $\beta(\text{O}i\text{-Pent})\text{R}_2$ ^1H δ (ppm) vs σ .

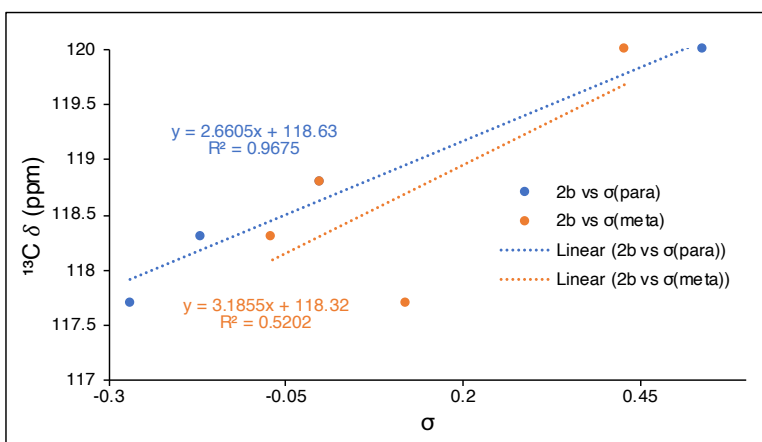


Figure 107. Plot of $\beta(\text{O}i\text{-Pent})\text{R}_2$ ^{13}C δ (ppm) vs σ .

| $\beta(\text{O}i\text{-Pent})\text{R}_2$ | 2b resonances | | | |
|---|-----------------------------|--------------------------------|------------|------------|
| | ^1H δ (ppm) | ^{13}C δ (ppm) | σ_m | σ_p |
| $\beta(\text{O}i\text{-Pent})\text{Ph}_2$ | 7.95 | 118.8 | 0.00 | 0.00 |
| $\beta(\text{O}i\text{-Pent})\text{Tol}_2$ | 7.87 | 118.3 | -0.07 | -0.17 |
| $\beta(\text{O}i\text{-Pent})(\text{PhOMe})_2$ | 7.81 | 117.7 | 0.12 | -0.27 |
| $\beta(\text{O}i\text{-Pent})(\text{PhCF}_3)_2$ | 7.98 | 120.0 | 0.43 | 0.54 |

Table 7. 2b resonances and Hammett parameters for $\beta(\text{O}i\text{-Pent})\text{R}_2$ Series.

5) Computational Analysis

For the computational analysis, we modeled four different substituents on the α - and β -NDT series along with an unfunctionalized species using non-relativistic density functional theory implemented in Gaussian 16. We use the non-relativistic methods due to the molecule only containing light elements (the heaviest being sulfur). We settled on the widele popular and well-performing global hybrid exchange correlation functional (XCF) B3LYP. The basis sets we used are the polarization-consistent sets developed by the Jensen group, which systematically reduces the basis set error. Each molecule initially underwent a geometry optimization before NMR calculations. The pc-2 basis set used for geometry optimisation and the B3LYP exchange correlation functional. After geometry optimisation, NICS scans were completed using the Aroma python package with Gaussian 16. The first NICS scan was done to determine the height needed about the plane for the NICS-XY scan. This initial scan was done in the center of each aromatic ring and scanning in 0.1 Å increments along the Z-axis outside of the plane. This was done to find the optimal height to perform an NICS-XY scan where the electrons of the σ -bond are removed and only the π -electron contribution is observed. The height of 1.7 Å was determined to be the optimal height to perform a NICS-XY scan to remove σ -bonding effects, consistent with others. Each scan was performed along the same path for each molecule using the aug-pcSseg-2 basis set and the B3LYP XCF. The aug-pcSseg-2 basis set contains extra tight exponents in the p functions to better describe the behaviour near the nucleus and optimised to the nuclear magnetic shielding constant, while also containing extra diffused functions to create a more complete basis. Overall reducing the basis set error for NMR calculations. Additionally, ^1H and ^{13}C NMR spectra were modeled using the GIAO method using the aug-pcSseg-2 basis set with the B3LYP XCF (the PBE0 XCF was tested as well, with the resultant NMR spectra being insensitive to the XCF employed).

$\alpha(\text{OMe})R_2'$ Series Models

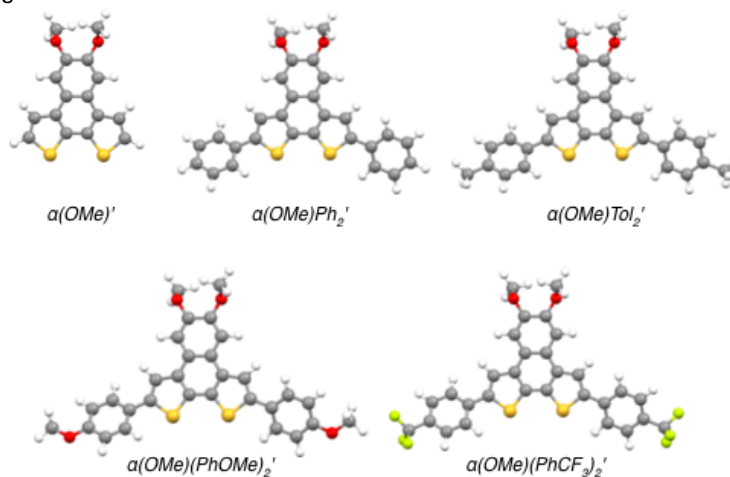


Figure 108. Optimized geometries of $\alpha(\text{OMe})R_2'$ Series.

| Model Compound | Total Energy (E_h) | ZPC (E_h) | Energy _{Total Energy + ZPC} (E_h) | IF |
|--|------------------------|---------------|--|----|
| $\alpha(\text{OMe})'$ | -1564.12683440 | 0.237891 | -1563.888943 | 0 |
| $\alpha(\text{OMe})\text{Ph}_2'$ | -2026.42019070 | 0.399396 | -2026.020795 | 0 |
| $\alpha(\text{OMe})\text{Tol}_2'$ | -2105.08669746 | 0.453568 | -2104.633129 | 0 |
| $\alpha(\text{OMe})(\text{PhOMe})_2'$ | -2255.56595208 | 0.463866 | -2255.102086 | 0 |
| $\alpha(\text{OMe})(\text{PhCF}_3)_2'$ | -2700.81348131 | 0.408085 | -2700.405396 | 0 |

Table 8. Computational data for optimized $\alpha(\text{OMe})R_2'$ models. ZPC = zero-point correction, IF = number of imaginary frequencies.

$\beta(\text{OMe})R_2'$ Series Models

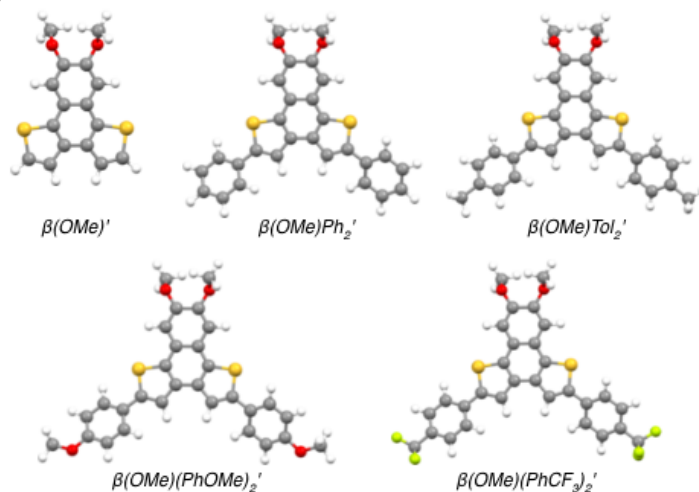


Figure 109. Optimized geometries of $\beta(\text{OMe})R_2'$ Series.

| Model Compound | Total Energy (E_h) | ZPC (E_h) | Energy _{Total Energy + ZPC} (E_h) | IF |
|--------------------------------|------------------------|---------------|--|----|
| $\beta(\text{OMe})'$ | -1564.12810479 | 0.237883 | -1563.890222 | 0 |
| $\beta(\text{OMe})Ph_2'$ | -2026.42118837 | 0.399338 | -2026.021850 | 0 |
| $\beta(\text{OMe})Tol_2'$ | -2255.56723982 | 0.453518 | -2255.113722 | 0 |
| $\beta(\text{OMe})(PhOMe)_2'$ | -2255.56723982 | 0.463811 | -2255.103429 | 0 |
| $\beta(\text{OMe})(PhCF_3)_2'$ | -2700.81449738 | 0.408029 | -2700.406468 | 0 |

Table 9. Computational data for optimized $\beta(\text{OMe})R_2'$ models. ZPC = zero-point correction, IF = number of imaginary frequencies.

Experimental vs Calculated Chemical Shift Analysis

The isotropic shieldings for the model compounds with the alkoxy groups simplified to methoxy groups were computed for both protons and carbons using the GIAO method with the aug-pcSseg-2 basis set and B3LYP XCF in Gaussian 16. The experimental chemical shifts (ppm) were extracted from ^1H - ^{13}C HSQC. Consistently across all molecules the interior 3b proton and carbon are underestimated.

$\alpha(\text{OHex})\text{Ph}_2$

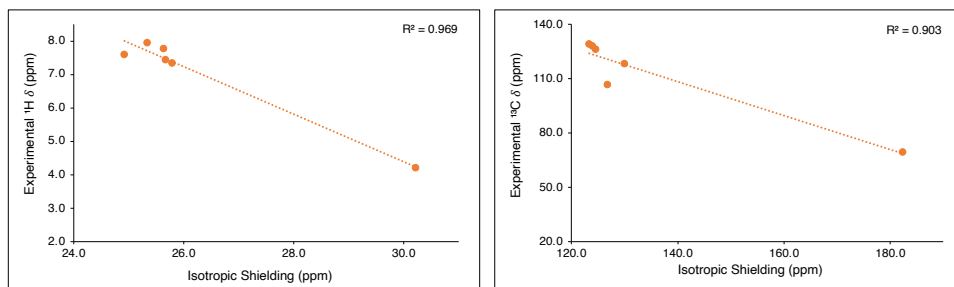


Figure 110. Comparison of experimental vs calculated ^1H (left) and ^{13}C (right) resonances (δ) for $\alpha(\text{OHex})\text{Ph}_2$ (experimental) and $\alpha(\text{OMe})\text{Ph}_2'$ (calculated).

$\alpha(\text{OHex})\text{Tol}_2$

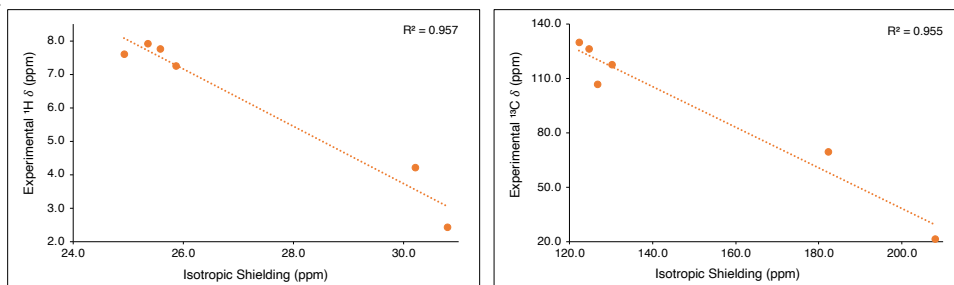


Figure 111. Comparison of experimental vs calculated ^1H (left) and ^{13}C (right) resonances (δ) for $\alpha(\text{OHex})\text{Tol}_2$ (experimental) and $\alpha(\text{OMe})\text{Tol}_2'$ (calculated).

$\alpha(\text{OHex})(\text{PhOMe})_2$

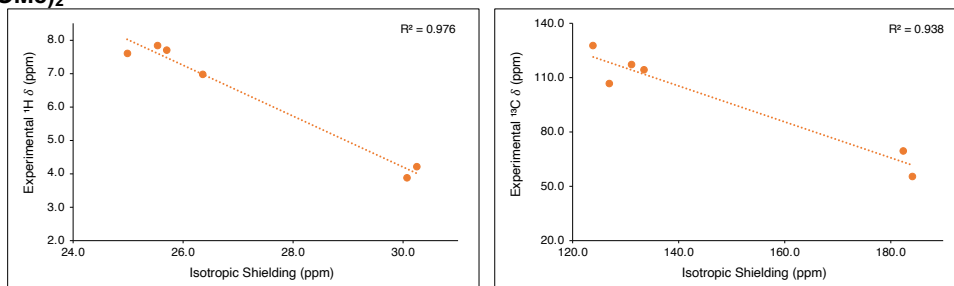


Figure 112. Comparison of experimental vs calculated ^1H (left) and ^{13}C (right) resonances (δ) for $\alpha(\text{OHex})(\text{PhOMe})_2$ (experimental) and $\alpha(\text{OMe})(\text{PhOMe})_2'$ (calculated).

$\alpha(\text{OHex})(\text{PhCF}_3)_2$

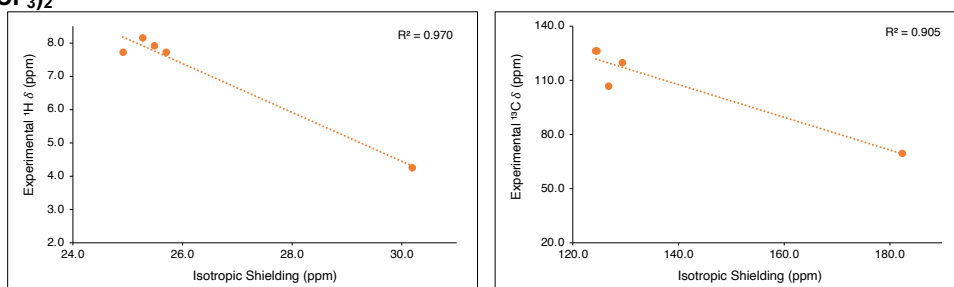


Figure 113. Comparison of experimental vs calculated ^1H (left) and ^{13}C (right) resonances (δ) for $\alpha(\text{OHex})(\text{PhCF}_3)_2$ (experimental) and $\alpha(\text{OMe})(\text{PhCF}_3)_2'$ (calculated).

$\alpha(\text{OMe})\text{Ph}_2$

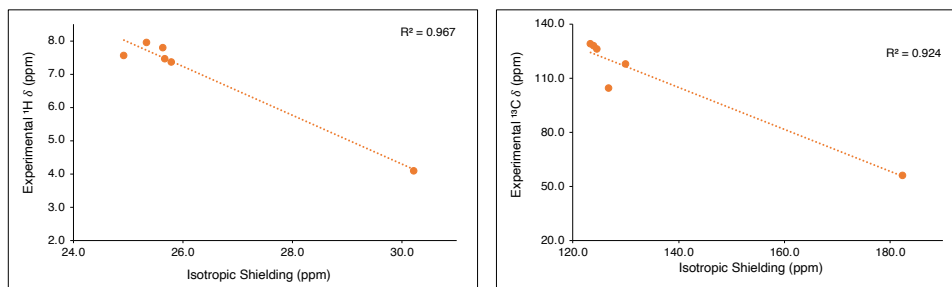


Figure 114. Comparison of experimental vs calculated ^1H (left) and ^{13}C (right) resonances (δ) for $\alpha(\text{OHex})\text{Ph}_2$ (experimental) and $\alpha(\text{OMe})\text{Ph}_2'$ (calculated).

$\alpha(\text{OMe})\text{Tol}_2$

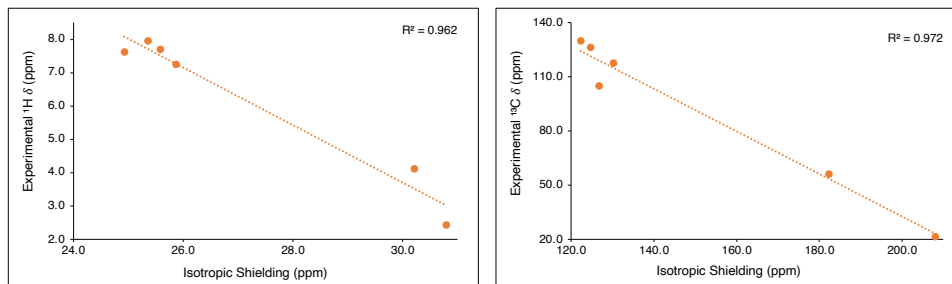


Figure 115. Comparison of experimental vs calculated ^1H (left) and ^{13}C (right) resonances (δ) for $\alpha(\text{OHex})\text{Tol}_2$ (experimental) and $\alpha(\text{OMe})\text{Tol}_2'$ (calculated).

$\alpha(\text{OMe})(\text{PhOMe})_2$

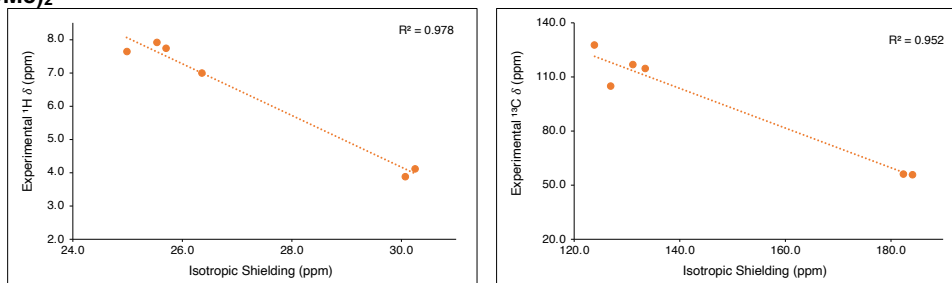


Figure 116. Comparison of experimental vs calculated ^1H (left) and ^{13}C (right) resonances (δ) for $\alpha(\text{OHex})(\text{PhOMe})_2$ (experimental) and $\alpha(\text{OMe})(\text{PhOMe})_2'$ (calculated).

$\alpha(\text{OMe})(\text{PhCF}_3)_2$

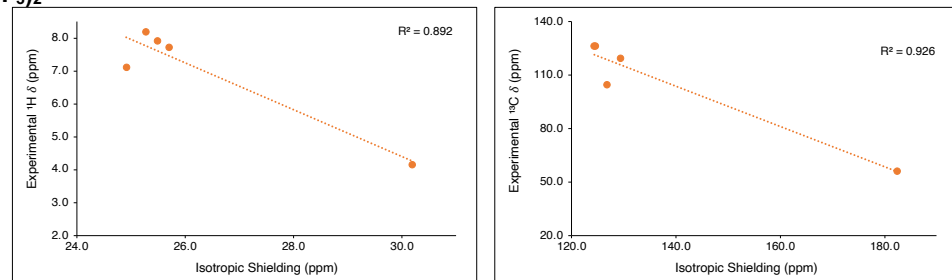


Figure 117. Comparison of experimental vs calculated ^1H (left) and ^{13}C (right) resonances (δ) for $\alpha(\text{OHex})(\text{PhCF}_3)_2$ (experimental) and $\alpha(\text{OMe})(\text{PhCF}_3)_2'$ (calculated).

$\beta(\text{O}i\text{-Pent})\text{Ph}_2$

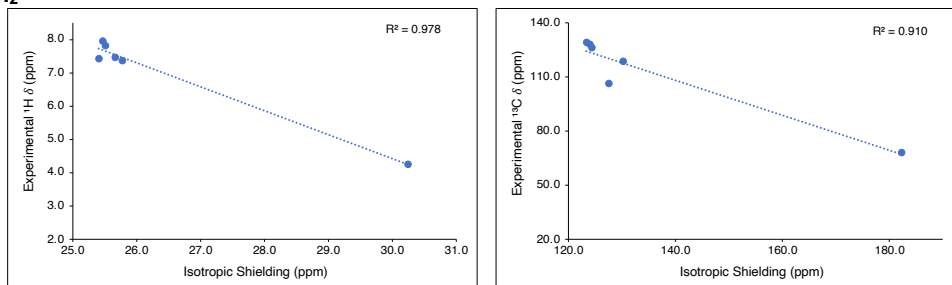


Figure 118. Comparison of experimental vs calculated ^1H (left) and ^{13}C (right) resonances (δ) for $\beta(\text{O}i\text{-Pent})\text{Ph}_2$ (experimental) and $\beta(\text{OMe})\text{Ph}_2'$ (calculated).

$\beta(\text{O}i\text{-Pent})\text{Tol}_2$

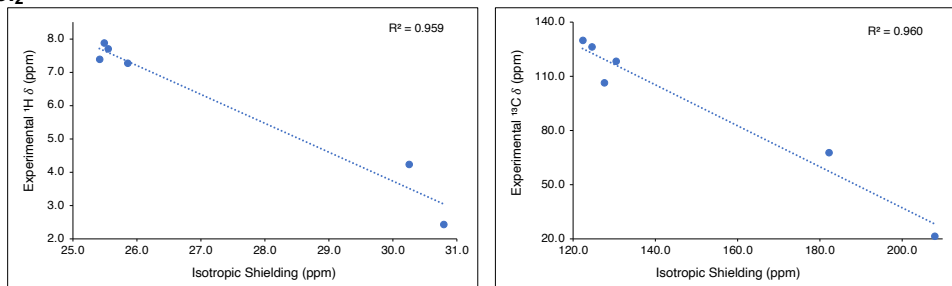


Figure 119. Comparison of experimental vs calculated ^1H (left) and ^{13}C (right) resonances (δ) for $\beta(\text{O}i\text{-Pent})\text{Tol}_2$ (experimental) and $\beta(\text{OMe})\text{Tol}_2'$ (calculated).

$\beta(\text{O}i\text{-Pent})(\text{PhOMe})_2$

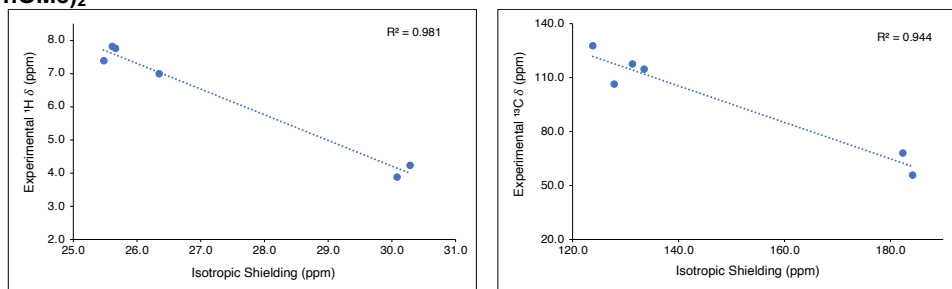


Figure 120. Comparison of experimental vs calculated ^1H (left) and ^{13}C (right) resonances (δ) for $\beta(\text{O}i\text{-Pent})(\text{PhOMe})_2$ (experimental) and $\beta(\text{OMe})(\text{PhOMe})_2'$ (calculated).

$\beta(\text{O}i\text{-Pent})(\text{PhCF}_3)_2$

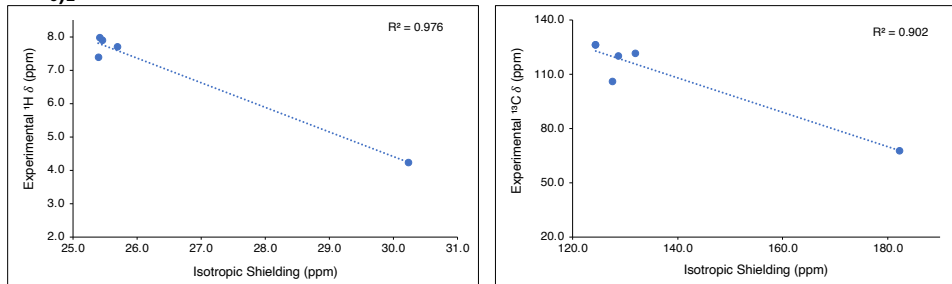


Figure 121. Comparison of experimental vs calculated ^1H (left) and ^{13}C (right) resonances (δ) for $\beta(\text{O}i\text{-Pent})(\text{PhCF}_3)_2$ (experimental) and $\beta(\text{OMe})(\text{PhCF}_3)_2'$ (calculated).

Nucleus Independent Chemical Shift (NICS)-XY Scans

Optimised geometries (given in Figures 108 and 109) were performed using the AROMA package⁸ and referenced against unsubstituted model compounds $\alpha(\text{OMe})'$ and $\beta(\text{OMe})'$.

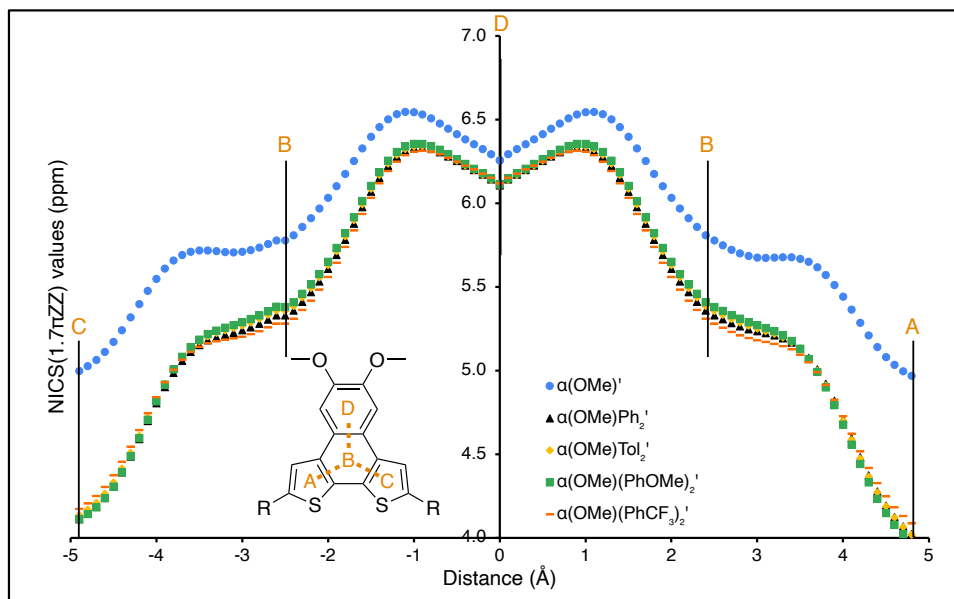


Figure 122. NICS_{1.7 π ZZ} scans for $\alpha(\text{OMe})R_2'$ Series.

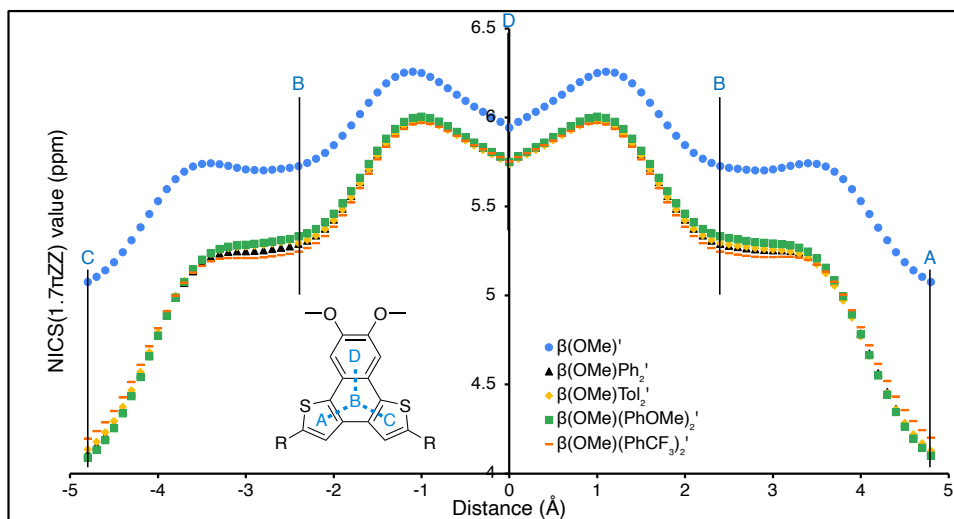


Figure 123. NICS_{1.7 π ZZ} scans for $\beta(\text{OMe})R_2'$ Series.

6) Crystallographic Analysis

Crystallographic analysis and data for $\alpha(\text{OMe})\text{Ph}_2$, $\alpha(\text{OMe})\text{Tol}_2$, $\alpha(\text{OMe})(\text{PhOMe})_2$, $\alpha(\text{OMe})(\text{PhCF}_3)_2$, and $\beta(\text{O}i\text{-Pent})\text{Tol}_2$ are presented below. Data were collected from a single crystal at 150(2) K on a Bruker AXS D8 Quest three circle diffractometer with a fine focus sealed tube X-ray source using a Triumph curved graphite crystal as monochromator and a PhotonII charge-integrating pixel array (CPAD) detector. The diffractometer was equipped with a low temperature device and used $\text{MoK}\alpha$ radiation ($\lambda = 0.71073 \text{ \AA}$). All data were integrated with SAINT and a multi-scan absorption correction using SADABS was applied.^{9,10} The crystal was solved by dual methods using SHELXT and refined by full-matrix least-squares methods against F^2 by SHELXL-2018/3.^{11,12} All non-hydrogen atoms were refined with anisotropic displacement parameters. All hydrogen atoms were refined isotropic on calculated positions using a riding model with their U_{iso} values constrained to 1.5 times the U_{eq} of their pivot atoms for terminal sp^3 carbon atoms and 1.2 times for all other carbon atoms. Disordered moieties were refined using bond lengths restraints and displacement parameter restraints. Tables and general reports were generated with FinalCif and edited accordingly.¹³ Any additional refinement notes are detailed below, all structures have been deposited in the Cambridge Crystallographic Data Centre (CCDC)¹⁴ with their deposition numbers given.

$\alpha(\text{OMe})\text{Ph}_2$

Single crystals of $\alpha(\text{OMe})\text{Ph}_2$ were obtained through vapor diffusion of hexanes into a saturated solution of $\alpha(\text{OMe})\text{Ph}_2$ in THF (Figure 124). One of the phenyl rings is disordered by a twist-rotation. The two disordered moieties were restrained to have similar geometries as the other not disordered phenyl ring. The ipso-C atom was omitted from the disorder. U_{ij} components of ADPs for disordered atoms closer to each other than 2.0 Å were restrained to be similar. Subject to these conditions the occupancy ratio refined to 0.501(3) to 0.499(3). CCDC number: 2361476

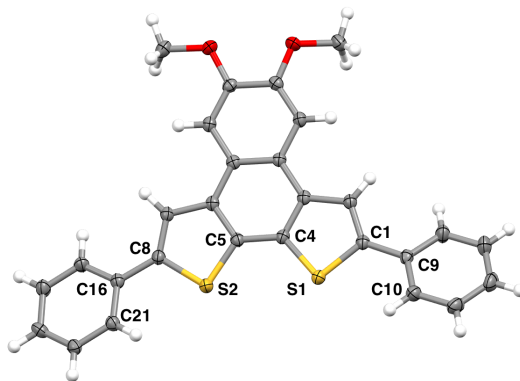


Figure 124. ORTEP diagram of $\alpha(\text{OMe})\text{Ph}_2$ (ellipsoids drawn at 50% probability). Hydrogens have been omitted for clarity. Select bond lengths (Å) and angles (°): C8–S2, 1.745(1); C5–S2, 1.720(1); C4–S1, 1.727(1); S1–C1, 1.743(1); C24–C23–C8–S2, 19.9(2); S2–C5–C4–S1, -3.4(2); S1–C1–C17–C18, -18.5(2).

| | a(OMe)Ph₂ |
|---|--|
| Empirical formula | C ₂₈ H ₂₀ O ₂ S ₂ |
| Formula weight | 452.56 |
| Temperature [K] | 150(2) |
| Crystal system | monoclinic |
| Space group (number) | <i>P</i> 2 ₁ / <i>c</i> (14) |
| <i>a</i> [Å] | 4.8146(4) |
| <i>b</i> [Å] | 20.525(2) |
| <i>c</i> [Å] | 21.556(3) |
| α [°] | 90 |
| β [°] | 90.453(5) |
| γ [°] | 90 |
| Volume [Å ³] | 2130.1(4) |
| <i>Z</i> | 4 |
| ρ_{calc} [gcm ⁻³] | 1.411 |
| μ [mm ⁻¹] | 0.275 |
| <i>F</i> (000) | 944 |
| Crystal size [mm ³] | 0.550×0.080×0.070 |
| Crystal color | yellow |
| Crystal shape | needle |
| Radiation | MoK α (λ =0.71073 Å) |
| 2 θ range [°] | 4.40 to 66.37 (0.65 Å) |
| Index ranges | -6 ≤ <i>h</i> ≤ 7 -31 ≤ <i>k</i> ≤ 31 -32 ≤ <i>l</i> ≤ 33 |
| Reflections collected | 40142 |
| Independent reflections | 7984 <i>R</i> _{int} = 0.0684 <i>R</i> _{sigma} = 0.0505 |
| Completeness to θ = 25.242° | 99.7 % |
| Data / Restraints / Parameters | 7984/216/337 |
| Goodness-of-fit on <i>F</i> ² | 1.028 |
| Final <i>R</i> indexes [$\geq 2\sigma(I)$] | <i>R</i> ₁ = 0.0425 <i>wR</i> ₂ = 0.0954 |
| Final <i>R</i> indexes [all data] | <i>R</i> ₁ = 0.0750 <i>wR</i> ₂ = 0.1081 |
| Largest peak/hole [eÅ ⁻³] | 0.41/-0.38 |

Table 10. Crystallographic data and structural refinement parameters, **a(OMe)Ph₂**.

$\alpha(\text{OMe})\text{Tol}_2$

Single crystals of $\alpha(\text{OMe})\text{Tol}_2$ were obtained through vapor diffusion of hexanes into a saturated solution of $\alpha(\text{OMe})\text{Tol}_2$ in THF (Figure 125). CCDC number: 2361477

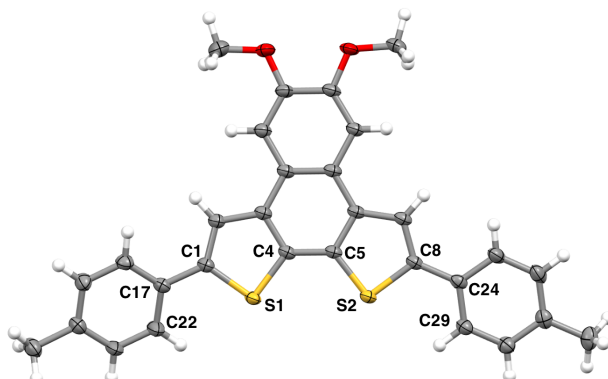


Figure 125. ORTEP diagram of $\alpha(\text{OMe})\text{Tol}_2$ (ellipsoids drawn at 50% probability). Hydrogens have been omitted for clarity. Select bond lengths (Å) and angles ($^\circ$): C1–S1, 1.745(1); C4–S1, 1.730(1); C5–S2, 1.721(1); C8–S2, 1.748(1); C22–C17–C1–S1, $-16.9(2)$; S1–C4–C5–S2, $-0.7(2)$; S2–C8–C24–C29, $8.3(2)$.

| $\alpha(\text{OMe})\text{Tol}_2$ | |
|--|--|
| Empirical formula | $\text{C}_{30}\text{H}_{24}\text{O}_2\text{S}_2$ |
| Formula weight | 480.61 |
| Temperature [K] | 150(2) |
| Crystal system | monoclinic |
| Space group (number) | $P2_1/n$ (14) |
| <i>a</i> [Å] | 13.7285(9) |
| <i>b</i> [Å] | 7.9848(5) |
| <i>c</i> [Å] | 21.6165(14) |
| α [$^\circ$] | 90 |
| β [$^\circ$] | 100.332(3) |
| γ [$^\circ$] | 90 |
| Volume [Å ³] | 2331.2(3) |
| <i>Z</i> | 4 |
| ρ_{calc} [gcm ⁻³] | 1.369 |
| μ [mm ⁻¹] | 0.255 |
| <i>F</i> (000) | 1008 |
| Crystal size [mm ³] | 0.450×0.280×0.230 |
| Crystal color | yellow |
| Crystal shape | rod |
| Radiation | MoK α ($\lambda=0.71073$ Å) |
| 2 θ range [$^\circ$] | 5.45 to 66.30 (0.65 Å) |
| Index ranges | $-21 \leq h \leq 20$ $-12 \leq k \leq 12$ $-33 \leq l \leq 32$ |
| Reflections collected | 37349 |
| Independent reflections | 8895 $R_{\text{int}} = 0.0444$ $R_{\text{sigma}} = 0.0443$ |
| Completeness to $\theta = 25.242^\circ$ | 99.8 % |
| Data / Restraints / Parameters | 8895/0/311 |
| Goodness-of-fit on F^2 | 1.024 |
| Final <i>R</i> indexes [$\geq 2\sigma(I)$] | $R_1 = 0.0444$ $wR_2 = 0.1049$ |
| Final <i>R</i> indexes [all data] | $R_1 = 0.0719$ $wR_2 = 0.1200$ |
| Largest peak/hole [eÅ ⁻³] | 0.39/-0.30 |

Table 11. Crystallographic data and structural refinement parameters, $\alpha(\text{OMe})\text{Tol}_2$.

$\alpha(\text{OMe})(\text{PhOMe})_2$

Single crystals of $\alpha(\text{OMe})(\text{PhOMe})_2$ were obtained through vapor diffusion of hexanes into a saturated solution of $\alpha(\text{OMe})(\text{PhOMe})_2$ in THF. $\alpha(\text{OMe})(\text{PhOMe})_2$ was obtained as a co-crystal with THF (shown in Figure 126). CCDC number: 2361478

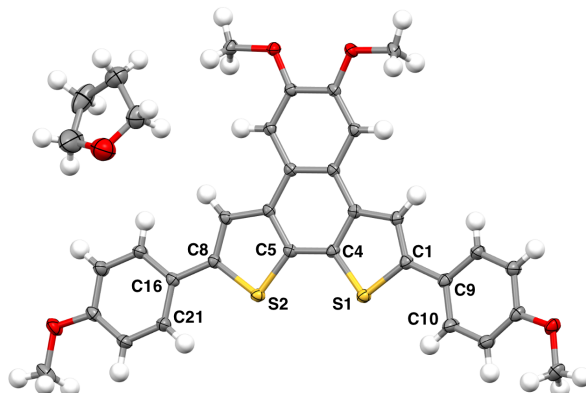


Figure 126. ORTEP diagram of $\alpha(\text{OMe})(\text{PhOMe})_2$ (ellipsoids drawn at 50% probability). Hydrogens have been omitted for clarity. Select bond lengths (Å) and angles (°): C5–S2, 1.729(1); C8–S2, 1.747(2); C4–S1, 1.733(2); C1–S1, 1.751(3); C21–C16–C8–S2, 7.7(2); S2–C5–C4–S1, -3.4(2); S1–C1–C9–C10, 1.3(2).

| $\alpha(\text{OMe})(\text{PhOMe})_2$ | |
|--|---|
| Empirical formula | $\text{C}_{34}\text{H}_{32}\text{O}_5\text{S}_2$ |
| Formula weight | 584.72 |
| Temperature [K] | 150(2) |
| Crystal system | monoclinic |
| Space group (number) | $P2_1$ (4) |
| <i>a</i> [Å] | 8.7673(7) |
| <i>b</i> [Å] | 6.2302(4) |
| <i>c</i> [Å] | 25.9473(19) |
| α [°] | 90 |
| β [°] | 93.533(3) |
| γ [°] | 90 |
| Volume [Å ³] | 1414.60(18) |
| <i>Z</i> | 2 |
| ρ_{calc} [gcm ⁻³] | 1.373 |
| μ [mm ⁻¹] | 0.232 |
| <i>F</i> (000) | 616 |
| Crystal size [mm ³] | 0.350×0.290×0.130 |
| Crystal color | yellow |
| Crystal shape | plate |
| Radiation | MoK α ($\lambda=0.71073$ Å) |
| 2 θ range [°] | 4.72 to 66.37 (0.65 Å) |
| Index ranges | -13 ≤ <i>h</i> ≤ 13 -9 ≤ <i>k</i> ≤ 9 -39 ≤ <i>l</i> ≤ 39 |
| Reflections collected | 65592 |
| Independent reflections | 10845 $R_{\text{int}} = 0.0377$ $R_{\text{sigma}} = 0.0243$ |
| Completeness to $\theta = 25.242^\circ$ | 99.8 % |
| Data / Restraints / Parameters | 10845/1/374 |
| Goodness-of-fit on F^2 | 1.049 |
| Final <i>R</i> indexes [$I \geq 2\sigma(I)$] | $R_1 = 0.0312$ $wR_2 = 0.0858$ |
| Final <i>R</i> indexes [all data] | $R_1 = 0.0333$ $wR_2 = 0.0871$ |
| Largest peak/hole [eÅ ⁻³] | 0.34/-0.29 |
| Flack X parameter | 0.029(10) |

Table 12. Crystallographic data and structural refinement parameters, $\alpha(\text{OMe})(\text{PhOMe})_2$.

$\alpha(\text{OMe})(\text{PhCF}_3)_2$

Single crystals of $\alpha(\text{OMe})(\text{PhCF}_3)_2$ were obtained through vapor diffusion of hexanes into a saturated solution of $\alpha(\text{OMe})(\text{PhCF}_3)_2$ in THF (Figure 127). CCDC number: 2361479

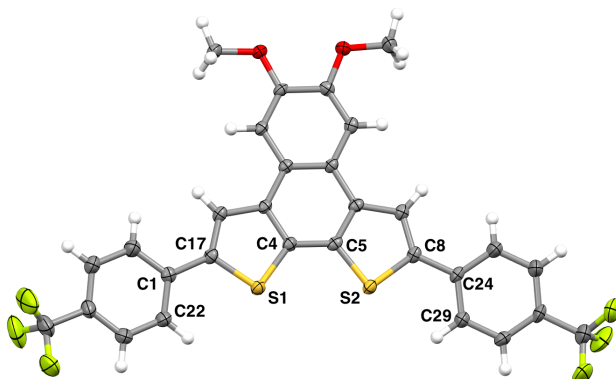


Figure 127. ORTEP diagram of $\alpha(\text{OMe})(\text{PhCF}_3)_2$ (ellipsoids drawn at 50% probability). Hydrogens have been omitted for clarity. Select bond lengths (Å) and angles (°): C4–S1, 1.731(3); C17–S1, 1.747(3); C5–S2, 1.722(3); C8–S2, 1.742(3); S1–C4–C5–S2, 2.5(4); C22–C1–C17–S1, -6.9(4); S2–C8–C24–C29, 9.5(4).

| | $\alpha(\text{OMe})(\text{PhCF}_3)_2$ |
|---|---|
| Empirical formula | $\text{C}_{30}\text{H}_{18}\text{F}_6\text{O}_2\text{S}_2$ |
| Formula weight | 588.56 |
| Temperature [K] | 150(2) |
| Crystal system | monoclinic |
| Space group (number) | $P2_1/n$ (14) |
| <i>a</i> [Å] | 17.861(5) |
| <i>b</i> [Å] | 8.2438(16) |
| <i>c</i> [Å] | 18.565(4) |
| α [°] | 90 |
| β [°] | 111.359(7) |
| γ [°] | 90 |
| Volume [Å ³] | 2545.8(10) |
| <i>Z</i> | 4 |
| ρ_{calc} [gcm ⁻³] | 1.536 |
| μ [mm ⁻¹] | 0.282 |
| <i>F</i> (000) | 1200 |
| Crystal size [mm ³] | 0.310×0.050×0.020 |
| Crystal color | yellow |
| Crystal shape | needle |
| Radiation | MoK α ($\lambda=0.71073$ Å) |
| 2 θ range [°] | 4.71 to 56.66 (0.75 Å) |
| Index ranges | -23 ≤ <i>h</i> ≤ 22 -10 ≤ <i>k</i> ≤ 10 -24 ≤ <i>l</i> ≤ 24 |
| Reflections collected | 36606 |
| Independent reflections | 6296 $R_{\text{int}} = 0.1603$ $R_{\text{sigma}} = 0.0903$ |
| Completeness to $\theta = 25.242^\circ$ | 100.0 % |
| Data / Restraints / Parameters | 6296/258/437 |
| Goodness-of-fit on F^2 | 1.008 |
| Final <i>R</i> indexes [$I \geq 2\sigma(I)$] | $R_1 = 0.0531$ $wR_2 = 0.1137$ |
| Final <i>R</i> indexes [all data] | $R_1 = 0.1142$ $wR_2 = 0.1400$ |
| Largest peak/hole [eÅ ⁻³] | 0.42/-0.41 |

Table 13. Crystallographic data and structural refinement parameters, $\alpha(\text{OMe})(\text{PhCF}_3)_2$.

$\beta(\text{O}i\text{-Pent})\text{ToI}_2$

Single crystals of $\beta(\text{O}i\text{-Pent})\text{ToI}_2$ were obtained through vapor diffusion of hexanes into a saturated solution of $\beta(\text{O}i\text{-Pent})\text{ToI}_2$ in THF. $\beta(\text{O}i\text{-Pent})\text{ToI}_2$ was obtained as a dimer crystal and is shown in Figure 128 with the rear molecule represented by a wireframe, with the top molecule as thermal ellipsoids. The metrics between the two molecules were averaged and are presented in the figure caption. The structure contains additional 4908 Ang³ of solvent accessible voids (ca. 30% of the cell volume). Fragments could be identified as partially occupied chloroform, disordered with other highly disordered solvate molecules that could not be recognised. The structure factors were instead augmented via reverse Fourier transform methods using the SQUEEZE routine¹⁵ as implemented in the program Platon. The resultant FAB file containing the structure factor contribution from the electron content of the void space was used in together with the original hkl file in the further refinement. (The FAB file with details of the Squeeze results is appended to the cif file). The Squeeze procedure corrected for 948 electrons within the solvent accessible voids. CCDC number: 2361480

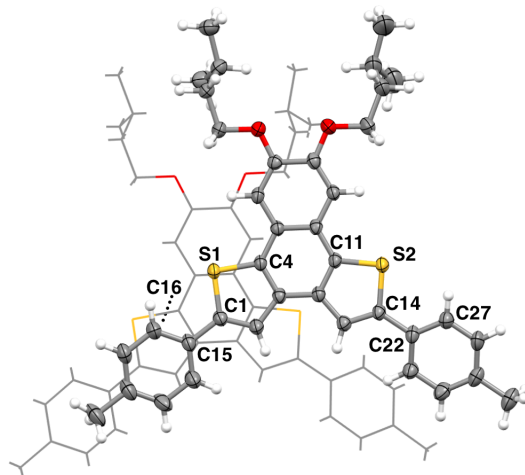


Figure 128. ORTEP diagram of $\beta(\text{O}i\text{-Pent})\text{ToI}_2$ (ellipsoids drawn at 50% probability). Crystallised as a dimer, bottom molecules given as wireframe. Average bond lengths (Å) and angles (°) of the dimers: C1–S1, 1.741; C4–S1, 1.735; C11–S2, 1.736; C14–S2, 1.743; C27–C22–C14–S2, -4.4; C16–C15–C1–S1, -8.2; S2–C8–C24–C29, 9.5(4).

| | β(<i>O</i>-Pent)Tol₂ |
|---|---|
| Empirical formula | C ₃₈ H ₄₀ O ₂ S ₂ |
| Formula weight | 592.82 |
| Temperature [K] | 150(2) |
| Crystal system | monoclinic |
| Space group (number) | C2/c (15) |
| <i>a</i> [Å] | 41.918(3) |
| <i>b</i> [Å] | 26.6997(19) |
| <i>c</i> [Å] | 15.3487(11) |
| α [°] | 90 |
| β [°] | 104.041(2) |
| γ [°] | 90 |
| Volume [Å ³] | 16665(2) |
| <i>Z</i> | 16 |
| ρ_{calc} [gcm ⁻³] | 0.945 |
| μ [mm ⁻¹] | 0.153 |
| <i>F</i> (000) | 5056 |
| Crystal size [mm ³] | 0.320×0.180×0.060 |
| Crystal color | colorless |
| Crystal shape | blade |
| Radiation | MoK α (λ =0.71073 Å) |
| 2 θ range [°] | 3.85 to 56.97 (0.75 Å) |
| Index ranges | -56 ≤ <i>h</i> ≤ 46 -35 ≤ <i>k</i> ≤ 35 -18 ≤ <i>l</i> ≤ 20 |
| Reflections collected | 54446 |
| Independent reflections | 20701 <i>R</i> _{int} = 0.0501 <i>R</i> _{sigma} = 0.0836 |
| Completeness to $\theta = 25.242^\circ$ | 99.7 % |
| Data / Restraints / Parameters | 20701/340/857 |
| Goodness-of-fit on <i>F</i> ² | 1.031 |
| Final <i>R</i> indexes [<i>I</i> ≥ 2 σ (<i>I</i>)] | <i>R</i> ₁ = 0.0774 <i>wR</i> ₂ = 0.2225 |
| Final <i>R</i> indexes [all data] | <i>R</i> ₁ = 0.1257 <i>wR</i> ₂ = 0.2622 |
| Largest peak/hole [eÅ ⁻³] | 1.06/-0.65 |

Table 14. Crystallographic data and structural refinement parameters, **β (*O*-Pent)Tol₂**.

7) References

- 1 A. M. Brouwer, *Pure Appl. Chem.*, 2011, **83**, 2213–2228.
- 2 D. P. Piet, H. J. Verheij, H. Zuilhof and E. J. R. Sudhölter, *J. Porphyr. Phthalocyanines*, 2003, **7**, 73–82.
- 3 J. G. Weis and T. M. Swager, *ACS Macro Lett.*, 2015, **4**, 138–142.
- 4 T. Chen, G. B. Pan, H. Wettach, M. Fritzsche, S. Höger, L. J. Wan, H. B. Yang, B. H. Northrop and P. J. Stang, *J. Am. Chem. Soc.*, 2010, **132**, 1328–1333.
- 5 G. Chamelot, M. Idir, M. Leclerc and J. F. Morin, *Polym. Chem.*, 2023, **1**, 1206–1212.
- 6 C. Huang, C. G. Zhen, S. Ping Su, C. Vijila, B. Balakrisnan, M. D. Joong Auch, K. Ping Loh and Z. K. Chen, *Polymer*, 2006, **47**, 1820–1829.
- 7 BindFit v0.5, <http://app.supramolecular.org/bindfit/>.
- 8 A. Rahalkar and A. Stanger, AROMA package, <http://chemistry.technion.ac.il/members/amnon-stanger/>.
- 9 Bruker, *SAINTE*, V8.40B, Bruker AXS Inc., Madison, Wisconsin, USA.
- 10 L. Krause, R. Herbst-Irmer, G. M. Sheldrick and D. Stalke, *J. Appl. Crystallogr.*, 2015, **48**, 3–10.
- 11 G. M. Sheldrick, *Acta Crystallogr. Sect. A Found. Crystallogr.*, 2015, **71**, 3–8.
- 12 G. M. Sheldrick, *Acta Crystallogr. Sect. C Struct. Chem.*, 2015, **71**, 3–8.
- 13 D. Kratzert, FinalCif, V123, <https://dkratzert.de/finalcif.html>.
- 14 C. R. Groom, I. J. Bruno, M. P. Lightfoot and S. C. Ward, *Acta Crystallogr. Sect. B Struct. Sci. Cryst. Eng. Mater.*, 2016, **72**, 171–179.
- 15 P. van der Sluis and A. L. Spek, *Acta Crystallogr. A* **46**, 1990, 194–201.